ISSN 0869-5938, Stratigraphy and Geological Correlation, 2021, Vol. 29, No. 4, pp. 450–494. © Pleiades Publishing, Ltd., 2021.
Russian Text © The Author(s), 2021, published in Stratigrafiya, Geologicheskaya Korrelyatsiya, 2021, Vol. 29, No. 4, pp. 71–117.

New Bio-, Chemo-, and Magnetostratigraphy of the Santonian–Campanian Boundary in the Kudrino and Aksu-Dere Sections (SW Crimea): Problems of Global Correlation and Selection of the Lower Boundary Stratotype of the Campanian. 1. Geological Framework, Sedimentology, Biostratigraphy

A. Yu. Guzhikov[a, *], E. Yu. Baraboshkin[b, c], G. N. Aleksandrova[c], I. P. Ryabov[a], M. A. Ustinova[c], L. F. Kopaevich[b], G. V. Mirantsev[d], A. B. Kuznetsov[e], P. A. Fokin[b], and V. L. Kosorukov[b]

[a] *Saratov State University, Saratov, 410012 Russia*
[b] *Moscow State University, Moscow, 119991 Russia*
[c] *Geological Institute, Russian Academy of Sciences, Moscow, 119017 Russia*
[d] *Paleontological Institute, Russian Academy of Sciences, Moscow, 117997 Russia*
[e] *Institute of Precambrian Geology and Geochronology, Russian Academy of Sciences, St. Petersburg, 199034 Russia*
**e-mail: aguzhikov@yandex.ru*

Received September 15, 2020; revised November 2, 2020; accepted December 17, 2020

Abstract—New complex data have been obtained for two sections of the Santonian–Campanian boundary of Southwestern Crimea. Article 1 presents detailed geological descriptions of sections, lithological, mineralogical, and paleoichnological materials, and the results of determining macro- (crinoids, ammonoids, belemnites) and micropaleontological (dinocysts, nannoplankton, benthic and planktonic foraminifers) remains. On the basis of the results of research, sea level fluctuations, variations in the activity of allogenic input (including pyroclastic material), and other features of sedimentation have been reconstructed. All macro- and micropaleontological data confirm the late Santonian–early Campanian age of the rocks; for each of the micropaleontological groups, biostratigraphic units have been established and a detailed division of the sections has been carried out.

Keywords: Upper Cretaceous, Santonian, Campanian, dinocysts, benthic foraminifers, planktonic foraminifers, nannoplankton, crinoids, ammonoids, belemnites, ichnoassemblages, Crimea

DOI: 10.1134/S086959382104002X

INTRODUCTION

The Santonian–Campanian sediments that compose a significant part of the Upper Cretaceous succession of the Crimean Mountains (Fig. 1a) are represented predominantly by limestones and marls. Many sections as thick as 200 m or more reported in the literature are located in the southwestern part of the Crimean Mountains. In spite of the extensive faunistic characterization and long history of investigation (Alekseev, 1989; Gozhik et al., 2013; Klikushin, 1980, 1981, 1985; Kopaevich, 2010; Kopaevich and Walaszczyk, 1990; Maslakova, 1959, 1967; Maslakova and Naidin, 1958; Naidin, 1953, 1959; Naidin et al., 1981; Weber and Malychev, 1923; etc.), detailed interregional correlations and the justification of the exact level of the lower boundary of the Campanian still remain actual stratigraphic problems for Southwestern Crimea and the Crimean Peninsula as a whole.

The most complete sections of the Santonian–Campanian boundary interval with reliable paleontological evidence are located in Southwestern Crimea, on the right slope of the Kacha River valley near the village of Kudrino (Fig. 1b). In one of them, the Aksu-Dere Ravine section, the Santonian–Campanian boundary was established earlier after integrated macro- and microfaunistic studies (Fokin et al., 2018). The main recognition criteria for this boundary were the finds of the crinoid *Marsupites testudinarius* (Schloth.), the last occurrence (LO) of which is proposed as the marker of the base of the Campanian Stage (Hancock et al., 1996). Of great value for the substantiation of this boundary are the finds of the belemnite species *Actinocamax verus* Miller and the ammonoid species

Parapuzosia (*P.*) cf. *leptophylla* (Sharpe) (Baraboshkin and Fokin, 2019).

After the additional paleontological studies and the acquisition of the magneto- and chemostratigraphic characteristics, the easily accessible and well-exposed sections in Southwestern Crimea can potentially be proposed as the Global Boundary Stratotype Section and Point (GSSP) or an auxiliary section of the Campanian Stage, which have not been determined by the International Union of Geological Sciences (IUGS) so far. At present, the candidates for the lower boundary stratotype of the Campanian are sections in Central Texas and Southern England (Hancock et al., 1996; Stratigraphy.org), but none of them fulfills all requirements on the selection of a limitotype (Remane et al., 1996), in particular, the demand for the fitness of rocks for paleomagnetic studies. The magnetostratigraphic data for the Upper Cretaceous in England (Montgomery et al., 1998) are controversial and are still a subject of discussion (Razmjooei et al., 2014, 2018; Thibault et al., 2016; etc.), whereas data for the Waxahachie Dam Spillway section in Texas (Gale et al., 2008) are absent entirely.

The Aksu-Dere section (Figs. 1b, 1c), in spite of sufficient abundance of micro- and macrofaunistic evidence of fossils such as crinoids, ammonoids, and belemnites (Baraboshkin and Fokin, 1919; Fokin et al., 2018), cannot be proposed as the lower boundary stratotype for this stage, because it contains clear indications of disconformity (erosion) and condensation immediately near the Santonian–Campanian boundary (Baraboshkin and Fokin, 2019; Fokin et al., 2018). At the same time, the nearby (approximately 2.2 km to the south) Kudrino-2 section (Figs. 1b, 1c) retains a more complete lithological succession of the boundary interval, and the composite Kudrino–Aksu-Dere section potentially satisfies the requirements on the completeness of the sequence imposed on GSSP. Microfauna was studied earlier at some levels of the Kudrino section (Kopaevich and Khotylev, 2014; etc.), but the precise position of the Santonian–Campanian boundary in this section has never been determined.

We performed detailed bio-, magneto-, and chemostratigraphic studies of two sections of the Santonian–Campanian boundary interval, Kudrino-2 and Aksu-Dere, in order to track the lower boundary of the Campanian from the stratotype area to the Crimean Mountains and to analyze the results of integrated studies in terms of justifying the interpretation of the Kudrino–Aksu-Dere composite section as the GSSP of the Campanian.

We obtained new paleontological (ammonoids, belemnites, crinoids, dinocysts, nannoplankton, planktonic and benthic foraminifers, paleoichnology), magnetostratigraphic (paleomagnetism and rock magnetism), isotopic-geochemical (stable carbon, oxygen, and strontium isotopes), and lithological-mineralogical (the results of thin-section petrography and insoluble residue composition studies) data. Samples for various types of analyses were selected using the "sample to sample" system. Oriented grab samples for paleomagnetic and rock-magnetic studies in the composite Kudrino–Aksu-Dere section were collected from a total of 109 levels. Nannoplankton identification was performed by analyzing samples from 28 levels; dinocysts and foraminifers, from 37 levels. Data on trace elements and carbon and oxygen isotopes were obtained for 27 levels, and data on strontium isotopes were obtained for 16 levels. The insoluble residue was studied at 18 levels in an interval 1.4 m thick near the Santonian–Campanian boundary established from paleontological and magnetostratigraphic data. The palynological and magneto- and chemostratigraphic studies of the Santonian and the lower Campanian of Southwestern Crimea were performed for the first time.

The field study and sampling of fossils were carried out by E.Yu. Baraboshkin, A.Yu. Guzhikov, and P.A. Fokin. Descriptions of geological sections, petrographic and ichnological studies, and cephalopod analysis were performed by E.Yu. Baraboshkin; crinoid analysis was performed by G.V. Mirantsev. Magnetostratigraphic data were obtained by Guzhikov; isotopic-geochemical data were obtained by A.B. Kuznetsov. Palynomorphs were studied by G.N. Aleksandrova; nannoplankton, by M.A. Ustinova; planktonic foraminifers, by L.F. Kopaevich; benthic foraminifers, by I.P. Ryabov; and the insoluble residue, by A.A. Fokin and V.L. Kosorukov.

Article 1 presents the descriptions of the lithology of geological sections and the results of sedimentological and biostratigraphic studies.

GEOLOGICAL DESCRIPTION OF THE SECTION

The studied sections are located in the Bakhchysarai district of the Republic of Crimea, west of the town of Bakhchysarai (Figs. 1a, 1b).

The Aksu-Dere Ravine section (observation point (o.p.) 3168; the apparent thickness is 31 m; Figs. 1c, 2a, 2b), located 2.2–2.3 km north of the village of Kudrino, begins at the top of the Prokhladnoe Formation (upper Turonian–lower Coniacian). The apparent base of the section is exposed in a deep gulley on the slope of the ravine (the coordinates of the base of the section are 44°43′27.0″ N, 33°56′52.0″ E). The section is built up further along the dirt road leading to the watershed and then along a shallow scour in the forest up to the crest of the river divide (the coordinates of sampling site 3168-42, in which the sampling of the section along this gulley resumed, are 44°43′26.9″ N, 33°56′54.6″ E).

The Kudrino-2 section (o.p. 3184; the apparent thickness is 43 m; Figs. 1c, 2c, 2d) is located at the northeastern outskirts of the village of Kudrino. The partially grass-covered base of the section is located on

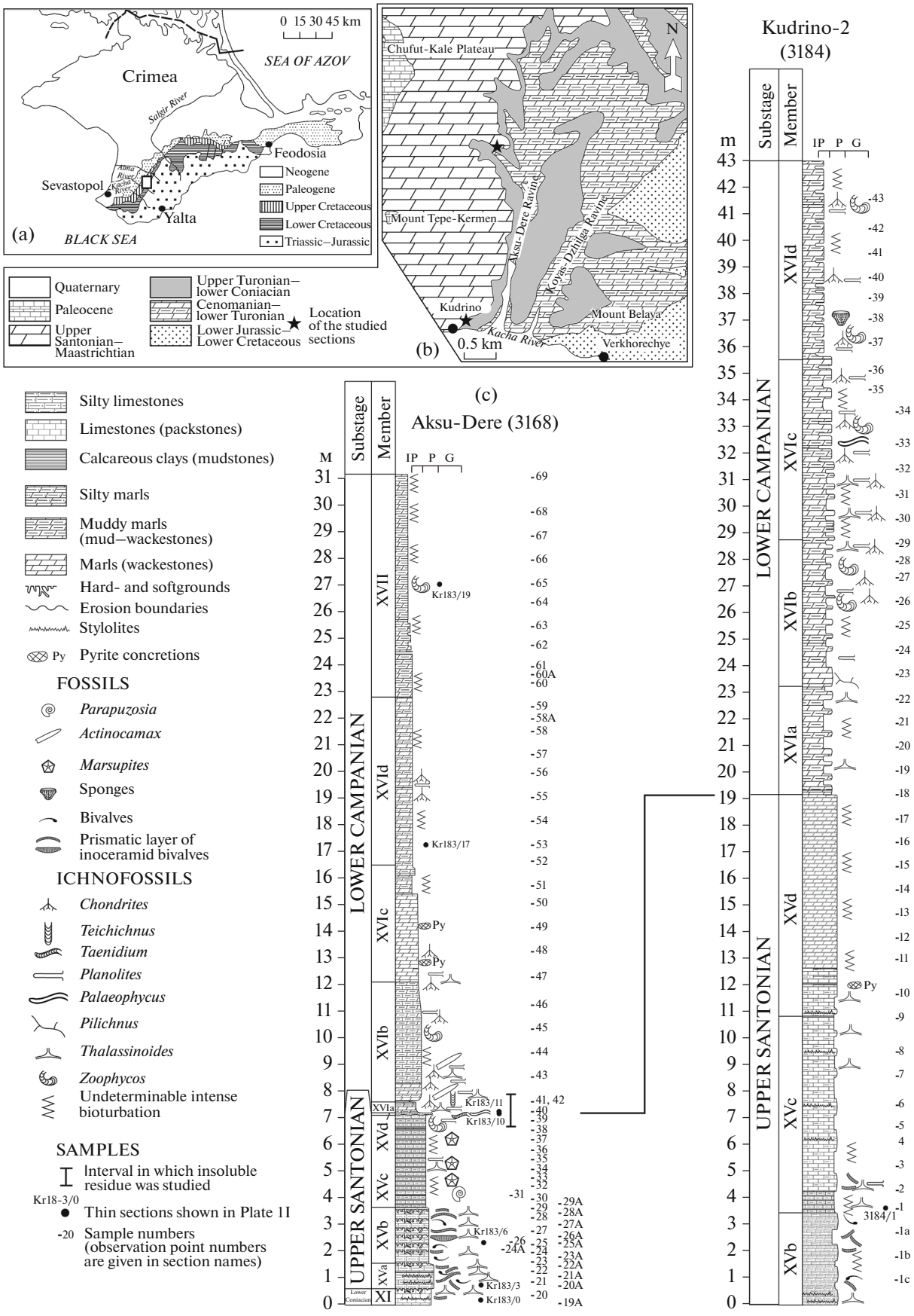
0 15 30 45 km
SEA OF AZOV
Crimea
Salgir River
Feodosia
Sevastopol
Alma River
Kacha River
Belbek River
Yalta
BLACK SEA
(a)
Neogene
Paleogene
Upper Cretaceous
Lower Cretaceous
Triassic–Jurassic
Quaternary
Paleocene
Upper Santonian–Maastrichtian
Upper Turonian–lower Coniacian
Cenomanian–lower Turonian
Lower Jurassic–Lower Cretaceous
Location of the studied sections
Chufut-Kale Plateau
N
Mount Tepe-Kermen
Aksu-Dere Ravine
Kyrk-Dzhilga Ravine
Kudrino
Mount Belaya
Kacha River
0.5 km
Verkhorechye
(b)
Silty limestones
Limestones (packstones)
Calcareous clays (mudstones)
Silty marls
Muddy marls (mud–wackestones)
Marls (wackestones)
Hard- and softgrounds
Erosion boundaries
Stylolites
Py Pyrite concretions
FOSSILS
Parapuzosia
Actinocamax
Marsupites
Sponges
Bivalves
Prismatic layer of inoceramid bivalves
ICHNOFOSSILS
Chondrites
Teichichnus
Taenidium
Planolites
Palaeophycus
Pilichnus
Thalassinoides
Zoophycos
Undeterminable intense bioturbation
SAMPLES
Interval in which insoluble residue was studied
Kr18-3/0 Thin sections shown in Plate 1I
-20 Sample numbers (observation point numbers are given in section names)
(c)
Aksu-Dere (3168)
M
Substage
Member
IP P G
UPPER SANTONIAN
LOWER CAMPANIAN
XVa
XVb
XVc
XVd
XVIa
XVIb
XVIc
XVId
XVII
XI
Lower Coniacian
Kr183/19
Kr183/17
Kr183/11
Kr183/10
Kr183/6
Kr183/3
Kr183/0
Py
Kudrino-2
(3184)
m
3184/1

Fig. 1. (a) Geological sketch map of Southwestern Crimea (square indicates location of the study area); (b) geological sketch map of the right bank of the Kacha River in the vicinity of the village of Kudrino and the Aksu-Dere Ravine; (c) lithological columns of the Kudrino-2 (observation point 3184) and Aksu-Dere (observation point 3168) sections.

the slopes of a small ravine just behind the houses (the coordinates of the base of the section are 44°42′15.0″ N, 33°56′49.5″ E), and the top of the section is located in a small washout at the extension of this ravine above the crossing with the dirt road that leads to the crest of the river divide (the coordinates of the top of the section are 44°42′17.8″ N, 33°56′47.6″ E). The base of the Santonian limestones of the Kudrino Formation is not exposed here.

The strata in both sections are conformably bedded and dip northwestward. Dip azimuths vary from 292° to 340° (mostly 310°–330°), and dip angles vary from 6°30″ to 19° (mostly 10°–13°).

The sections are similar in structure and differ in thicknesses of members; for this reason, we give a uniform description indicating the thicknesses. The Prokhladnoe Formation (upper Turonian–lower Coniacian) is represented by hard white limestones overlain by pinkish limestones with stylolites at the top. The upbuilding Kudrino Formation (upper Santonian–Maastrichtian) is composed of limestones and muddy limestones in the Santonian interval and marls and muddy marls in the Campanian interval. All deposits are bioturbated in full volume with a bioturbation index (Bi) of 5 (Droser and Bottjer, 1986).

Because the exposure is fragmentary, the nature of cyclicity and cementation of the relief forming rocks is poorly visible. Therefore, the members and submembers were recognized on the basis of a variety of signatures—lithology, rock microscopy (Plate I), slope morphology, and petromagnetic characteristics. At the same time, we tried to preserve numbering of members adopted in (Alekseev, 1989).

The following succession is exposed in the section from the base upward (Fig. 1c).

Prokhladnoe Formation. Member XI. Slightly muddy white hard limestones; in the upper part (40–50 cm), pinkish, Fe-colored, with numerous continuous stylo-

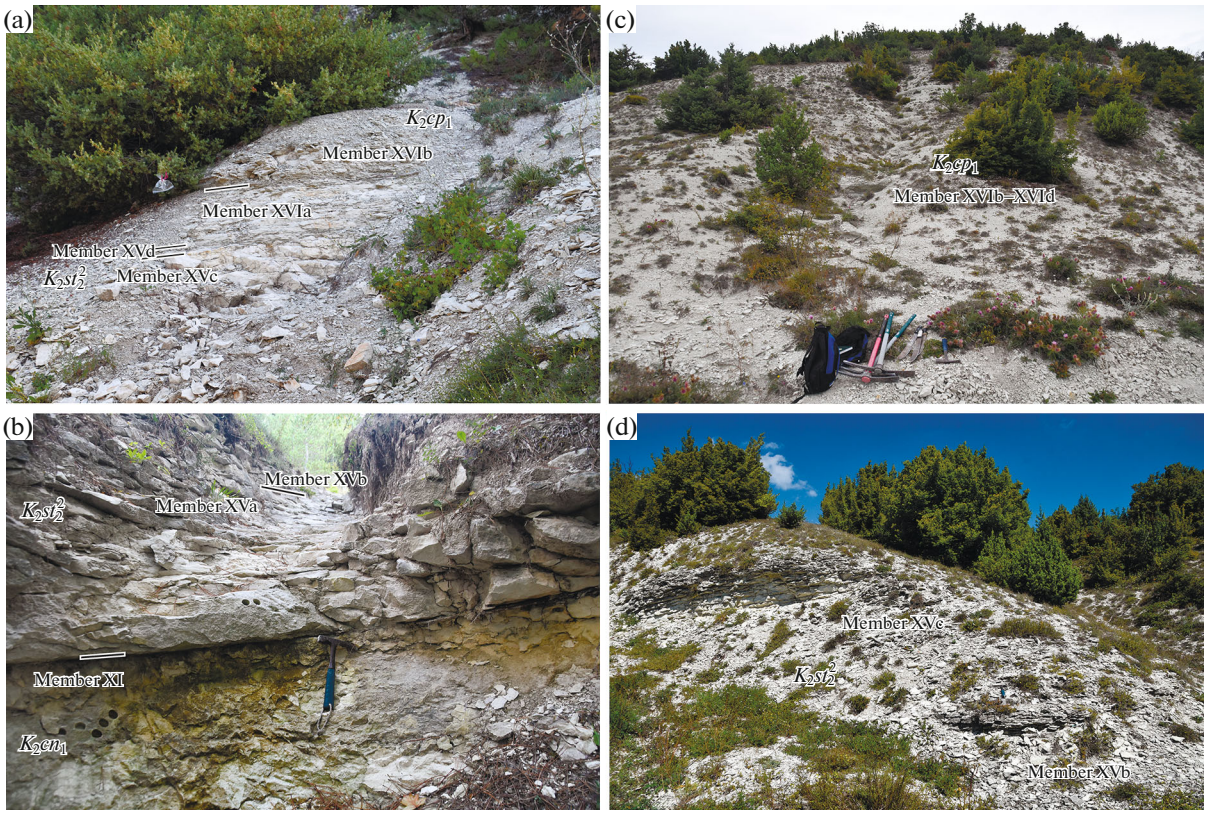

Fig. 2. Photographs of the Aksu-Dere (a, b) and Kudrino-2 (c, d) sections, taken by Baraboshkin in 2018–2019. (a) The outcrops of the lower part of the Kudrino Formation in the Santonian–Campanian boundary interval; (b) the base of the section; the boundary between the Coniacian limestones of the Prokhladnoe Formation and the Santonian limestones of the Kudrino Formation; (c) the lower part of the Kudrino Formation in the Santonian–Campanian boundary interval; (d) the upper (Campanian) part of the sequence of the Kudrino Formation.

lites (the height of the teeth is up to 1–2 cm) marked by greenish clay 1–5 mm thick along them. Microscopically, they are calcispheric–foraminiferal packstones (Plate I, fig. a) with large well-preserved foraminifers, single silt-size glauconite and quartz grains, and the fragments of the prismatic layer of inoceramid bivalve shells. The top of the member (Fig. 2b) is eroded and penetrated by the burrows of crustaceans *Thalassinoides suevicus* (Reith) and *T. paradoxica* (Woodward) to a depth of 5–10 cm. The erosion surface is marked by a thin (up to 1 cm) greenish carbonate clay layer. This member forms the steep slopes of the cuestas. Its apparent thickness in the Aksu-Dere section is more than 0.6 m. According to (Alekseev, 1989; Kopaevich and Walaszczyk, 1990; Naidin et al., 1981), the age of this member is early Coniacian.

Kudrino Formation. Member XV. This member constitutes the upper parts of steep slopes and the armoring top layers of the cuestas. It has been subdivided into four submembers, the lowermost of which was encountered only in the Aksu-Dere section.

Submember XVa (Fig. 2b). Slightly muddy light gray limestones with numerous fragments of the prismatic layer of inoceramid bivalve shells, stylolites (teeth heights are up to 0.5 cm), and numerous subvertical centimeter-thick burrows of *Thalassinoides suevicus* (Reith). In thin sections the rocks are represented by calcispheric-foraminiferal wackestone–packstones and microbreccias (Plate I, fig. b) with small poorly preserved foraminifers, numerous silt-size glauconite and quartz grains, and numerous small fragments of the prismatic layer of inoceramid bivalve shells. In the middle of the submember is a thin (0.5 cm) mudstone–marl layer, and the top is represented by a hardground surface. The submember is characterized by poorly represented thick slab jointing (30–40 cm); its total thickness is 0.9–1 m.

Submember XVb (Fig. 2b). It is similar to the previous submember, but differs from it in a thinner (20–25 cm) slab jointing of the limestones, caused by numerous hardground surfaces with *Thalassinoides suevicus* (Reith). Microscopically, it consists of foraminiferal packstones (Plate I, fig. b) with numerous (up to 5%) coarsely silt-size glauconite and quartz grains, poorly preserved foraminifers, and the fragments of the prismatic layer of inoceramid bivalve shells and echinoderm shells. The thickness of the submember is 2–2.1 m. The thickness increases southward, and the apparent thickness of the submember in the Kudrino-2 section (Fig. 2d) is 3.4 m.

Submember XVc (Fig. 2a). Slightly muddy light gray limestones (10–15 cm) interbedded with greenish marl–mudstones (0.5–1 cm). At a distance of 0.5 m above the base and below the top are thicker (3–5 cm) muddy interbeds. Microscopically, the rocks are similar to those of the previous submember, but the number of glauconite and quartz grains is somewhat smaller. The rocks contain ichnofossils *Thalassinoides suevicus* (Reith), *Planolites beverleyensis* (Bil.), and *Taenidium crassum* Broml., Ekd., Richt. (Plate II, fig. 13) and *Palaeophycus* isp. and *Zoophycos* isp. (in the upper part). The plates of the crinoid *Marsupites*, including *M. laevigatus* (Forbes) (Plate III, figs. 4, 5) and *M. testudinarius* (Schlotheim) (Plate III, fig. 6), are found in this submember of the Aksu-Dere section precisely. The inner mold of a large ammonoid *Parapuzosia* (*P.*) cf. *leptophylla* (Sharpe) (Plate III, fig. 1) (Baraboshkin and Fokin, 2019) was found in its lower part. The top is eroded and ocherized. The thickness of the submember is 3.4–3.5 m.

In the Kudrino-2 section, the thickness of this submember increases to 7.3 m (Fig. 2d). It is characterized by coarse rhythmicity, which is expressed topographically on the slope by the alternation of more or less cemented interbeds of limestones with occasional stylolites (the thickness of the interbeds that differ in the extent of cementing is ~0.5 m in the lower part and ~0.2–0.3 m in the upper part). The lower layer 0.8 m thick at the base of the submember contains centimeter-thick mudstone interbeds.

Submember XVd. Slightly muddy light gray and pinkish silty limestones. In thin sections, these rocks are calcispheric–foraminiferal wackestone–packstones with small poorly preserved foraminifers and thinly crushed fragments of the prismatic layer of inoceramid bivalve shells and echinoderm shells. The base of the submember in the Aksu-Dere section (Plate I, fig. e) displays erosion; the bioclasts are more strongly deformed, and the coarsely silt-size glauconite (up to 10%) and quartz grains are more numerous than in the Kudrino-2 section (Plate I, fig. d); plagioclase grains are present in both sections. More details of the composition of the noncarbonate fraction are given in the "Composition of the Insoluble Residue" section. The submember contains ichnofossils *Thalassinoides suevicus* (Reith) and

Plate I. Petrographic characteristics of the geological section. Thin sections are from the Aksu-Dere section in figs. (a–c) and (e–h) and from the Kudrino-2 section in fig. (d) (location is shown in Figs. 1 and 3). The photographs were shot in non-polarized light using an Axiocam ICc5 camera under a Zeiss Axio Lab Alpol microscope. (a) Sample Kr18-3/0, calcispheric–foraminiferal packstone, Member XI; (b) Sample Kr18-3/3, calcispheric–foraminiferal packstone with fragments of the prismatic layer of inoceramid bivalve shells, Submember XVa; (c) Sample Kr18-3/6, calcispheric–foraminiferal packstone, Submember XVb; (d) Sample 3184/1, calcispheric–foraminiferal wackestone–packstone, Submember XVb; (e) Sample Kr18-3/10, foraminiferal–calcispheric wackestone–packstone, Submember XVd; (f) Sample Kr18-3/11, foraminiferal packstone, base of Submember XVIa; (g) Sample Kr18-3/17, foraminiferal wackestone, Submember XVId; (h) Sample Kr18-3/19, foraminiferal wackestone, Member XVII. Abbreviations: e, echinoid spine fragments; gl, glauconite; q, quartz; pl, plagioclase; p, prismatic layer of bivalves; s, sponge spicules; si, silicification of foraminifers.

Plate I

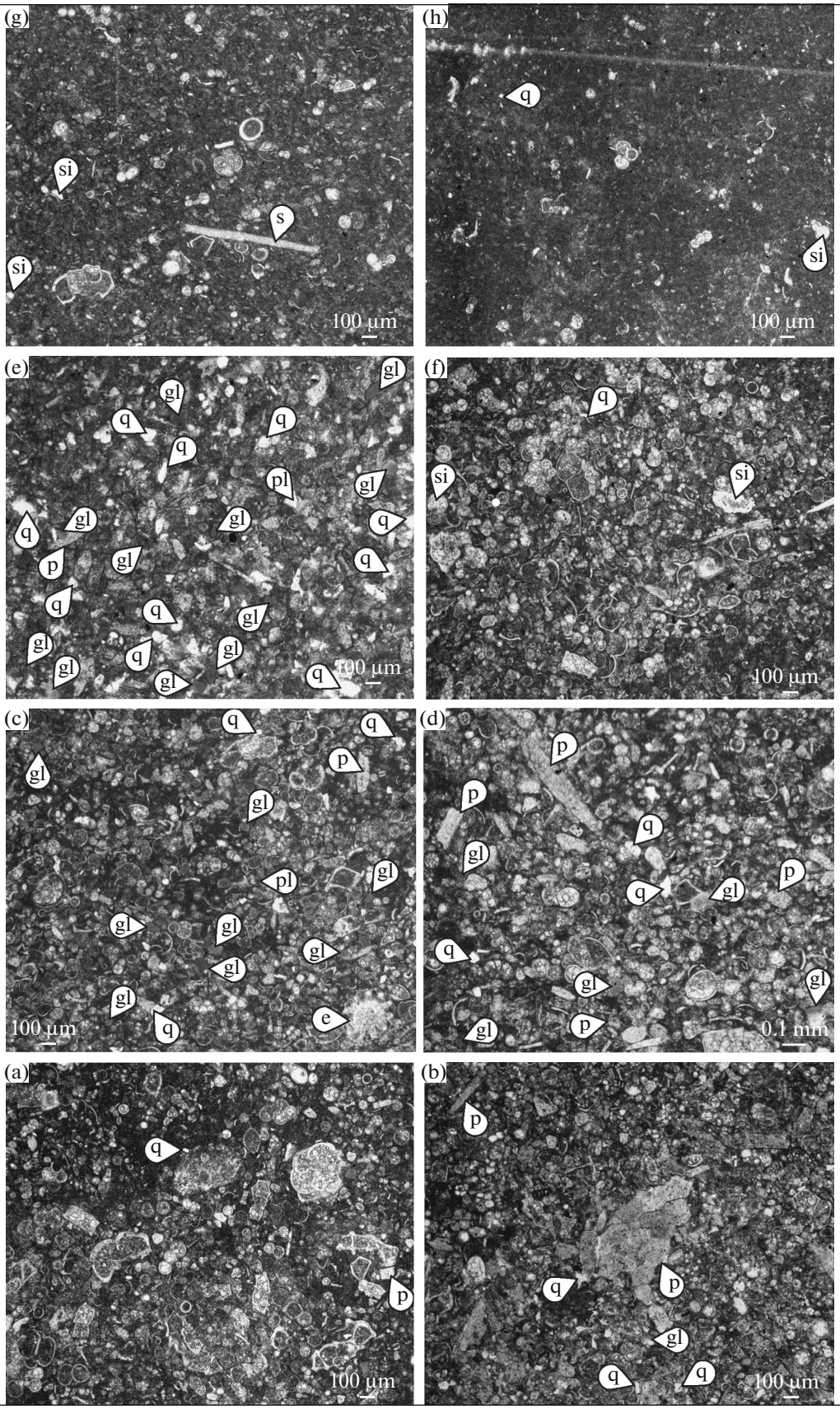
(g)
si
s
si
100 μm
(h)
q
si
100 μm
(e)
gl
q
q
q
pl
gl
q
gl
gl
q
p
gl
q
q
q
gl
gl
gl
q
gl
gl
q
100 μm
(f)
q
si
si
100 μm
(c)
q
q
p
gl
gl
pl
gl
gl
gl
gl
gl
gl
gl
e
q
100 μm
(d)
p
p
q
gl
p
q
gl
q
gl
gl
p
gl
0.1 mm
(a)
q
p
100 μm
(b)
p
q
p
gl
q
q
100 μm

Plate II

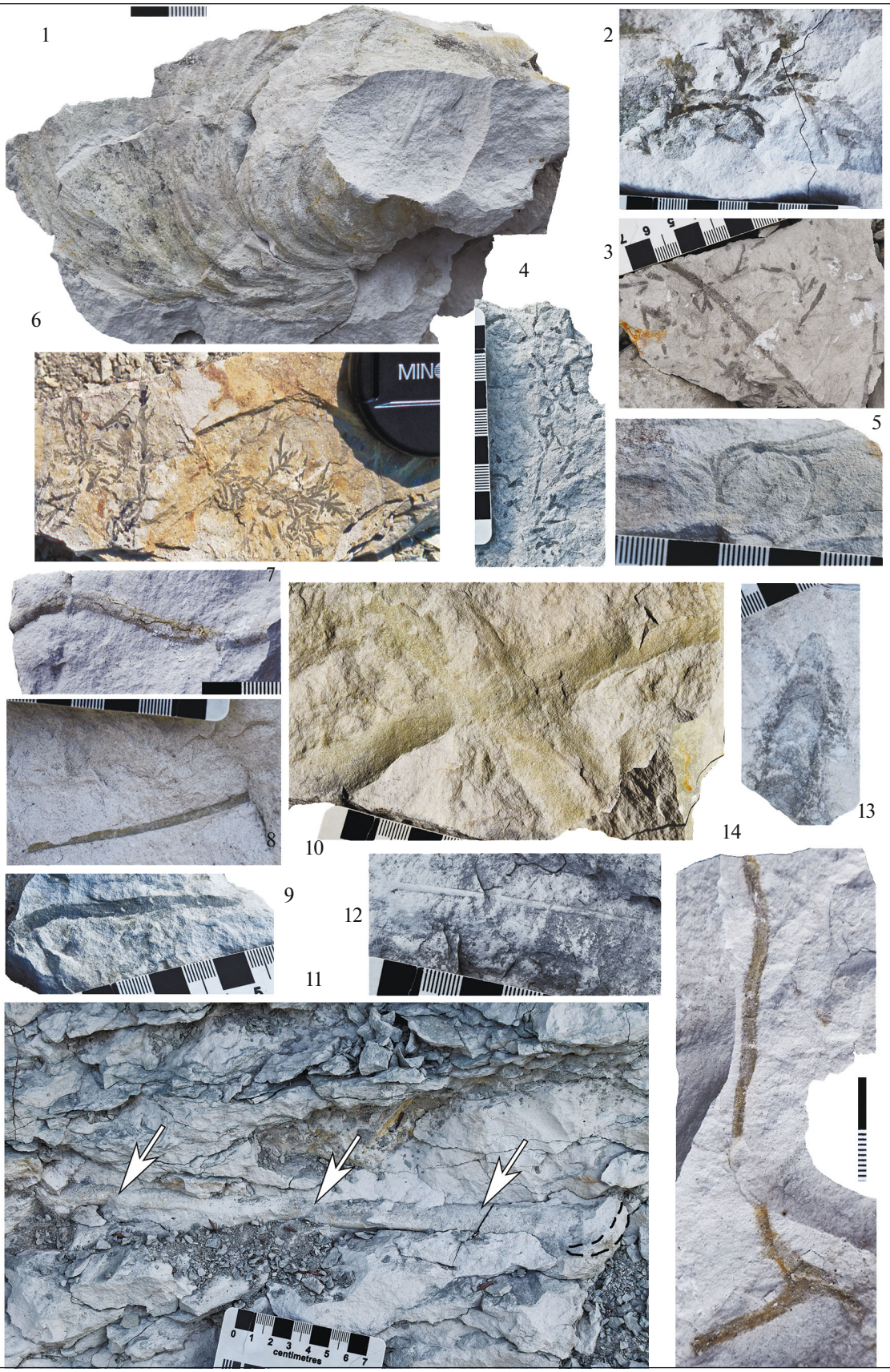

Plate II. Ichnofossils from the Santonian–Campanian sediments of Southwestern Crimea. Figs. 1, 2, 6, 7, 14 are from a 5-m-thick interval of the lower Campanian in a small quarry at the northwestern outskirts of the village of Kudrino (Kudrino-1 section), which strips a bentonite (kil) clay layer and immediately upbuilds the Kudrino-2 section; figs. 3 and 10 are from the Kudrino-2 section; figs. 4, 5, 8, 9, 11–13 are from the Aksu-Dere section. All samples are stored at the Earth Science Museum of Moscow State University (ESM MSU), collection no. 140. (1) *Zoophycos villae* Massalongo, Sample ESM MSU 140/1; (2) *Chondrites caespitosus* (Fisch.-Oost.), Sample ESM MSU 140/2; (3) *Ch. targionii* (Brongn.), Sample ESM MSU 140/3, Submember XVIc; (4) *Ch. intricatus* (Brongn.), Sample ESM MSU 140/4, Submember XVIb; (5) *Ch. patulus* Fisch.-Oost., Sample ESM MSU 140/5, Submember XVIb; (6) *Ch. caespitosus* (Fisch.-Oost.); (7–9) *Palaeophycus tubularis* Hall: (7) Sample ESM MSU 140/6; (8) Sample ESM MSU 140/7, Submember XVIb; (9) Sample ESM MSU 140/8, Submember XVIb; (10) *Thalassinoides suevicus* (Reith), Sample ESM MSU 140/9, Submember XVc; (11) *Teichichnus rectus* Seilacher, Sample ESM MSU 140/10, Submember XVIa; (12) *Planolites beverleyensis* (Bil.), Sample ESM MSU 140/11, Submember XVIb; (13) *Taenidium crassum* Broml., Ekd., Richt., Sample ESM MSU 140/12, Submember XVc; (14) *Palaeophycus heberti* (de Saporta), Sample ESM MSU 140/1.

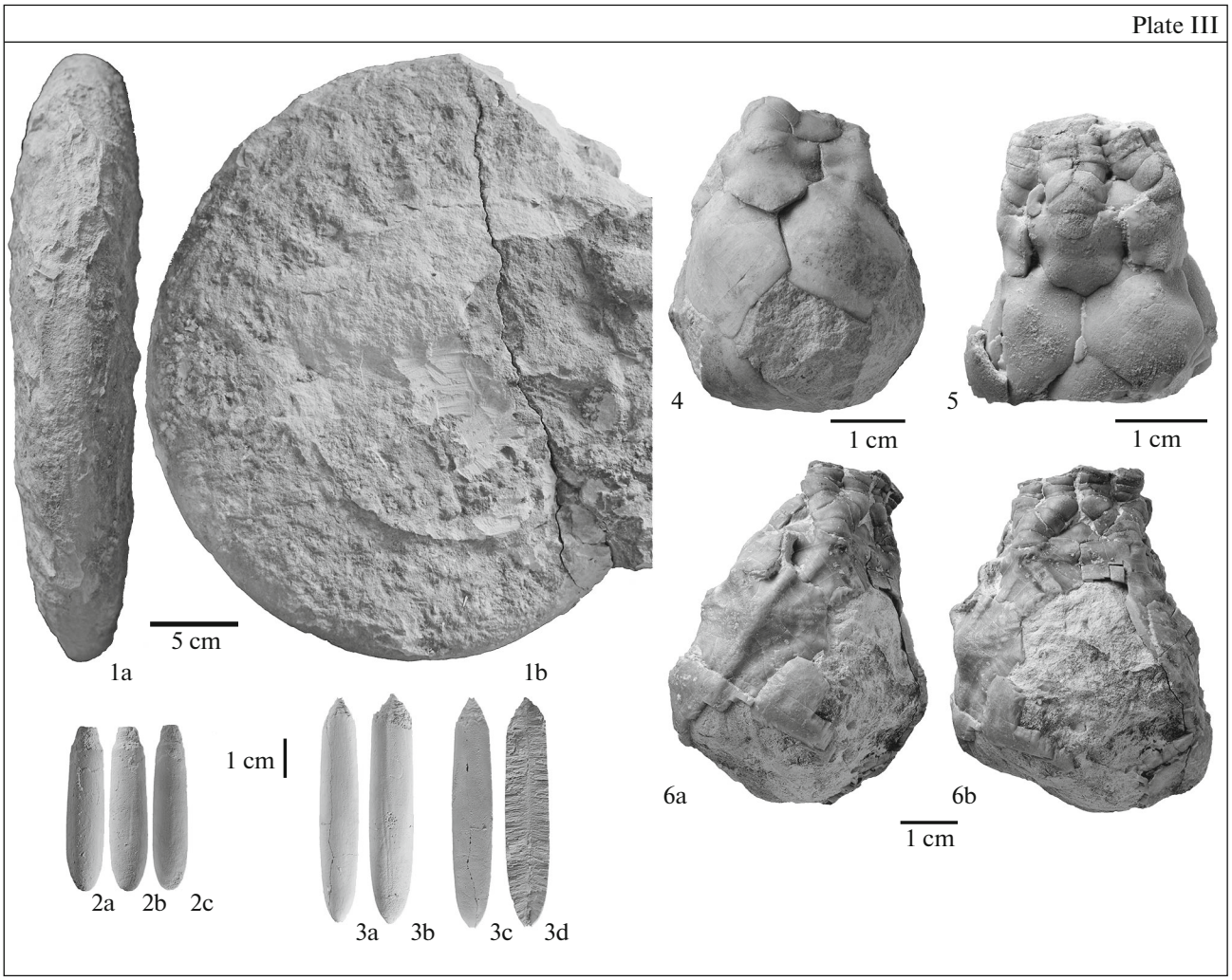

Plate III. Macrofaunal finds from the Aksu-Dere section. Collected by Fokin in 2012 (fig. 1) and 2018 (fig. 2), Baraboshkin in 2019 (fig. 3), Sautkina in 2011 (fig. 5), and Sumarokov in 2012 (fig. 6). Samples 2 and 3 are covered with ammonium chloride. Samples the names of which include the abbreviation ESM MSU are stored in the Earth Science Museum of Moscow State University, Collection no. 136. (1) *Parapuzosia (P.)* cf. *leptophylla* (Sharpe), Sample ESM MSU 136/1: (a) ventral view; (b) side view; upper Santonian, Submember XVc; (2) *Actinocamax* cf. *verus* Miller, Sample ESM MSU 136/2: (a) ventral view; (b) dorsal view; (c) side view; lower Campanian, Submember XVIb; (3) *A. verus* Miller, Sample ESM MSU 136/3: (a) cutaway in dorsal–ventral direction; (b) dorsal view; (c) side view; (d) ventral view; lower Campanian, debris 1.5 m above the base of Submember XVIb; (4) *Marsupites laevigatus* (Forbes), crown, upper Santonian, from a road cut at the level of Submember XVc; (5) *M. laevigatus* (Forbes), crown, upper Santonian, debris at the level of Submember XVc; (6a, 6b) *M. testudinarius* (Schlotheim), crown, upper Santonian, debris at the level of Submember XVc.

Planolites isp. The submember is as thin as 5–7 cm in the Aksu-Dere section (Fig. 2a) and thickens up to 8.3 m in the Kudrino-2 section. The submember here is composed of limy marl layers (20–40 cm) with *Thalassinoides*, alternating with thin (~0.5 cm) calcareous mudstone interbeds.

Member XVI constitutes the feet of the slopes of the next cuesta level. It has been subdivided into four submembers.

Submember XVIa. Light gray and greenish irregularly slabby muddy-silty limestones or limy marls. Muddy component distribution and cementing are irregular. Microscopically, the rocks are foraminiferal packstones (Plate I, fig. f) with well-preserved foraminifers, some of which are silicified, with a small number of calcispheres, fragments of the prismatic layer of inoceramid bivalve shells, echinoderms, and scarce silt-size glauconite and quartz grains. The submember contains ichnofossils *Thalassinoides suevicus* (Reith) (Plate II, fig. 11), *Palaeophycus* isp., *Planolites* isp., and *Chondrites* isp.; in addition, *Teichichnus rectus* Seilacher (Plate II, fig. 11) was encountered 10–12 cm below the boundary with the overlying submember. The submember is as thin as 0.5 m in the Aksu-Dere section (Fig. 2a) and thickens up to 4 m in the Kudrino-2 section, where it is represented by a sequence of more or less muddy marl interbeds with approximately equal thicknesses (~20 cm) containing occasional *Thalassinoides*.

Submember XVIb. Light gray and greenish muddy marls. The Aksu-Dere section (Fig. 2a) has a 5-cm-thick calcareous mudstone interbed, which resembles a "mudstone interbed" type sole mark (Baraboshkin et al., 2002) at the sole of this submember, and the lower 60 cm of the sequence are lithologically similar to the previous submember. The overlying part of the section is muddier and is poorly exposed. In thin sections, the rocks are foraminiferal packstone–wackestones with scarce fragments of the prismatic layer of inoceramid bivalve shells and occasional silt-size quartz and glauconite grains. The submember contains ichnofossils *Chondrites targionii* (Brongn.), *Ch. intricatus* (Brongn.) (Plate II, fig. 4), *Ch. patulus* Fisch.-Oost. (Plate II, fig. 5), *Palaeophycus tubularis* Hall (Plate II, figs. 8, 9), *Planolites* isp., *Palaeophycus* isp., and *Zoophycos* isp. In addition, the belemnites *Actinocamax* cf. *verus* Miller (Plate III, fig. 2) and *A. verus* Miller (Plate III, fig. 3) were encountered 0.3 and 1.2 m above the base, respectively (Baraboshkin and Fokin, 2019). The thickness of the submember in the Aksu-Dere section is 4.5 m.

In the Kudrino-2 section, the submember is represented by a sequence of alternating more or less muddy varieties of bioturbated marls (interbeds approximately 20 cm thick) with a bed of more calcareous rocks 70 cm thick, which contains limonitized *Pilichnus* isp. burrows, at the base. The overlying part of the sequence contains ichnofossil *Planolites* isp., *Chondrites* isp., *Zoophycos* isp., and scarce *Thalassinoides* isp. Microscopically, the rocks are similar to those in the Aksu-Dere section. The thickness of the submember in the Kudrino-2 section is 5.4–5.5 m.

Submember XVIc. Light gray and greenish marls, irregularly (the average interbed thickness is ~15 cm) alternating with more muddy marls and calcareous mudstones; limonitized pyrite concretions are present. Microscopically, the rocks are foraminiferal wackestones similar to those in the previous submember but with a larger proportion of micrite and without the fragments of the prismatic layer of inoceramid bivalve shells. Occasional fine silt-size quartz and glauconite grains are still present. This submember contains *Planolites* isp., *Palaeophycus* isp., *Chondrites targionii* (Brongn.) (Plate II, fig. 3), *Ch. intricatus* (Brongn.), *Ch.* isp., *Zoophycos* isp., scarce *Thalassinoides* isp., and complex *Thalassinoides-Chondrites* ichnofossils. The thickness of the submember is 4.4 m in the Aksu-Dere section and 6.7 m in the Kudrino-2 section.

Submember XVId. Light gray and greenish muddy marls (10–60 cm thick each) interbedded with more muddy varieties and calcareous mudstones (10–15 cm thick each). Interbed thicknesses slightly increase upward. Microscopically, the rocks are foraminiferal wackestones (Plate I, fig. g) with small, sometimes silicified foraminifers with a varying extent of preservation, dispersed spicules, and scarce fine silt-size quartz and glauconite grains. The submember contains scarce sponge remains, ichnofossils *Planolites* isp., *Chondrites* ispp., *Zoophycos* isp., and scarce *Thalassinoides* isp. Somewhat above these, *Zoophycos villae* Massalongo (Plate II, fig. 1), *Chondrites caespitosus* (Fisch.-Oost.) (Plate II, figs. 2, 6), *Palaeophycus tubularis* Hall (Plate II, fig. 7), and *Palaeophycus heberti* (de Saporta) (Plate II, fig. 14) were encountered at the base of the Kudrino-1 section, which upbuilds the Kudrino-2 section after an erosion interval of unknown thickness (presumably not thicker than 10–20 m). The thickness of the submember in the Aksu-Dere section is 6.3 m; its apparent thickness in the Kudrino-2 section is more than 7.5 m.

Member XVII. It constitutes cuesta slopes and has been studied only in the Aksu-Dere section, where it is poorly exposed. The member is composed of a sequence of alternating more or less muddy marls and calcareous mudstones, but alternation character is not distinct. Microscopically, the rocks are foraminiferal wackestones and mudstones (Plate I, fig. h) with disseminated small "globigerinids," sometimes silicified, and occasional fine silt-size quartz grains. Glauconite was not encountered in thin sections. *Zoophycos* isp. structures are present. The apparent thickness of the member is more than 8 m.

DEPOSITIONAL ENVIRONMENTS

Petrographic Characteristics

Rock microscopy data allow one to indicate three sediment accumulation stages in the studied interval of the section.

According to E. Flügel's model (Flügel, 2010), the Coniacian rocks of Member XI (Plate I, fig. a) correspond to the standard microfacies (SMF) 3: "Pelagic lime mudstone and wackestone with planktonic microfossils"; they characterize basinal facies or the outer shelf. Single quartz grains are fine silt-size (0.02–0.06 mm) and are presumably the results of eolian transport; occasional glauconite grains of a similar size have been encountered. Planktonic foraminifers are numerous, diversified, and well preserved; numerous calcispheres, single spherical radiolarians, and the fragments of the prismatic layer of inoceramid bivalve shells are found. The composition of limestones in Member XI is indicative of their formation in the environment of open outer shelf and calm water.

The limestones and muddy limestones of Member XV differ markedly from the underlying rocks of Member XI. Microscopically, these rocks are calcispheric–foraminiferal wackestones–packstones and microbreccias (Plate I, figs. b–e) with the remains of various predominantly poorly preserved foraminifers; abundant fragments of the crushed prismatic layer of inoceramid bivalve shells; echinoderm fragments; and comparatively abundant (a few percent) clastic impurity and glauconite, which peaks in Submember XVd. All bioclasts are destroyed to a various degree. This microfacies type also corresponds to SMF 3 (see above) and, partially, SMF 4: "Microbreccia, bio/lithoclastic packstone or rudstone" (Flügel, 2010), which is interpreted as talus, debris, and basinal facies. The "talus and debris" interpretation is unusual for the conventional understanding of the sedimentology of these deposits, but is not excluded completely, when one considers the substantial variations in thickness of Member XV in the Aksu-Dere section as compared with the Kudrino-2 section. However, the abrupt shallowing of the basin (Alekseev, 1989), which led to decrease in sedimentation rate and hardground and erosion surface formation breaks, observed in the Aksu-Dere section, seems more probable. To summarize, this was a shelf-type open-marine basin, although shallower than the Coniacian one.

The rocks of the upper part of the section (Members XVI–XVII) correspond to the same SMF 3 microfacies (Flügel, 2010), but they display a distinct trend: the foraminiferal packstones in the lower part of the section are succeeded upward first by muddy wackestones and then by mudstones. In addition, the comparatively rich foraminiferal assemblages in the lower part give way to the impoverished assemblages with predominantly *Globigerina*-type forms having smaller shells, some of which are silicified. Moreover, the bioclasts of the prismatic layer of the inoceramid bivalve shells gradually disappear upward; the glauconite grains decrease in number and size (and disappear altogether at the top), giving way to sponge spicules. The single fine silt-size quartz grains occur throughout the section, probably related to eolian processes. The signatures mentioned above indubitably indicate the deepening of the basin and the development of an outer shelf environment with muddy carbonate sedimentation.

Composition of the Insoluble Residue

The insoluble residue from the Santonian–Campanian boundary interval (from the top of Submember XV to the base of Submember XVIb) was studied in detail in the Aksu-Dere section. Samples for this purpose were collected additionally at an interval of 10 cm from 18 levels within a sequence 1.4 m thick and at an interval of several centimeters at the soles of submembers XVd and XVIb near disconformity planes (Fig. 3).

Aliquots of grab samples which had been dried and decontaminated were dissolved in 10% acetic acid solution; the residue was separated by elutriation into pelitic and granular fractions (i.e., into sand-size and silt-size grains of detrital and authigenic origin). After weighing accurate to 0.01 g, both fractions were studied by X-ray diffraction analysis at the Laboratory of Lithology and Facies Analysis of Moscow State University (MSU). The granular fraction was studied by bulk mineral analysis; pelitic fraction (<0.002 mm) was studied by the "texturized preparation" method, with imaging in three stages: air-dry sample, sample saturated with ethylene glycol, and sample after ignition. Imaging was performed with a Dron-3m X-ray diffractometer equipped with an X-ray tube with a Co anticathode; the operating current was 20 mA, and the operating voltage was 30 kV. The results are shown in Fig. 3.

The established homogeneity of the composition of the noncarbonate components of the studied rocks indicates the similarity in depositional environment between the late Santonian and early Campanian basins. The elevated concentrations of the terrigenous clastic and pelitic components (up to 4.75 and 18.75%, respectively) at the boundary between Submembers XVc and XVd mark a break of sediment accumulation. The amount of allogenic (clastic) components rapidly decreases up the section. The slow increase in pelitic material content in Submember XVIa can be due to the lagging of carbonate accumulation in the basin against the accelerated transgression. The deepening of the basin was accompanied by a certain deterioration of the gas conditions in bottom and entrapped (sludge) water, presumably expressed by the increase in marcasite content in the noncarbonate fraction of the rocks and the frequency of *Chondrites* in Submember XVIa.

Worthy of mention is the periodic occurrence of hornblende grains, most probably of pyroclastic ori-

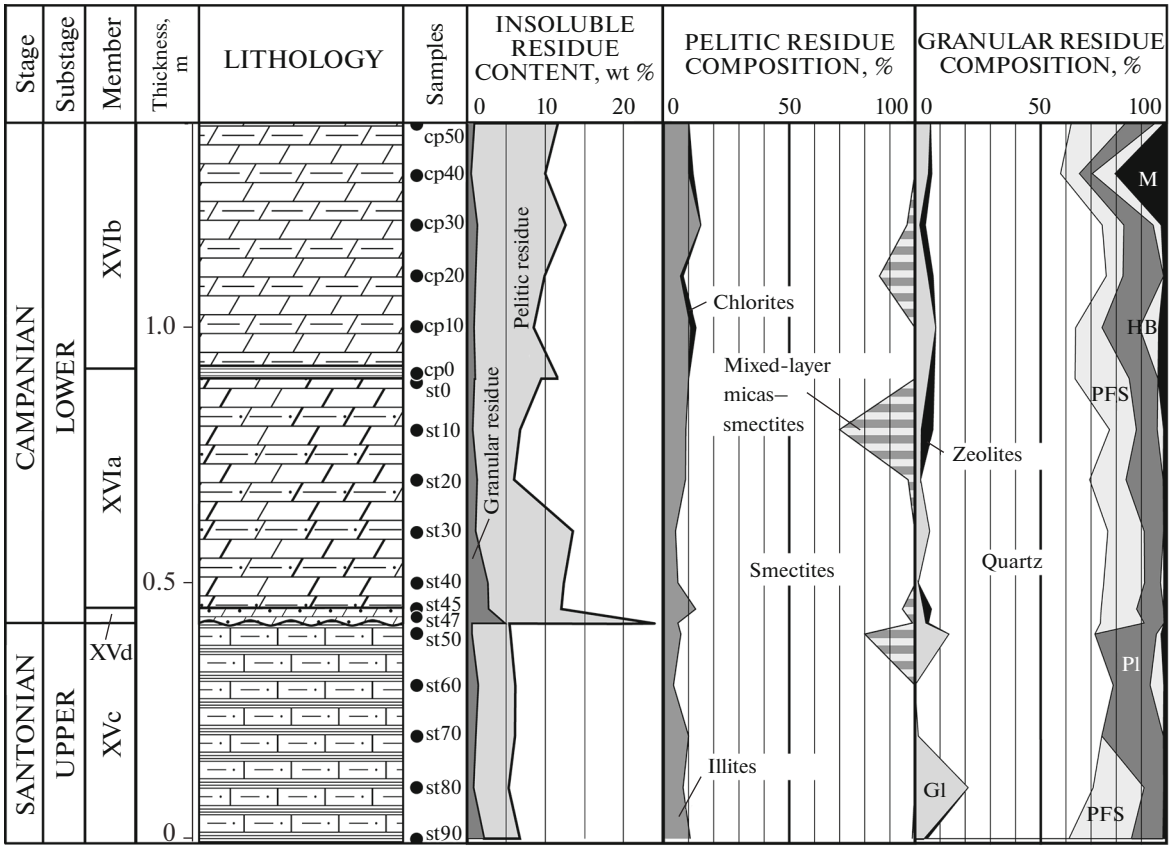

Fig. 3. Composition of the noncarbonate residue of the Santonian–Campanian boundary sediments in the Aksu-Dere section. Abbreviations: Gl, glauconite; PFS, potassium feldspar; M, marcasite; PL, plagioclases; HB, hornblende. See Fig. 1 for the rest of the legend.

gin, in the insoluble residue. The increase in its concentration and frequency in the lower Campanian sediments along with the basic–intermediate ash decomposition products such as zeolite and chlorite can be interpreted as a signature of increase in volcanic activity during the Campanian Age. The sources of fine pyroclastic material could have been the Eastern Pontide and Central Anatolian island arc belts, where volcanic activity was found to have peaked precisely during the Campanian (Okay and Nikishin, 2015). Some plagioclases are probably also of volcanic origin; therefore, the increase in the proportion of plagioclases at the top of the Santonian along with the simultaneous disappearance of potassium feldspar and the appearance of hornblende may indicate the increase in ash material supply into the basin.

In other respects the composition of the sand-size to silt-size fraction of the clastic material with a high quartz concentration and elevated potassium feldspar and plagioclase content is similar to the products of cratonic origin from an unknown source.

Ichnological Characteristics

The studied section is irregularly characterized by ichnofossils. Notwithstanding that all rocks have a high bioturbation index (Bi = 5), the ichnofossils proper are in most cases poorly preserved. Therefore, we additionally used the finds from the Kudrino-1 section in a small open-pit mine in the northwestern outskirts of the village of Kudrino, where a bentonite clay ("kil") layer, approximately corresponding to the upper part of Submember XVId–Member XVII (Guzhikov et al., 2020), is exposed, for a more complete characterization of the ichnofossil assemblage. Some information about the ichnoassemblages from the studied sections is given in (Baraboshkin, 2020).

Two different ichnofossil assemblages have been recognized in the section. The lower ichnofossil assemblage corresponds to Members XI and XV. It is dominated by the living chambers of the crustacean *Thalassinoides suevicus* (Reith) and less frequent *T. paradoxica* (Woodward). These burrows are characteristic of the *Cruziana*, *Skolithos*, and *Glossifungites* ichnofacies (Knaust, 2017). They are also found in deeper water ichnofacies, but are much scarcer. In many Crimean sections, such burrows are associated with the development of hardground surfaces, associated with a short break in sedimentation. Traces of vital activities characteristic of deeper marine environments, including *Planolites beverleyensis* (Bil.), *Taenidium crassum* Broml., Ekd., Richt. (Plate II, fig. 13), *Palaeophycus*

isp., and *Zoophycos* isp., reappear only at the very top of Submember XVc.

The upper ichnofossil assemblage occurs in members XVI–XVII. It is characterized by widespread sediment eating structures *Palaeophycus tubularis* Hall (Plate II, fig. 7), *P. heberti* (de Saporta) (Plate II, fig. 14), *P.* isp., *Planolites* isp., *Teichichnus rectus* Seilacher, *Palaeophycus tubularis* Hall (Plate II, figs. 8, 9), *Zoophycos villae* Massalongo (Plate II, fig. 1), and *Z.* isp., as well as farming structures *Chondrites caespitosus* (Fisch.-Oost.) (Plate II, figs. 2, 6), *Chondrites targionii* (Brongn.), *Ch. intricatus* (Brongn.) (Plate II, fig. 4), *Ch. patulus* Fisch.-Oost. (Plate II, fig. 5), *C.* isp., and *Pilichnus* isp., although the scarce *Thalassinoides suevicus* burrows are still present. The most numerous here are the representatives of the ichnogenus *Chondrites*. This is due not only to the fact that their makers (wormlike organisms) could have existed in reduced-oxygen environments but also mostly to the fact that they occupied the lowermost bioturbation level. This means that their burrows moved upward and reworked the burrows of all preexisting bioturbators in the course of sediment accumulation. This ichnofossil assemblage is characteristic of the deeper water distal *Cruiziana* ichnofacies and the *Zoophycos* ichnofacies and indicates the deepening of the basin and a change of the character of the substrate.

In summary of the analyzed data on the vertical distribution of ichnofossils, Members XI–XV can be ascribed to the *Cruziana* ichnofacies, and Members XVI–XVII can be ascribed to the deeper water *Zoophycos* ichnofacies. This agrees with other data, such as the upward decrease in the amount of silt-size clasts and shell detritus, decrease in size and impoverishment of foraminifer assemblages, and appearance of sponge spicules and silicification, reflecting the trend of basin deepening and increase in sedimentation rate during the first half of the Campanian Age.

Therefore, the obtained data confirm the existing idea (Alekseev, 1989) of the depositional environment during the Santonian–Campanian time and detail it to a certain extent. By the end of the Coniacian and during the Santonian Age, the present-day territory of Southwestern Crimea was occupied by a fairly deep marginal sea with normal marine conditions. During the late Santonian, it underwent certain shallowing, which led to a decrease in sedimentation rate and occasional sedimentation breaks, including the hardground breaks, and enrichment in terrigenous material and authigenic glauconite concentration. From the beginning of the Campanian, the basin underwent rapid deepening, an increase in sedimentation rate, and a tendency to acquire the outer (deeper) shelf environment. In addition, the background mudstone–carbonate sedimentation in the basin was supplemented by ash material supply from the south. It should be noted that the relatively dissected topography of the basin, enabling rapid changes in section thickness and completeness during the Coniacian–Santonian time, gave way to its topographic leveling during the Campanian. This was probably caused by a decrease in tectonic activity in the region and the opening of the Black Sea basin.

BIOSTRATIGRAPHIC CHARACTERISTICS

Cephalopods

Macrofossils in the Santonian–Campanian boundary interval are quite rare, and the finds of cephalopods (the primary orthostratigraphic group of the Late Mesozoic invertebrates) are few. The ammonoids *Pachydiscus* sp. were reported from the study area (Jolkichev and Naidin, 1999), and *Nowakites* (?) *savini* (de Grossouvre) and *Eupachydiscus* cf. *sayni* (de Grossouvre) were found in the Belbek River basin (Klikushin, 1985). These ammonoids are not depicted, and the correctness of their identification cannot be confirmed. The ammonoid *Eupachydiscus* sp. (Fokin et al., 2018) reported from Submember XVc of the Aksu-Dere section, which was redetermined as *Parapuzosia (Parapuzosia)* cf. *leptophylla* (Sharpe) (Baraboshkin and Fokin, 2019; see Plate III, fig. 1), confirms the Santonian age of the submember.

The belemnite *Actinocamax quasiverus* Naidin and *Gonioteuthis* sp. (Alekseev, 1989; Alekseev et al., 2005, p. 86) were reported from Member XVI at the base of the Campanian. A photo of the rostrum of a Coniacian–early Campanian belemnite *Gonioteuthis* sp. indet. is given in (Iolkichev and Naidin, 1999, Fig. 5, figs. 7, 8). A drawing of *Actinocamax verus verus* Miller from the Bakhchysarai district in the Crimean Mountains is given, without specifying the exact location, in (Naidin, 1964, Fig. 5, fig. 9), and photographs of the rostra of *Actinocamax verus* are given in (Naidin, 1959, Plate XIX, figs. 11, 12). However, a later publication (Jolkichev and Naidin, 1999) does not contain even a reference to the presence of this species in the lower Campanian, and the belemnites from the lower Campanian deposits depicted in this paper (Jolkichev and Naidin, 1999, Fig. 5, figs. 9, 10) are ascribed to *Actinocamax quasiverus* Naidin, 1953, first described on the basis of a single rostrum (Naidin, 1953).

Baraboshkin and Fokin (2019) figured and described the finds of the belemnite *Actinocamax* cf. *verus* Miller from the outcrop 30 cm above the base of Member XVIb (Plate III, fig. 2) and *A. verus* Miller (Plate III, fig. 3) found in the talus at the level of Member XVI of the Aksu-Dere section. *A. verus* is widespread in the Santonian–lower Campanian of Western Europe and the Turonian (?)–lower Campanian of the Russian Platform and Crimea and is indicated from the Santonian sediments on the eastern slope of the Northern Urals (Baraboshkin and Fokin, 2019). These finds cannot refine the position of the Santonian–Campanian boundary but do help us to confirm the presence of this species in Crimea and

raise the issue of the relationship between the species *A. verus* and *A. quasiverus*. In addition, the occurrence of *Actinocamax verus* in the sequences of Northern Europe and at higher latitudes (Baraboshkin and Fokin, 2019) suggests the inflow of relatively cool waters from the North European to the Crimean basin at the boundary between the Santonian and Campanian ages. Probably this was among the factors responsible for the numerous sedimentation breaks in the Santonian–Campanian boundary interval of the Aksu-Dere section.

To summarize, the cephalopod finds from the studied sections confirm the Santonian age of Submember XVc but are insufficient for confirming the position of the Santonian–Campanian boundary.

Echinoderms

Fossil echinoderms, the stemless crinoids of the order Uintacrinida (genera *Marsupites* and *Uintacrinus*), in particular, are also of paramount stratigraphic importance for the characterization of the Santonian–Campanian boundary sediments. These two genera are widespread virtually worldwide. The wide geographic and narrow stratigraphic distribution, well-defined morphological features, and the easy identification of these genera enabled their use in global chronostratigraphy. The first occurrence of the index species *Uintacrinus socialis* is proposed as the marker of the lower boundary of the upper Santonian. The last occurrence (LO) of the index species *Marsupites testudinarius* is recommended as the main criterion for the Santonian–Campanian boundary (Gale et al., 2008; Hampton et al., 2007; Hancock et al., 1996; Ogg and Hinnov, 2012; Schulz et al., 1984; etc.).

The paleobiogeographic distribution of *Marsupites* and *Uintacrinus* encompasses the boreal paleolatitudes in the Northern Hemisphere (between 20° and 50° N) and the austral latitudes in the Southern Hemisphere (between 25° and 50° S) (Gale et al., 2008; Mitchell, 2009). The species *Uintacrinus socialis* is encountered in all sections at the base of Beds with *Uintacrinus* and *Marsupites*, whereas only *Marsupites* is found in their upper parts. The second species of the genus *Uintacrinus—U. anglicus* Rasmussen, 1961—was initially established at the top of the *Marsupites* Beds in the sections of Southern England. Later, the same succession of crinoid zones (Marsupites testudinarius–Uintacrinus anglicus) was also reported in other regions: Yorkshire, Mangyshlak, Texas, and Western Australia (Hancock et al., 1996; Mitchell, 1994).

The species composition of the genus *Marsupites* is a matter of discussion. According to one version, it is restricted to the type species *M. testudinarius*. The rest of the species, in turn, are its morphological variations. This is substantiated by the joint occurrence of various morphotypes in the same bed. Nevertheless, Klikushin (1985) demonstrated the chronological consistency and uniqueness of a number of forms at the subspecies level on the basis of the data on sections in Southwestern Crimea. For instance, forms with large plates having a protuberance in the central part (*M. testudinarius laevigatus* (Forbes, 1850)) are found in the lower part of Beds with *Marsupites*; specimens with large plates with a pronounced sculpture of radial series of tubercles (*M. testudinarius testudinarius* (Schlotheim, 1820)) are found in the middle part of the beds; and small plates with a central protrusion and radial acuminate ridges (*M. testudinarius ornatus* (Miller, 1821)) were reported in the uppermost part. A similar succession of the sculptural morphotypes of *Marsupites* was reported in the sections in England, Germany, and Mangyshlak. The data on the Waxahachie Dam Spillway section in North Texas (Gale et al., 2008) demonstrated the presence of two morphological and stratigraphic *Marsupites* populations, *M. laevigatus* and *M. testudinarius*. In addition, sporadic plates of a new morphotype—*M. testudinarius* forma *granulatus*—were encountered in the upper part of the M. testudinarius Zone. To summarize, we may presently speak about four successive crinoid zones for the Santonian–Campanian interval: Uintacrinus socialis–Marsupites laevigatus–Marsupites testudinarius–Uintacrinus anglicus. However, the U. socialis and M. laevigatus zones may slightly overlap each other in a number of sections in Crimea, Mangyshlak, Turkmenistan, England, Germany, and Western Australia.

Marsupites finds in the Aksu-Dere section in the Bodrak River valley were reported at the uppermost Santonian in Member XVc (slightly muddy foraminiferal packstones) of the Kudrino Formation. The thickness of the member is around 4 m, which is thinner than in the similar sections in the Belbek River valley, where the thickness of the layer with *Uintacrinus* and *Marsupites* varies in the range of 10–25 m (Klikushin, 1981). The specimens originate from several levels. We have two cups and separate plates from the Aksu-Dere section (collected by students of the Faculty of Geology of Moscow State University and by G.V. Mirantsev) at our disposal. The relatively smooth *M. laevigatus* with indistinct sculpture (Plate III, figs. 4, 5) and the ornamented *M. testudinarius* (Plate III, fig. 6), characteristic of the terminal part of the upper Santonian, were found. In addition, *M. testudinarius* is represented by several morphotypes with different sculpture on the plates. One more *Marsupites testudinarius testudinarius* cup from the middle part of the Beds with *Marsupites* in the Aksu-Dere section (collected by Naidin (1956)) was earlier depicted in Klikushin (1985).

The cups and separate plates of the crinoids *Marsupites* and *Uintacrinus* from Crimea were repeatedly mentioned and depicted in the literature earlier many times, mostly by Klikushin (1980, 1981, 1985), in detailed descriptions of the Santonian–Campanian boundary sections in the southeastern part of the Belbek River valley. Giving the paleofaunistic characterization of

the *Marsupites* Beds in these sections, Klikushin (1981) reconstructed them as a sponge–inoceramid paleocenosis and noted the scarcity of the fauna.

On the basis of the currently available finds, two crinoid zones have been substantiated in the Aksu-Dere section, Marsupites laevigatus and Marsupites testudinarius. The latter species is more important, because its last occurrence is recommended as the main criterion for establishing the base of the Campanian Stage. From this point of view, the Santonian–Campanian boundary passes between Members XVc and XVd, because the last occurrence of *M. testuidinarius* is marked in the upper part of Member XVc. The species *U. socialis* and *U. anglicus*, which characterize the base of the upper Santonian and the lower Campanian, respectively, have not been found in the studied sections so far. Probably this is due to the comparative scarcity of the genus *Uintacrinus* and its mostly fragmentary preservation as isolated plates.

Palynology

The chemical treatment of palynological samples was performed according to the procedure adopted by the Laboratory of Paleofloristics of the Geological Institute, Russian Academy of Sciences (GIN RAS) (Aleksandrova et al., 2012). Nine samples from the Kudrino-2 outcrop section (o.p. 3184) and 27 samples from the Aksu-Dere outcrop section (o.p. 3168) were studied (Figs. 4, 5). Of them, 20 samples contained palynomorphs of satisfactory or poor preservation. The recognized palynological associations are represented by numerous dinocysts and, at some levels, together with pollen and spores, prasinophytes, and taxa of unknown systematics.

The recognized dinocyst assemblages were compared with the zonal assemblages of the Upper Cretaceous sections in England (Pearce, 2010; Pearce et al., 2020; Prince et al., 1999, 2008). Dinocyst assemblages of Western Siberia (Lebedeva, 2006), Greenland (Nøhr-Hansen, 1996; Nøhr-Hansen et al., 2019), the Norwegian and Barents seas (Radmacher et al., 2014, 2015), and Belgium (Slimani, 2001) either significantly differ from a systematic point of view or are established in the sections with the hiatus corresponding to the Santonian–Campanian boundary; this is why their direct comparison with those of southwestern Crimea is impossible.

Changes in the composition of dinocyst associations allowed recognizing one dinocyst assemblage in the Kudrino-2 section (DK) and three in the Aksu-Dere section (DAD). The assemblages were recognized on the basis of the presence/first occurrence of stratigraphically important taxa and/or according to certain quantitative characteristics of palynomorph association. The stratigraphic distribution of palynomorphs is shown in Figs. 4 and 5. The images of the most typical species are given in Plates IV, V, and VI. For the interpretation of possible paleoenvironments, dinoflagellate cysts were arranged into 11 groups: (1) *Canningia* and *Senoniasphaera*; (2) *Chatangiella* and *Isabelidinium*; (3) *Surculosphaeridium*; (4) *Spiniferites*; (5) *Dinogymnium*; (6) *Acanthaulax wilsonii*; (7) *Palaeohystrichophora infusorioides*; (8) *Odontochitina*; (9) *Trithyrodinium*; (10) other gonyaulacoids; (11) green algae. Plant pollen and spores were included in group (12).

Dinocyst assemblage with *Senoniasphaera macroreticulata–Surculosphaeridium longifurcatum* (DK-1) (Kudrino-2 section, o.p. 3184, Submembers XVIa–XVIc, Samples 20–35). Quantitatively and taxonomically, the dinocyst association at the base of Submember XVIa (Sample 20) is extremely poor. The species recognized here *Senoniasphaera protrusa* Clarke et Verdier, *Senoniasphaera macroreticulata* Prince et al., *Canningia glomerata* sensu Fensome et al., 2019, *C. colliveri* Cookson et Eisenack, *C. senonica* Clarke et Verdier, and *Dinogymnium denticulatum* (Alberti) Evitt et al., ex gr. *Cassidium fragile* (Harris) Drugg are represented by scarce (often single) poorly preserved specimens.

Higher in the section dinocyst diversity and abundance increase (Figs. 4, 5). Thus, *Spiniferites* spp. are predominant; *Chatangiella* (*Chatangiella* sp., *Ch.* "*spinosa*" sensu H. Nøhr-Hansen, *Ch.* cf. *manumii* (Vozzhennikova) Lentin et Williams), *Surculosphaeridium longifurcatum* (Firtion) Davey et al., and *Canningia glomerata* are numerous. Species *Isabelidinium microarmum* (McIntyre) Lentin et Williams, *Acanthaulax wilsonii* Yun Hyesu, *Surculosphaeridium* sp., *Exochosphaeridium* sp., *Ex. phragmites* Davey et al., *Ex. bifidum* (Clarke et Verdier) Clarke et al., *Hystrichosphaeropsis obscura* Habib, *Apteodinium deflandrei* (Clarke et Verdier) Lucas-Clark, cf. *Riculacysta pala* Kirsch, *Subtilisphaera pontis-mariae* (Deflandre) Lentin et Williams, *Trithyrodinium evittii* Drugg, *Culversphaera velata* (Clarke et Verdier) Prince et al., *Trimuridinium whitenessense* (Prince et al.) Fensome et al., *Palaeohystrichophora infusorioides* Deflandre, and *Dinogymnium* spp. occur constantly.

The interval of the dinocyst assemblage DK-1 demonstrates fluctuations in dominance of different species (Fig. 6). For instance, *Surculosphaeridium longifurcatum*, *Spiniferites* spp., *Canningia glomerata*, and *Isabelidinium microarmum* dominate in the middle of Submember XVIa (Sample 25). At the base of Submember XVIc (Sample 30) *Isabelidinium microarmum* decreases abruptly, whereas the quantity of *Chatangiella* spp. and *Acantaulax wilsonii* increases. Abundant *Palaeohystrichophora infusorioides* and frequent *Subtilisphaera pontis-mariae* are recognized in the upper part of this submember (Sample 35), whereas *Chatangiella* spp. and *Acantaulax wilsonii* here are few.

On the basis of the simultaneous occurrence of species *Senoniasphaera macroreticulata*, *S. protrusa*, *T. whitenessense*, *Raetiaedinium truncigerum* (Deflandre) Kirsch, *Whitecliffia spinosa* (Clarke et Verdier) Pearce,

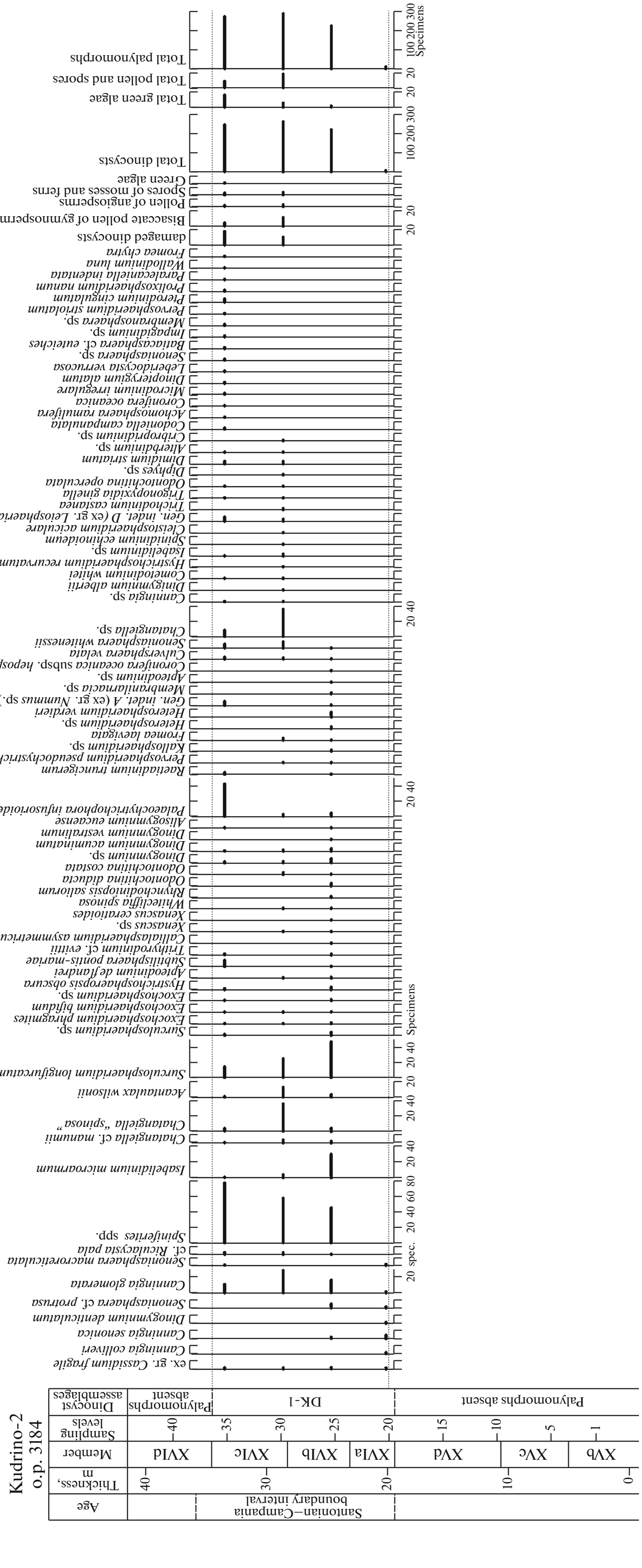

Fig. 4. Distribution of palynomorphs in the Kudrino-2 section.

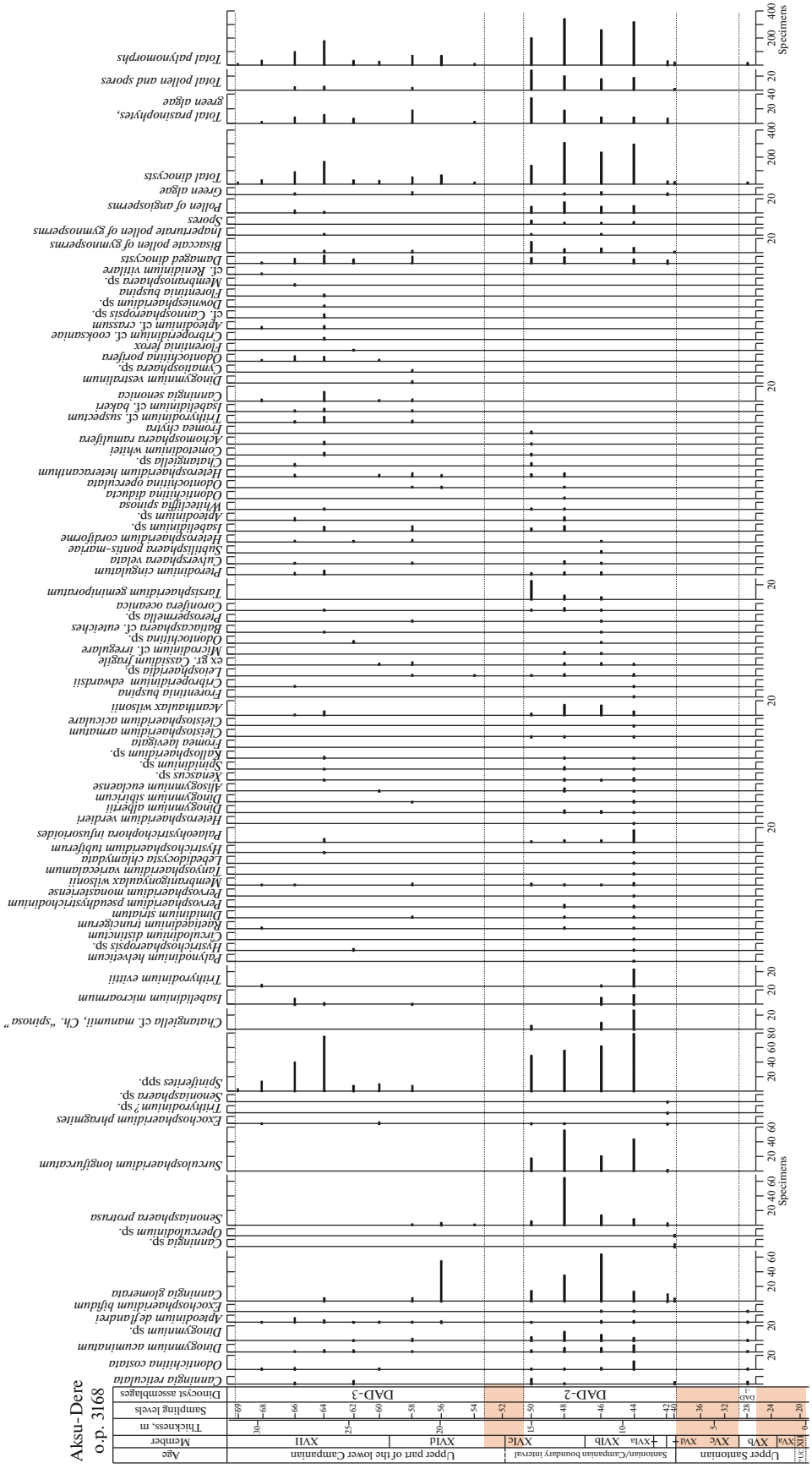

Fig. 5. Distribution of palynomorphs in the Aksu-Dere section.

and *Surculosphaeridium? Longifurcatum*, as well as the presence of abundant *Chatangiella*, the dinocyst assemblage-1 is comparable with one from the Newhaven Chalk Formation of the White Island and the Margate Chalk Formation (Pearce et al., 2020; Prince et al., 1999, 2008), corresponding to the Marsupites testudinarius–Offaster pilula zones of the Santonian–Campanian boundary interval (Fig. 7).

According to the data from the Santonian–Campanian sediments in England, the first occurrence of *Trimuridinium whitenessense* is established in the upper Santonian Uintacrinus socialis Zone of the White Ness section in Eastern Kent (Prince et al., 2008), whereas a similar event in the Trunch borehole section is recorded from a higher stratigraphic level—the lower Campanian Offaster pillula Zone (Pearce et al., 2020). Species *Senoniasphaera macroreticulata* was described and recognized only from the upper Santonian–lowermost Campanian Uintacrinus socialis Zone of the White Ness section and Marsupites–Uintacrinus anglicus zones of the Foreness Point section. This allows us to restrict the upper boundary of our dinocyst assemblage-1 to the lowermost Campanian.

The frequent occurrence of Boreal peridinioid genera *Isabelidinium* and *Chatangiella* in the interval from the middle of Submember XVIa to the base of Submember XVIc along with the general low diversity of dinocysts indicates the development of relatively cold-water and highly productive depositional environments.

Dinocyst assemblage DAD-1 (o.p. 3168, Aksu-Dere, Member XVb, Sample 28). Dinocyst associations are extremely poor in terms of abundance and species diversity (Fig. 5). Only single specimens of *Canningia reticulata* Cookson et Eisenack, *Odontochitina costata* Alberti, *Dinogymnium acuminatum* Evitt et al., *Dinogymnium* sp., *Apteodinium deflandrei*, and *Exochosphaeridium bifidum* are recognized here. All these taxa are largely distributed through the Late Cretaceous, which disables any conclusions on the precise stratigraphic age of sediments.

Dinocyst assemblage with *Cannigia glomerata–Surculosphaeridium longifurcatum* (DAD-2) (o.p. 3168, Aksu-Dere, Submembers XVIa–XVIc, Samples 40–50). Samples 40 and 42 contain only few not diversified dinocysts (14 and 20 specimens, respectively) (Fig. 5). This interval is represented by *Canningia* sp., *C. glomerata* sensu Fensome et al., 2019, *Senoniasphaera* sp., *S. protrusa*, *Surculosphaeridium longifurcatum*, *Exochosphaeridium phragmites*, *Operculodinium* sp., and *Trithyrodinium*? sp. Dinocyst diversity and abundance increase higher in the sequence, from Sample 44. Predominant taxa are *Canningia glomerata*, *Senoniasphaera protrusa*, *Surculosphaeridium longifurcatum*, *Spiniferites* spp., *Acanthaulax wilsonii*, and *Chatangiella* spp. Species *Odontochitina costata*, *Dinogymnium acuminatum*, *Dinogymnium* sp., *Apteodinium deflandrei*, *Exochosphaeridium bifidum*, *Membranigonyaulax wilsonii* Slimani, and *Palaeohystrichophora infusorioides* are constantly present. Starting from Sample 46, *Coronifera oceanica* Cookson et Eisenack, *Pterodinium cingulatum* (Wetzel) Below, and prasinophytes *Tarsisphaeridium geminiporatum* W. Riegel are present, while from Sample 48 species *Whitecliffia spinosa* and *Odontochitina diducta* Pearce occur; other dinocyst taxa are distributed irregularly. The palynological assemblage is characterized by the constant relatively frequent presence of pollen grains (from 5.5 to 13% of the total assemblage) (Fig. 6).

The interval of DAD-2 demonstrates changes in the content of dominant species. Thus, Sample 44 is characterized by the dominance of *Spiniferites* spp. and *Surculosphaeridium longifurcatum* and by the common occurrence of *Chatangiella*, *Isabelidinium*, *Trythirodinium*, *Dinogymnium* spp., and *Palaeochystrichophora infusorioides*. Higher in the section (Samples 46–50) the numbers of *Canningia glomerata* and *Senoniasphaera protrusa* increase significantly (up to 30%); *Spiniferites* spp. and *Surculosphaeridium longifurcatum* are frequent, and the other taxa occur in an insignificant amount.

Dinocyst assemblage DAD-2 is close to the assemblage DK-1 from the Kudrino-2 section, but differs by the absence of *Senoniasphaera macroreticulata*, *Trimuridinium whitenessense*, *Canningia colliveri*, and *C. senonica* and the generally large number of Areoligeraceae (*Senoniasphaera* and *Canningia*) (Fig. 6). It should be noted that the dinocyst assemblage DAD-2 is taxonomically similar to the one from the Member 2–basal Member 3 of the Alan-Kyr section (Guzhikov et al., 2019).

Dinocyst assemblage DK-1 from the Kudrino-2 section is dated to the terminal Santonian to early Campanian. According to the available data on the eustatic changes, this time interval is characterized by the consecutive frontal development of a major marine transgression ("*Marsupites* transgression") and the positive isotope excursion event SCBE (Santonian–Campanian Boundary Event; Haq et al., 1987; Jarvis et al., 2002, 2006; Jenkyns et al., 1994; McArthur et al., 1992, 1993; etc.). The high-resolution chemostratigraphic data for the upper Cretaceous sections in England suggest that the inception of the CIE-SCBE is dated to the late Santonian (the middle of *Marsupites* Zone), while its termination corresponds to the base of the Campanian, below the first occurrence of *Offaster pilula* (Jarvis et al., 2002, 2006).

The abundance of Areoligeraceae in the dinocyst assemblage DAD-2 indicates the deposition of sediments in shallow-water environments with a high hydrodynamics during the transgressive phase of the basin evolution. Moreover, the high numbers of *Spiniferites* and *Surculosphaeridium* indicate the maximum flooding surface (mfs) conditions (Prauss, 2001), while the pollen abundance suggests a significant sediment supply from the adjacent land. In general, the decrease in the abundance of *Chatangiella* and *Isabelidinium* up

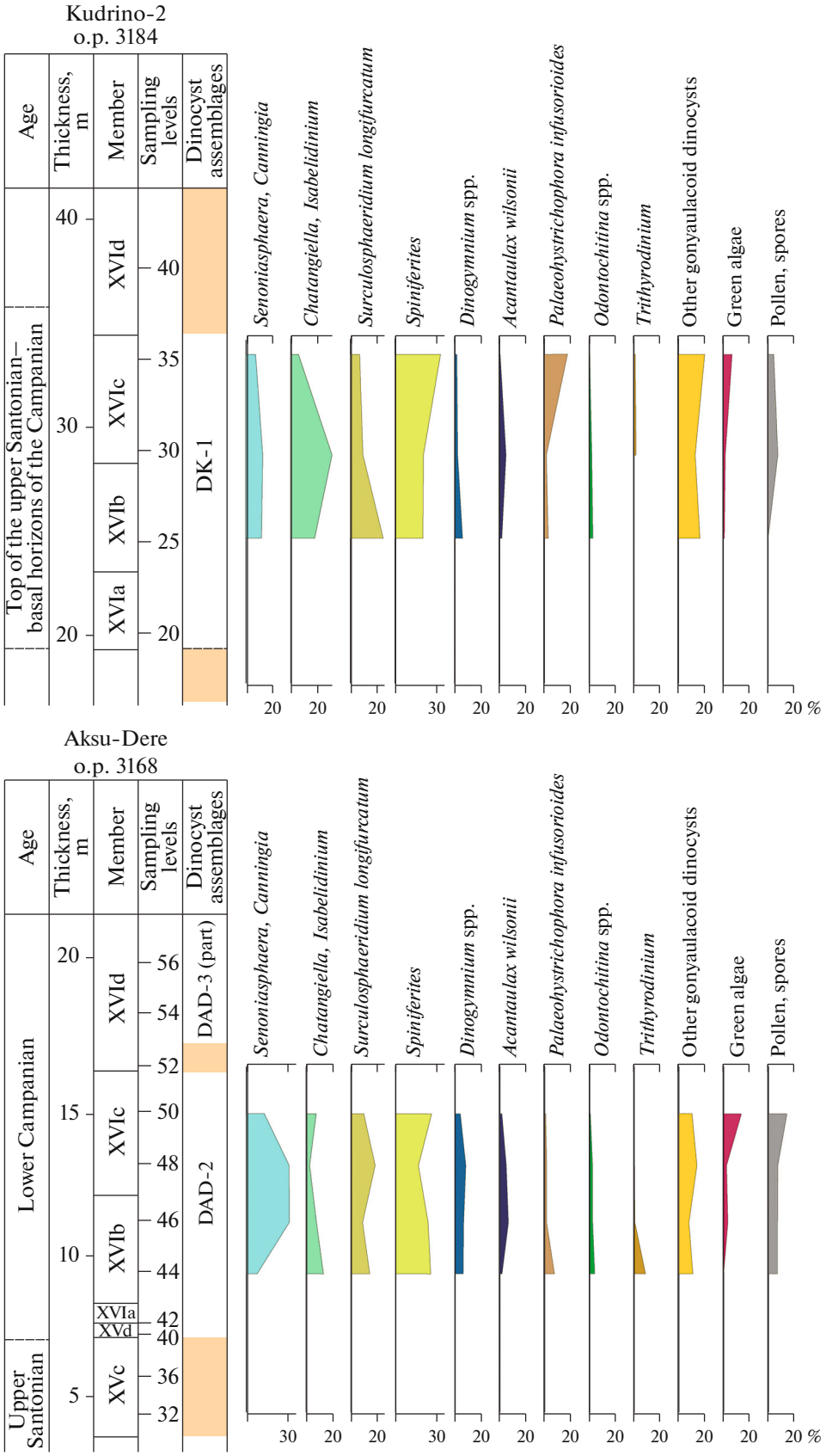

Fig. 6. Proportions of various palynomorph groups in DK-1 assemblage from the Kudrino-2 section and DAD-2 assemblage from the Aksu-Dere section.

the section indicates the gradual water warming during the accumulation of Submembers XVa–XVIa. These data suggests that the DAD-2 assemblage is stratigraphically younger than the dinocyst assemblage DK-1 from the Kudrino-2 section.

Dinocyst assemblage with *Odontochitina porifera* (DAD-3) (o.p. 3168, Aksu-Dere, Submember XVId–Member XVII, Samples 54–69). This interval is characterized by an extreme scarcity of dinocysts; in the most part of this interval of the section, all taxa occur in small amounts (mostly singly) and sporadically, except *Spiniferites* spp. (Fig. 5). Pollen grains and spores are also sporadically present.

Most dinocyst taxa from the dinocyst assemblage DAD-2 are present here. Additionally, *Odontochitina porifera*, *Dinogymnium vestralinum*, *Florentinia ferox*, *Cribroperidinium* cf. *cooksaniae*, *Apteodinium* sp., *Apteodinium* cf. *crassum*, cf. *Cannosphaeropsis* sp., *Downiesphaeridium* sp., and *Membranosphaera* sp. are recognized for the first time in this section. On the other hand, species *Surculosphaeridium longifurcatum*, *Chatangiella* cf. *manumii*, *Ch. "spinosa,"* and *Exochosphaeridium bifidum*, present in the DAD-2, are not encountered. The last occurrences of *Senoniasphaera protrusa*, *Dimidinium striatum*, *Pervosphaeridium pseudhystrichodinium*, and *P. monasteriense* are noted in Sample 58.

The present list of dinocyst species does not make it possible to judge the exact age of sediments in this part of the Aksu-Dere section. In British sections, many of these taxa disappear within the interval of the Offaster pilula Zone; in addition, the first single occurrence of *Odontochitina porifera* is known from the middle of the Coniacian, and its common occurrences are known from the upper Santonian, from the Uintacrinus socialis Zone interval (Pearce et al., 2020; Prince et al., 1999, 2008) (Fig. 7). The absence of *Surculosphaeridium longifurcatum* in the DAD-3 assemblage indicates that the lower boundary of this assemblage is not older than the middle part of the Offaster pilula Zone. The last occurrences of *R. truncigerum* and *S. protrusa* at the top of the Offaster pilula Zone, considered to be synchronous in England, occur at different levels of the Aksu-Dere section: the last *S. protrusa* was encountered at the top of Member XVI and the last *R. truncigerum* was found in Member XVII, almost at the top of the section.

The co-occurrence of *O. porifera* and *Ap. deflandrei* in the sections of Helvetic and Ultra-Helvetic nappes in Germany is established within the dinocyst Zone 4 Areoligera coronata, encompassing the larger part of the Campanian from the middle of the Globotruncanita elevata Zone to the Radotruncana calcarata Zone of planktonic foraminifers (Kirsch, 1991). The occurrence of these taxa in Austrian and Hungarian sections is recognized in the lower Campanian dinocyst Apeodinium deflandrei Subzone of the Odontochitina operculata Zone, corresponding to the nannoplankton CC18 (B. parca)–CC19 (C. ovalis) (first half) zones (Siegl-Farkas and Wagreich, 1996; Siegl-Farkas, 1997). The first occurrence of *O. porifera* in the Polar Ural zones is noted at the base of the lower Campanian Beds with *Chatangiella niiga* (Lebedeva, 2005, 2006). On the basis of the presence of the index species, this part of the section may be also correlated with the dinocyst Beds with *Odontochitina porifera* of the Pudovkino Formation from the Lower Volga region, characterized by the benthic foraminifera *Cibicidoides temirensis/Bolivinoides decoratus* Zone (LC13), and with the radiolarian Beds with *Prunobrachium crassum–Archaeospongoprunum salumi* of early Campanian age (Aleksandrova et al., 2012).

Taking into account all data mentioned above as well as the position of the interval with the DAD-3 assemblage in the section, we suggest the early Campanian age of Members XVI and XVII (Fig. 7).

The dinocyst assemblages recognized in Crimea are generally close to the late Santonian–early Campanian assemblages from England. On the basis of the occurrence of dinocyst index species in the studied sections, the dinocyst assemblage DK-1 from the Kudrino-2 section is stratigraphically older than the dinocyst assemblage DAD-2, and taking into account significant content of Boreal genera, it probably corresponds to the Santonian–Campanian boundary interval and the SCBE. The DAD-2 assemblage in the Aksu-Dere section characterizes relatively warm shallow-water paleoenvironments. The taxonomically poor DAD-3 assemblage, recognized in the upper part of the Aksu-Dere section, is questionably dated to the early Campanian.

The problem of the exact correlation between the DK-1 and DAD-2 assemblages, as well as their relationships to the one from the Alan-Kyr section, remains unresolved: all of them are recognized in different sections, and their continuous succession was not observed.

Nannoplankton

Nine samples from the Kudrino-2 section and 21 samples from the Aksu-Dere section were analyzed. All of them contain nannoplankton. Samples were prepared according to the standard procedure (Bown and Young, 1998) and studied under a BiOptik200 polarizing microscope under parallel and crossed nicols with a magnification of ×1000. Photographs were shot using a Canon EOS 550D digital camera with a Canon camera adapter. In order to estimate the relative numbers of certain species, counting was performed in 100 fields of vision at a run within an arbitrarily selected slide area. Species diversity was estimated within the entire sample on the slide with an area of 24 × 24 mm. Nannofossil preservation varies from bad (significant dissolution and recrystallization) to moderate (secondary alteration is insignificant). In spite of

the poor preservation, all nannofossils proved to be identifiable to the species level.

The Upper Cretaceous calcareous nannoplankton from the Aksu-Dere section was studied for the first time by S.I. Shumenko (Shumenko and Stetsenko, 1978), who recognized zonal assemblages. In 2016, its study was continued by E.A. Shcherbinina (Shcherbinina and Gavrilov, 2016). Since then, many new data on the taxonomic diversity and the stratigraphic and lateral distribution of zonal markers have been accumulated. This enables the correlation of remote sections and adjustment of the boundaries of the recognized zones. At present, the biostratigraphic chart of the Upper Cretaceous by nannoplankton developed by Burnett (1998) is the most suitable for the solution of these problems, although the chart developed by Sissingh (1977) for the sediments of this age has not lost its significance and agrees well with the chart by Burnett (1998).

Sixty-eight nannoplankton species were identified in the Kudrino-2 and Aksu-Dere sections. Most of them represent the genera *Broinsonia*, *Prediscosphaera*, *Zeugrhabdotus*, and *Watznaueria*.

The calcareous nannoplankton assemblage of the **Kudrino-2 section** is relatively poor in terms of species diversity: only 46 species were identified (Fig. 8). The **lower Campanian UC13 and UC14a zones** were recognized here conventionally. The former zone was established from the first occurrence of *Arkhangelskiella cymbiformis* Vekshina; the second, from the first occurrence of *Broinsonia parca parca* (Stradner) Bukry (Burnett, 1998). However, because the second species was identified only in one sample and as a single specimen, the boundary between the zones within Submember XVd was drawn provisionally (Fig. 8).

The nannoplankton assemblage identified **in the Aksu-Dere section** is more diversified in terms of species and has individual specific features (Fig. 9, Plate VII). Four zones have been recognized in this section (Fig. 9). Although the Coniacian Stage is not discussed in this paper, it should be noted that samples from Member XI contain *Lucianorhabdus cayeuxii* Deflandre. This taxon appears at the base of **Subzone UC11c of the upper Coniacian** (Burnett, 1998), which contradicts the age of this member determined by foraminifers, inoceramids, and other macrofauna (Alekseev, 1989; Kopaevich and Walaszczyk, 1990; Naidin et al., 1981). **Zone UC12 of the upper Santonian** is devoid of the species which are unique to it (Burnett, 1998), and its boundary with the overlying **Zone UC13 of the lower Campanian** is identified by the first occurrence of *Arkhangelskiella cymbiformis*, which we encountered at the top of Submember XVb (Fig. 9, Plate VII). **Zone UC14 of the lower Campanian** is represented by two subzones, **UC14a**, the base of which was established in the middle of Submember XVc in view of the first occurrence of *Broinsonia parca parca*, and **UC14b**, the base of which was established in the lower part of Member XVII in view of the first occurrence of *Broinsonia parca constrica* Hattner et al. (Burnett, 1998) (Fig. 9, Plate VII). The recognized zones and nannofossil assemblages correlate well with coeval zones of the upper Santonian–lower Campanian in the Southern Carpathians (Melinte-Dobrinescu, 2018), Northern Limestone Alps (Wolfgring et al., 2018), Southern England, and Southern Poland (Dubicka et al., 2017). At the same time, correlation with the Alan-Kyr section in Central Crimea is complicated by the poor nannoplankton preservation in the latter (Kopaevich et al., 2020; Ovechkina et al., 2021).

A specific feature of the nannoplankton assemblages of the Aksu-Dere section is that the index species of the zones occur as single specimens rather than in large quantities (Fig. 9). However, this is also characteristic of the West European sections (Dubicka et al., 2017; Melinte-Dobrinescu, 2018; Wolfgring et al., 2018). They also contain the species atypical of the lower Campanian as single specimens. For instance, the existence of *Zeugrhabdotus scutula* (Bergen) Rutledge et Bown is limited to the Hauterivian–Santonian, but apparently it is also sporadically found in the Campanian (Mikrotax.org). It has been identified in four samples from the Aksu-Dere section and in one sample from the Kudrino-2 section (Fig. 8) in the amount of 1–2 specimens (Fig. 9, Plate VII). This suggests that this taxon was redeposited or that it has a wider stratigraphic range. Also interesting is the stratigraphic distribution of *Reinhardtites levis* Prins et Sissingh in Sissingh. Its first occurrence in Burnett's biostratigraphic chart corresponds to the base of the UC14d Zone (Burnett, 1998). But the first occurrence of this taxon has been reported in the lower Campanian Zone UC14a in the section of borehole 763 on the Exmouth Plateau, NW shelf of Australia, and at the base of Subzone UC14a in the section of borehole 1138 on the Kerguelen Plateau (Russo, 2012–2013). Its earlier appearance was also established in the Alan-Kyr section (Kopaevich et al., 2020; Ovechkina et al., 2021).

The late Turonian–Maastrichtian interval of the Late Cretaceous is considered as the time of global cooling and the reduced amount of nutrients in surface waters (Linnert et al., 2014, 2018), which could not but have affected the taxonomic composition of nannoplankton. Nevertheless, the analysis of changes in the relative abundance of nannofossils in the Aksu-Dere section suggests that the periods of increase in temperature took place as well. For instance, the increase in abundance of *Watznaueria barnesiae* (Black in Black et Barnes) Perch-Nielsen, *Calculites obscurus* (Deflandre) Prins et Sissingh in Sissingh, and *Lucianorhabdus cayeuxii* (Fig. 9) may indicate the increase in the temperature of a shallow basin where they dwelled (Sanjary et al., 2019). In the Aksu-Dere section, a substantial increase in the abundance of *W. barnesiae* (more than 50 specimens/100 fields of vision) was encountered at many levels of the section, starting from Submember XVc upward (Samples 32,

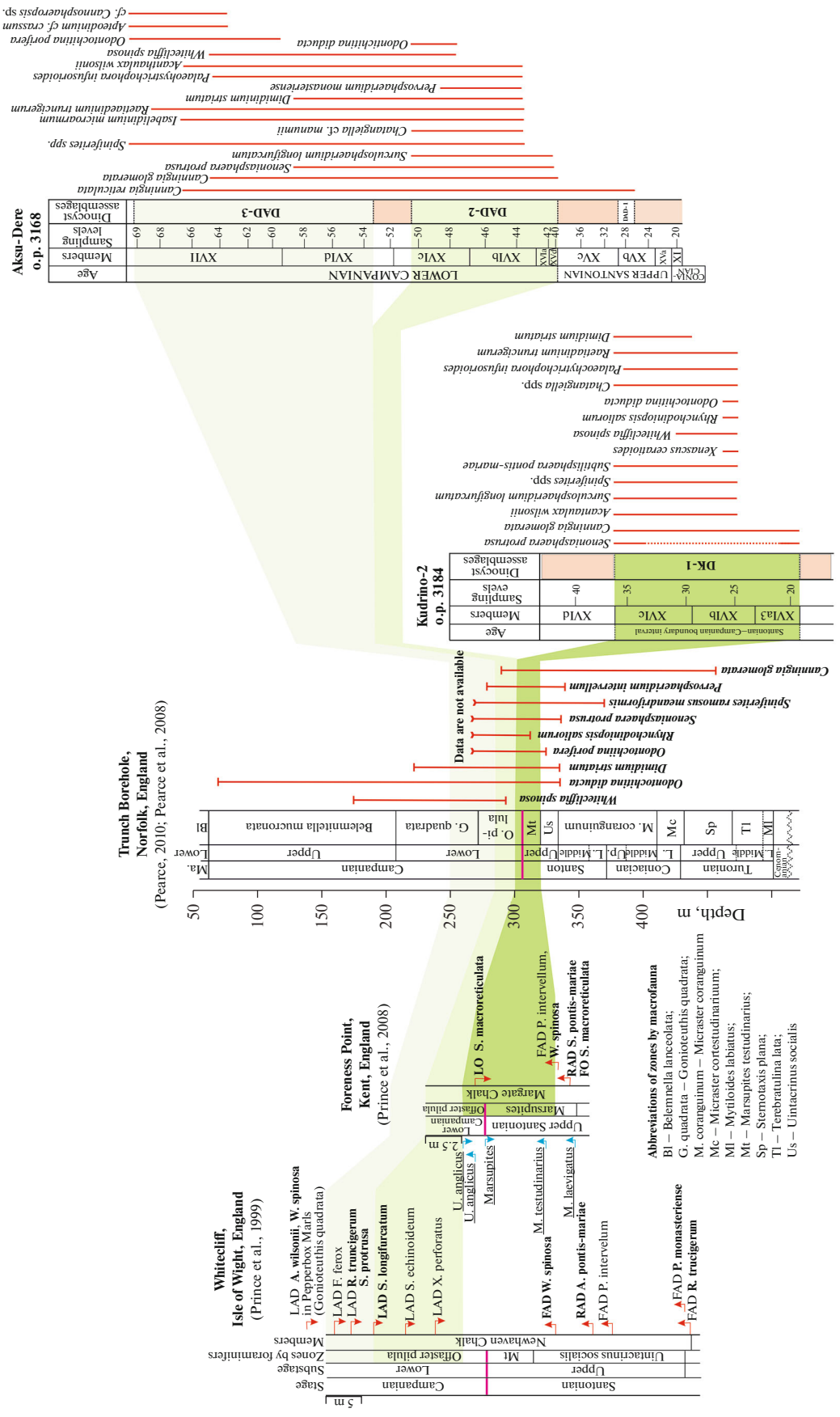

Fig. 7. Correlation of the Kudrino-2 and Aksu-Dere sections with sections in England.

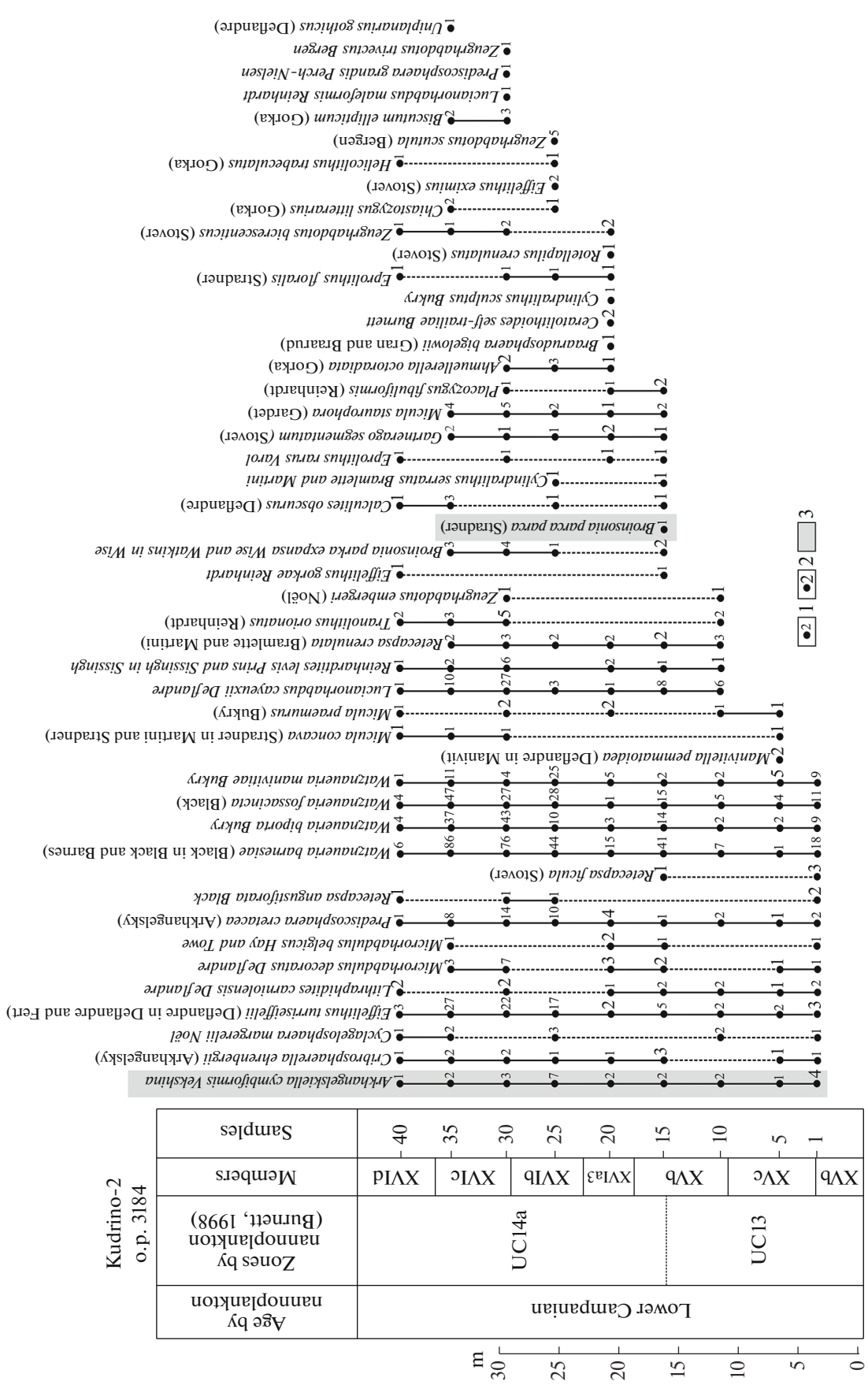

Fig. 8. Nannoplankton distribution in the Kudrino-2 section. (1) Number of specimens per 100 fields of vision at a run; (2) total number of specimens within the slide; (3) the occurrence of zonal index species in the sequence.

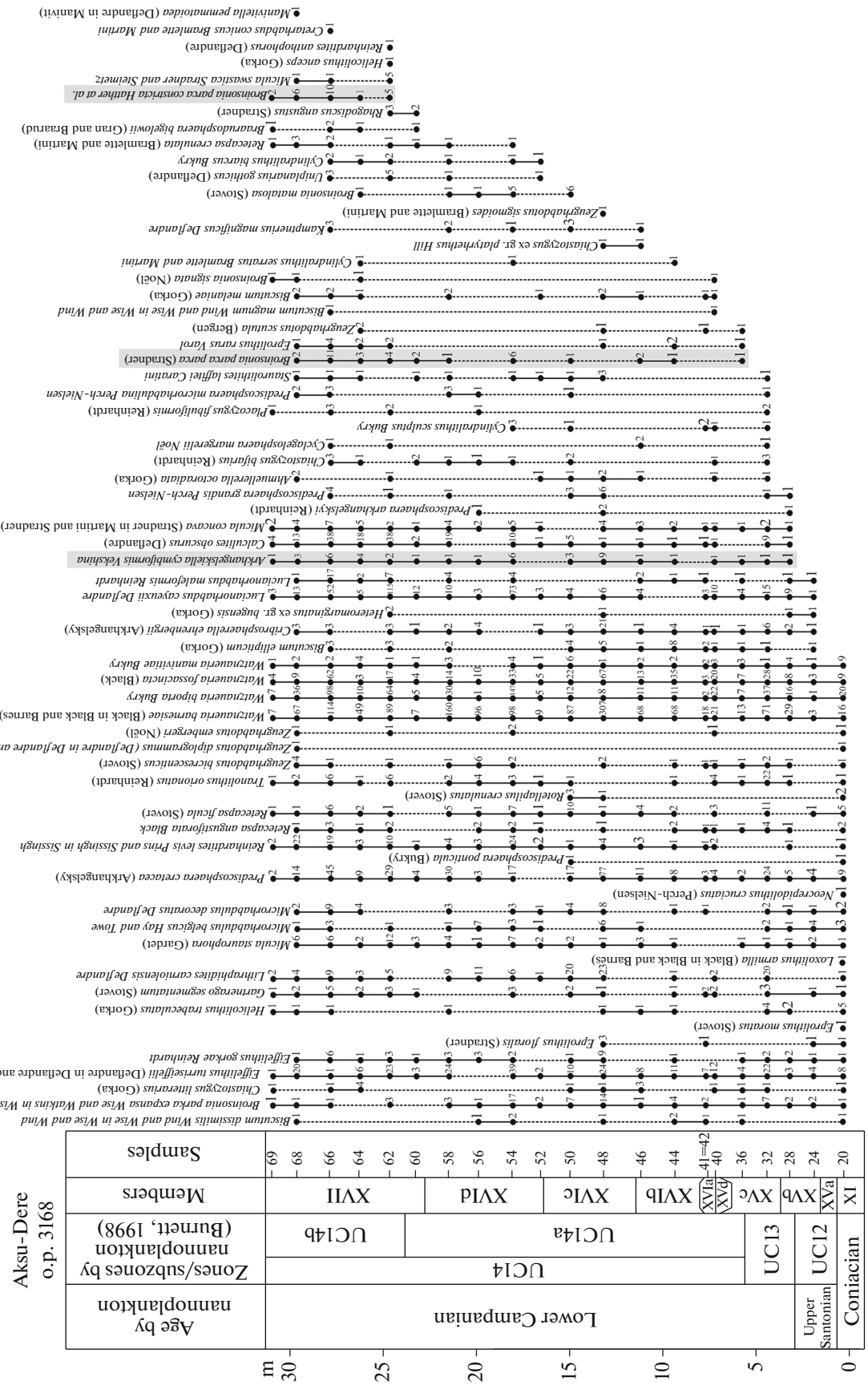

Fig. 9. Nannoplankton distribution in the Aksu-Dere section. See Fig. 8 for the legend.

44–50, 54–58, 62, and 66–68) (Fig. 9). An abrupt increase in the abundances of the two other species were reported only at the very top of the section: *C. obscurus* (more than 30 specimens/100 fields of vision) was established in Member XVII (Samples 62, 66); *Lucianorhabdus cayeuxii* (more than 50 specimens/100 fields of vision) was established in Submember XVId (Sample 54) and Member XVII (Samples 62 and 66).

A significant increase in the abundance of *W. barnesiae* in the Kudrino-2 section was reported only in Submember XVIc (Samples 30–35), where it is accompanied by the increase in the abundance of *L. cayeuxii* (up to 10–27 specimens/100 fields of vision), whereas *C. obscurus* occurs as single specimens (Fig. 8).

Benthic Foraminifers

Benthic foraminifer (BF) assemblages from the Santonian–Campanian interval of the Aksu-Dere section were studied on samples collected from 28 levels. In order to extract foraminifer tests, the method of soaking rocks with a saturated solution of Glauber's salt was applied, but the result was unsatisfactory, so the powder was treated additionally with glacial acetic acid, which provided the required effect. The <0.2 mm size fraction of the obtained material was examined under an MC-2 ZOOM stereoscopic microscope. A coarser fraction was not obtained for technical reasons.

Nine samples were collected from the Kudrino-2 section for the studies of BF assemblages. They were treated using the procedure with soaking in glacial acetic acid and subsequent washing over a sieve with 0.1 mm mesh. The dried powder was divided into <0.4 and >0.4 mm fractions, which afterwards were studied under the MC-2 ZOOM microscope.

Detailed images of single specimens, which provided a clearer understanding of foraminifer test morphology, were obtained at the Laboratory of Diagnostics of Nanomaterials and Structures of Saratov State University using a Tescan MIRA 2 LMU autoemission scanning electron microscope.

On the basis of the results of the studies of BF assemblages, biostratigraphic units in the rank of beds were identified. The comparison of the earlier microfaunistic data on the Santonian–Campanian in Crimea (Beniamovsky and Kopaevich, 2016; Bragina et al., 2016; Maslakova, 1959) with zones by BF established in other regions (Beniamovsky, 2008a, 2008b; Hart et al., 1989; Koch, 1977; Vishnevskaya et al., 2018; Walaszczyk et al., 2016) revealed a number of "stratigraphic collisions" (Beniamovsky and Kopaevich, 2016), e.g., the occurrence of *Pseudovalvulineria clementiana clementiana* (d'Orbigny), the zonal species of the Campanian in the East European Craton, in the Santonian sediments with *Marsupites testudinarius*. Similar cases analyzed in detail by Beniamovsky and Kopaevich (2016) proved the prematurity of the optimistic conclusion that the Beds with BF in the Santonian–Campanian of Central Crimea "correlate easily with the charts proposed for the European paleobiogeographic region" (Bragina et al., 2016).

Aksu-Dere section. BF assemblages in this section were established in all samples. Approximately 40 species were identified, including index species that determine the age of host rocks (Plate VIII). The following units in the rank of beds were recognized in the section (Fig. 10): Beds with *Pseudovalvulineria stelligera/Stensioeina gracilis/St. perfecta* (upper Santonian); Beds with *Bolivinoides strigillatus/B. culverensis/Pseudovalvulineria* ex gr. *thalmanni* (Santonian–Campanian transitional interval); Beds with *Pseudogavelinella clementiana clementiana* (Santonian–Campanian transitional interval); and Beds with *Bolivinoides granulatus* (lower Campanian).

Beds with *Pseudovalvulineria stelligera/Stensioeina gracilis/S. perfecta* (BFAD-4) were recognized in the interval of Samples 25–37 (Submembers XVb, XVc) by the presence of index species and a significant number of the representatives of the genus *Osangularia*, which enables their correlation with the Pseudovalvulineria stelligera (LC10a) Subzone of the upper Santonian of Beniamovsky's chart (Beniamovsky, 2008b). The assemblage is characterized by good preservation and, in addition to the index BF, includes the agglutinating *Spiroplectammina rosula* (Ehrenberg), *Arenobulimina presli* (Reuss), and *Heterostomella carinata* Franke, as well as the secreting *Cibicidoides eriksdalensis* (Brotzen), *Gavelinella pertusa* (Marsson), *Eponides concinnus* Brotzen, *Osangularia whitei* (Brotzen), *Eouvigerina aculeata* (Ehrenberg), and *Quadrimorphina* sp. *Eouvigerina* sp., *Fursenkoina* cf. *polonica* (Gawor-Biedowa), *Loxostomum eleyi* (Cushman), and *Sitella gracilis* (Cushman) appear in the upper part of the beds (Sample 30 and higher). *S. gracilis* is characteristic of the upper Santonian, which is mentioned by Beniamovsky in the study of the Alan-Kyr section (Beniamovsky and Kopaevich, 2016). The level of the first occurrence (as a single species) of the species *Bolivinoides strigillatus* (Chapman), which is the index species of the upper Santonian zone of the same name in a number of regional charts (Beniamovsky, 2008a, 2008b; Hart et al., 1989; Vishnevskaya et al., 2018; Walaszczyk et al., 2016), was established in Sample 35.

Beds with *Bolivinoides strigillatus/Bolivinoides culverensis/Pseudovalvulineria* ex gr. *thalmanni* (BFAD-5) were recognized by the first occurrence of *B. culverensis* (Barr) and the constant joint occurrence of index species at the level of Submembers XVd, XVIa, and XVIb (interval of Samples 40–46). The assemblage is replenished by the secreting *Stensioeina pommerana* Brotzen, *Gavelinella costulata* Marie, *Valvulineria lenticula* Reuss, *V. laevis* Brotzen, *Reussella kelleri* (Vassilenko), and *Sitella laevis* (Beissel). Scarce *Neoflabellina* cf. *suturalis praecursor* (Wedekind) and the first occurrence of the scarce representatives of the genus

Quadrimorphina were noted in the upper part of the beds (Sample 44).

The first occurrence of *Pseudovalvulineria* ex gr. *thalmanni* (Brotzen) is also noted in the Submember XVd of the Kudrino-2 section, where this species is characterized by a similar interval of occurrence; in this connection, a decision was taken to include this form in the name of the beds as an index species. It differs from the typical "*thalmanni*" by the absence of distinct tubercles on the dorsal side, probably due to specific paleoecology.

The B. culverensis Zone, recognized by the joint occurrence of *strigillatus* and *culverensis*, was established for the lower Campanian of the zonal scheme for Cis-Carpathian Poland (Walaszczyk et al., 2016). The first occurrence of *B. culverensis* (Barr) was also mentioned at the base of the lower Campanian within the territory of Southern England (Bailey et al., 2009), Poland, and Western Ukraine (Dubicka and Peryt, 2016). In Crimea, the level of the joint occurrence of these species, according to the conclusion of Beniamovsky and Kopaevich (2016), corresponds to the upper Santonian. On this basis, the BFAD-5 Beds were dated to the Santonian–Campanian transitional interval. The first occurrence of *Stensioeina pommerana* Brotzen—the upper Santonian–lower Campanian representative of the genus *Stensioeina*—does not contradict these conclusions but confirms the similarity between the BF assemblages of the Aksu-Dere and Kudrino-2 sections at the level of Sample 40.

Beds with *Pseudogavelinella clementiana clementiana* (BFAD-6). The lower boundary of the beds is drawn on the basis of the occurrence of the index species and disappearance of *Bolivinoides strigillatus*. The assemblage is established in the interval of Samples 46–60 (Submembers XVIb–XVId) and is characterized by good preservation. In terms of species composition, it is similar with the assemblage in underlying sediments. The last occurrence of *B. culverensis* (Barr), *Stensioeina exculpta* (Reuss), and *Valvulineria laevis* Brotzen was noted in the lower part of the beds. *Neoflabellina asema* Koch (successor of *Neoflabellina suturalis praecursor*), the occurrence of which was noted in the upper Santonian (sporadic)–lower Campanian (constant) of Northwestern Germany (Koch, 1977), appears for the first time within the beds (Sample 49). *Cibicidoides eriksdalensis* Brotzen, *Pseudovalvulineria* ex gr. *thalmanni* (Brotzen), *Eouvigerina* sp., and *Loxostomum eleyi* (Cushman) disappear at the top of the beds.

In terms of the composition of BF associations, the BFAD-6 Beds correspond to the lower Campanian LC12 Zone of Beniamovsky chart (Beniamovsky, 2008b). The species *Pseudogavelinella clementiana clementiana* is the marker of the lower Campanian within the East European Craton (Olfer'ev and Alekseev, 2005), but in Crimea, it was established in sediments with crinoid *Marsupites testudinarius* Schlotheim, considered as the index species of the upper Santonian (Beniamovsky and Kopaevich, 2016; Maslakova, 1959). Therefore, the BFAD-6 Beds are also dated as late Santonian–early Campanian.

Beds with *Bolivinoides granulatus* (BFAD-7) were recognized within Member XVII (interval of Samples 61–69) by the first occurrence of the index species. The assemblage consists of well preserved tests, but its composition is slightly impoverished by the disappearance of a number of species and replenished by the appearance of index species. The occurrence of *Bolivinoides* cf. *laevigatus* (Marie), a descendant of the lower Campanian form *Bolivinoides granulatus* (Hofker), was noted at the level of Sample 66. At the base of the beds, there are numerous *Stensioeina gracilis* Brotzen, the number of which decreases markedly toward the top.

On the basis of the occurrence of *Bolivinoides granulates*, BFAD-7 Beds correlate with the lower Campanian Bolivinoides granulatus/Stensioeina gracilis Zone of the chart for the Carpathian Foredeep (Walaszczyk et al., 2016).

Kudrino-2 section. Foraminifers were established in all nine samples. The assemblages are well preserved and display significant species diversity: about 38 species including index species, which define the age of host rocks, were identified (Plate IX).

The Kudrino-2 section was subdivided into the following units in the rank of beds (Fig. 11): Beds with *Pseudovalvulineria stelligera/Stensioeina gracilis/St. perfecta* (upper Santonian); Beds with *Heterostomella praefoveolata* (top of the upper Santonian); Beds with *Bolivinoides strigillatus/B. culverensis/Pseudovalvulineria* ex gr. *thalmanni* (Santonian–Campanian boundary interval); and Beds with *Pseudogavelinella clementiana clementiana* (Santonian–Campanian boundary interval).

Beds with *Pseudovalvulineria stelligera/Stensioeina gracilis/Stensioeina perfecta* (BFK-1) were established in the interval of Samples 1–5 (Submembers XVb, XVc); they are similar in the identified assemblage to the BFAD-4 Beds (upper Santonian) recognized in the Aksu-Dere section and described above.

Plate IV. Palynomorphs from the Kudrino-2 and Aksu-Dere sections. All figures are at the same magnification. (1) *Canningia colliveri* Cookson et Eisenack, Kudrino-2, Sample 20; (2, 3, 5) *Senoniasphaera macroreticulata* Prince et al., Kudrino-2, Sample 20; (4, 7) *Isabelidinium microarmum* (McIntyre) Lentin et Williams: (4) Aksu-Dere, Sample 44; (7) Kudrino-2, Sample 25; (6) *Odontochitina porifera* Cookson, Aksu-Dere, Sample 62; (8) *Surculosphaeridium longifurcatum* (Firtion) Davey et al., Kudrino-2, Sample 25; (9) *Acanthaulax wilsonii* Yun Hyesu, Kudrino-2, Sample 25; (10) *Dinogymnium acuminatum* Evitt et al., Kudrino-2, Sample 25; (11) *D. denticulatum* (Alberti) Evitt et al., Kudrino-2, Sample 20; (12) *Heterosphaeridium verdieri* Yun Hyesu, Kudrino-2, Sample 25.

Plate IV

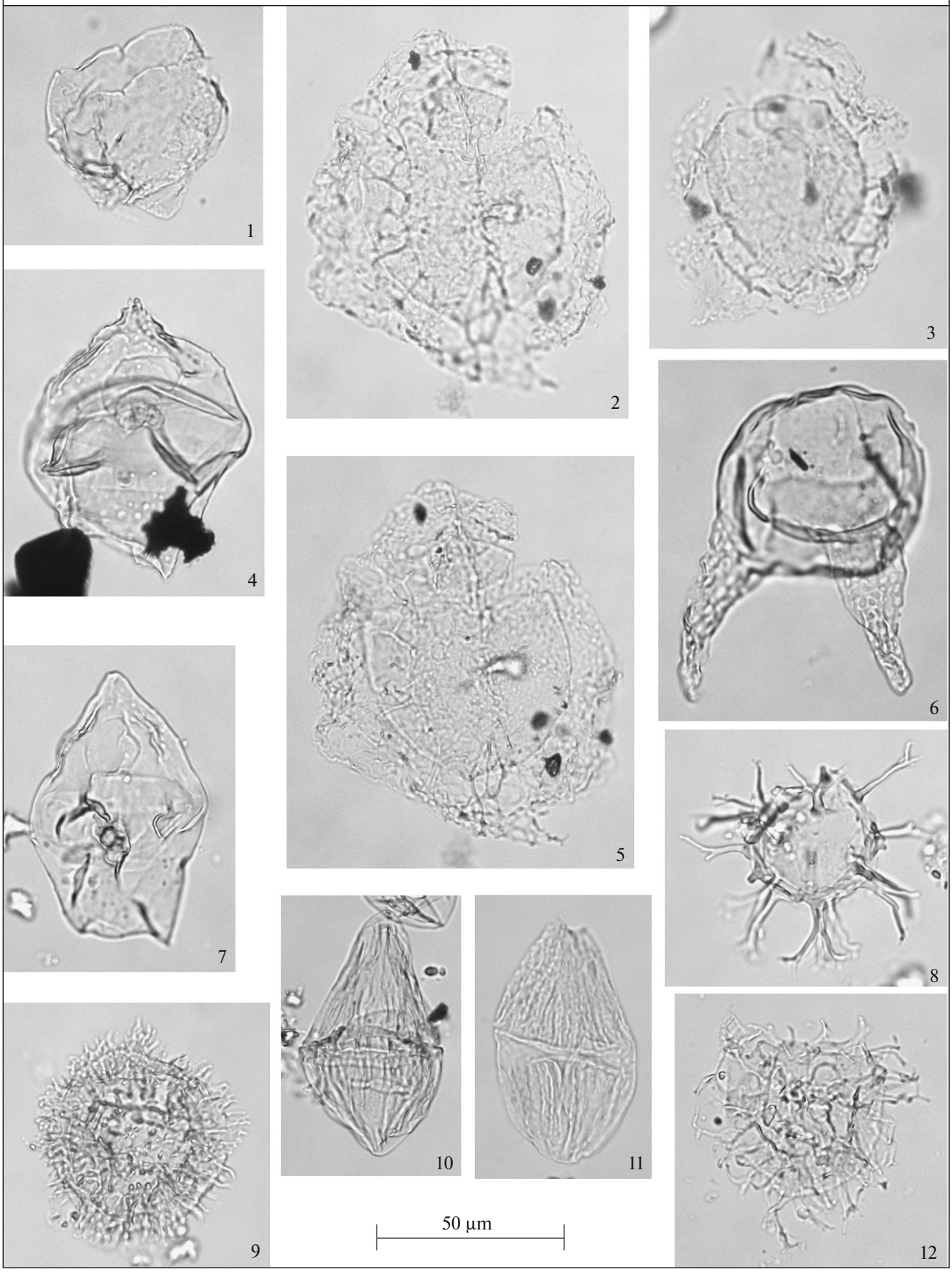

Beds with *Heterostomella praefoveolata* (BFK-2) were distinguished by the first occurrence of the index species in the lower part of Submember XVd at the level of Sample 10. The assemblage is replenished by the agglutinating *Ataxophragmium crassum* (d'Orbigny) and secreting *Neoflabellina* sp., *Globorotalites mischelianius* (d'Orbigny), *Eouvigerina* sp., *Fursenkoina* cf. *polonica* (Gawor-Biedowa), and *Sitella gracilis* (Cushman). The first occurrence of *Stensioeina* forms transitional from "perfecta" to "pommerana" was noted. The lower boundary of BFK-2 was drawn provisionally along the base of Submember XVd.

According to the chart developed by Beniamovsky (2008b), *Heterostomella praefoveolata* (Mjatluk) is characteristic of the communities of the upper Santonian Stensioeina pommerana (LC11) Zone. The typical *S. pommerana* in the Kudrino-2 section appears above the level of the first finds of *H. praefoveolata*; therefore, the age of the BFK-2 Beds can be defined as late Santonian.

Beds with *Bolivinoides strigillatus/B. culverensis/Pseudovalvulineria* ex gr. *thalmanni* (BFK-3) were recognized in Sample 15 (upper part of Member XVd) by the joint occurrence of the index species and a notable replenishment of the assemblage by the agglutinating *Marssonella* sp., *Gaudryina laevigata* Franke, *Arenobulimina minutissima* Gawor-Biedowa, and *Heterostomella* ex gr. *carinata* and the secreting *Ammodiscus cretacea* (Reuss), *Neoflabellina* cf. *suturalis praecursor* (Wedekind), *Pseudogavelinella clementiana clementiana* (d'Orbigny), *Stensioeina pommerana* Brotzen, *Gavelinella pertusa* Marsson, *Valvulineria lenticula* (Reuss), *Sitella gracilis* (Cushman), *Eouvigerina aculeata* (Ehrenberg), *Loxostomum eleyi* (Cushman), and *Praebulimina reussi* (Morrow). The upper boundary of BFK-3 is provisionally drawn along the top of Submember XVd.

BFK-3 Beds correlate with BFAD-5 Beds in Aksu-Dere and are also dated to the Santonian–Campanian boundary interval.

Beds with *Pseudogavelinella clementiana clementiana* (BFK-4) were recognized by the presence of the index species, absence of *Bolivinoides strigillatus* (Chapman) in the lower part of the beds, and the presence of a specific assemblage identified in Samples 20–40 (Member XVI). Foraminifer tests are characterized by good preservation. In terms of species composition, the assemblage is similar to the BF assemblage from the underlying sediments. The presence of *Angulogavelinella grodnoensis* (Akimetz), characteristic of the lower Campanian in Poland (Gawor-Biedowa, 1992), was noted at the base of the beds (Samples 20–25). *Pseudovalvulineria* ex gr. *thalmanni* disappear in the lower part of the beds. The epibole (acmezone) of *Heterostomella praefoveolata* (Mjatluk) and the first occurrences of *Neoflabellina* cf. *asema* Koch, 1977 and *Cibicides beaumontianus* (d'Orbigny) were noted within the beds (Sample 25). *B. culverensis* (Barr) and *Neoflabellina suturalis suturalis* (Cushman)—the species characteristic of both the late Santonian and the early Campanian—are present in the upper part of the beds. Considering the similarity between the BFK-4 and BFAD-6 assemblages, the age of the beds is also characterized as transitional late Santonian–early Campanian.

Planktonic Foraminifers

The technical treatment of samples for the studies of the tests of planktonic foraminifers (PF) was performed by P.A. Proshina at the Laboratory of Micropaleontology of GIN RAS (Moscow) and I.P. Ryabov at the Laboratory of Stratigraphy and Paleontology of the Lower Volga Scientific Research Institute of Geology and Geophysics (LVSRIGG), Saratov. At GIN RAS, the samples were treated using the method of soaking with sodium hyposulfite (thiosulfate) followed by treatment in an ultrasonic bath, and at LVSRIGG, the samples were treated according to the standard procedure using glacial acetic acid. PF were photographed on a TESCAN2300 scanning electron microscope at the Paleontological Institute of the Russian Academy of Sciences (Moscow) and on a JEOL JSM-6480LV electron microscope at the Chair of Petrology of the Faculty of Geology of Moscow State University (Moscow). PF test images are given in Plates X and XI. The PF distribution is shown in Fig. 12 for the Kudrino-2 section and in Fig. 13 for the Aksu-Dere section.

PF from the upper Santonian–lower Campanian interval of the Kudrino-2 (in 9 samples) and Aksu-Dere (in 24 samples) sections were studied. Twenty-two PF species of ten genera were identified. Tests of PF in the Aksu-Dere display moderate, rarely poor preservation and not evenly distributed along the section. PF tests in the Kudrino-2 section are well preserved, and PF assemblages are taxonomically diversified. The most representative PF assemblage in the Aksu-Dere section occurs in the lower part of the sec-

Plate V. Palynomorphs from the Kudrino-2 and Aksu-Dere sections. All figures are at the same magnification. (1, 2) *Senoniasphaera protrusa* Clarke et Verdier, Kudrino-2, Sample 25; (3) *Dinogymnium albertii* Clarke et Verdier, Kudrino-2, Sample 30; (4) *Alisogymnium euclaense* (Cookson et Eisenack) Lentin et Vozzhennikova, Aksu-Dere, Sample 44; (5, 6) *Canningia reticulata* Cookson et Eisenack, Aksu-Dere, Sample 58; (7) *Fromea laevigata* (Drugg) Stover et Evitt, Kudrino-2, Sample 25; (8) *Apteodinium deflandrei* (Clarke et Verdier) Lucas-Clark, Kudrino-2, Sample 25; (9) *Chatangiella* cf. *manumii* (Vozzhennikova) Lentin et Williams, Aksu-Dere, Sample 44; (10) *Dinogymnium muticum* (Vozzhennikova) Lentin et Williams, Aksu-Dere, Sample 46; (11, 12) *Chatangiella* "*spinosa*" sensu Nohr-Hansen et al., 2019: (11) Aksu-Dere, Sample 44; (12) Kudrino-2, Sample 25; (13, 14) *Isabelidinium microarmum* (McIntyre) Lentin et Williams: (13) Kudrino-2, Sample 25; (14) Aksu-Dere, Sample 44.

Plate V

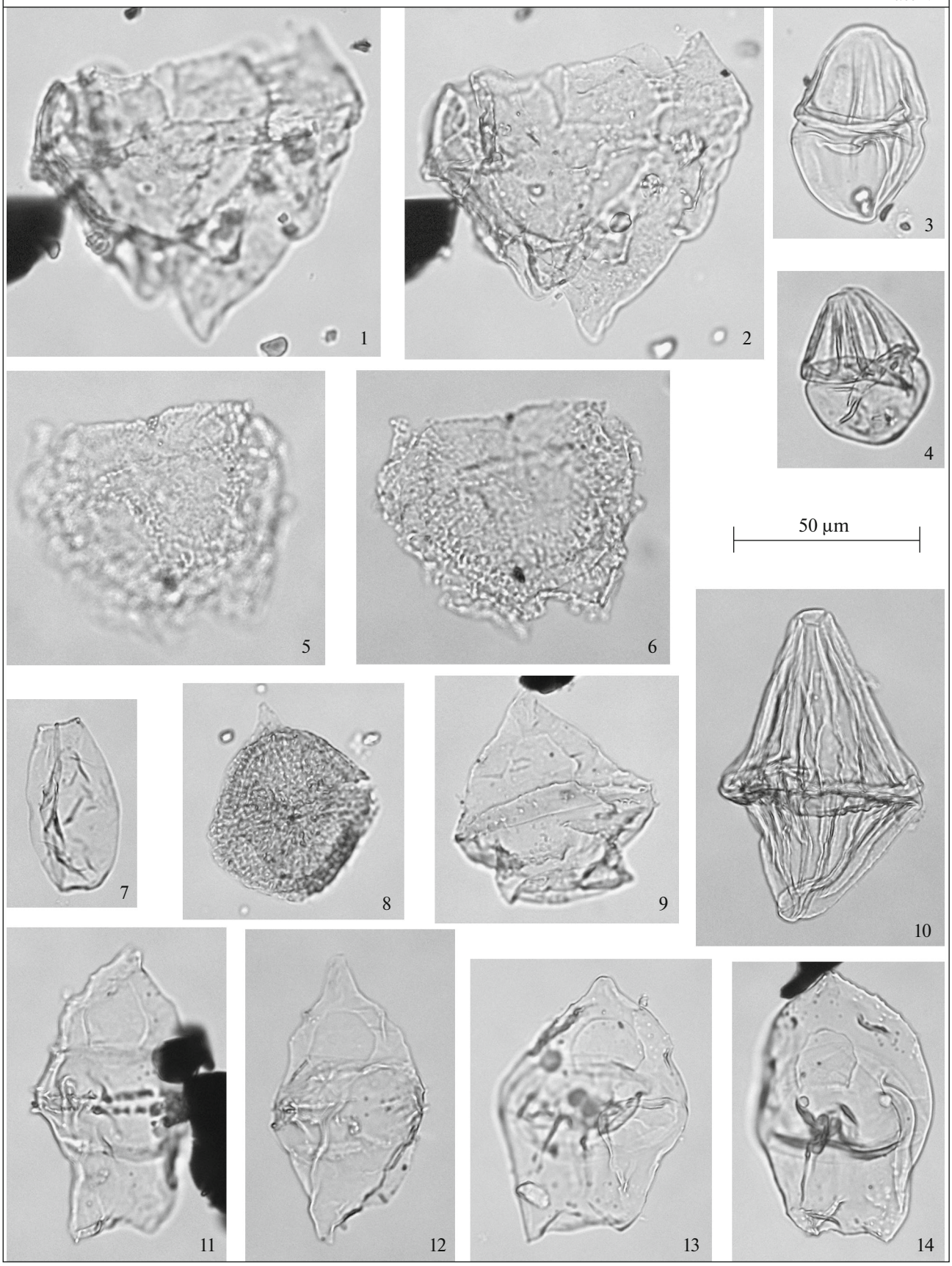

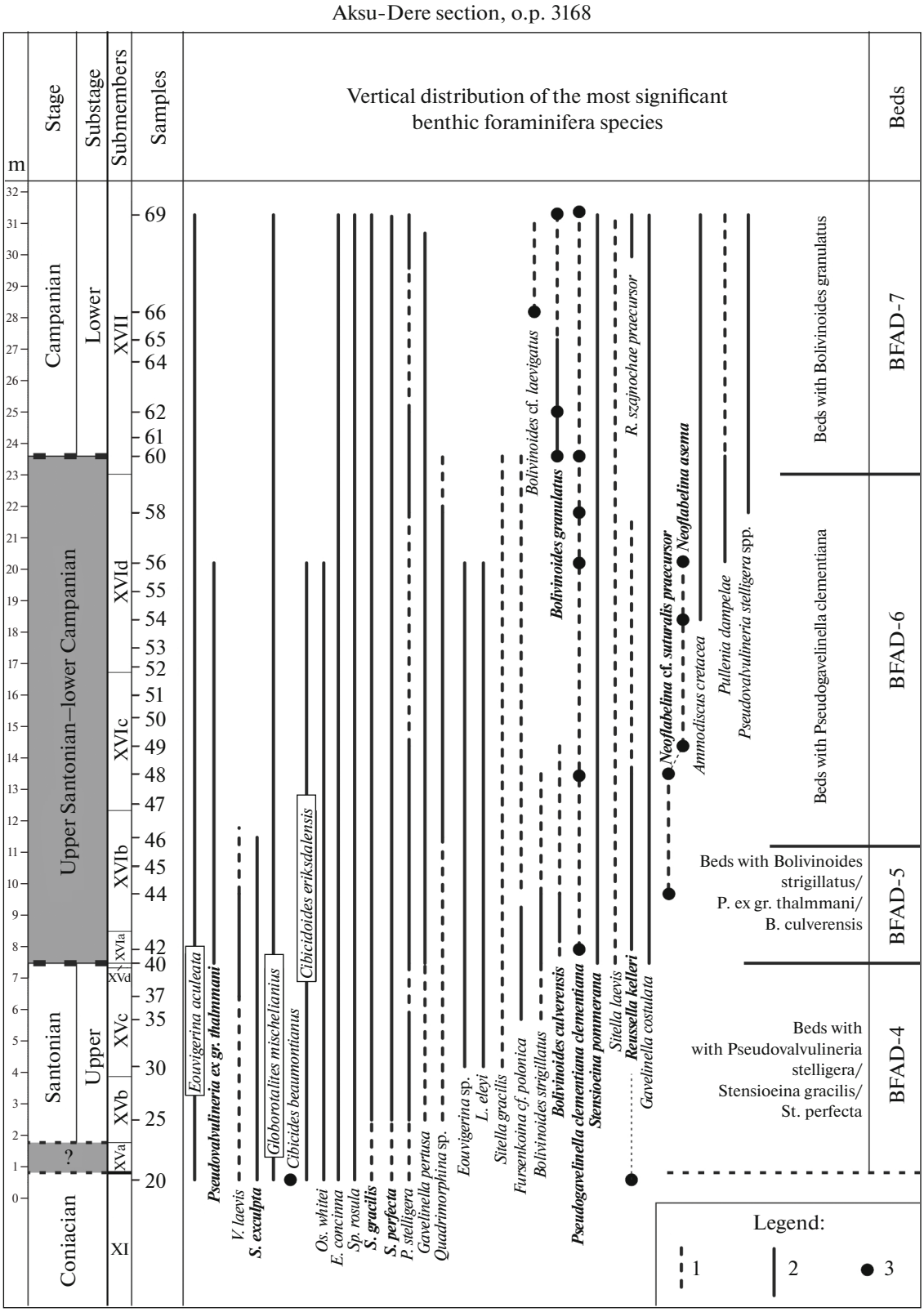

Fig. 10. Distribution of benthic foraminifers in the Aksu-Dere section. (1) Sporadic occurrence; (2) repeated occurrence; (3) plausible find of the species. Stratigraphically important species are given in bold.

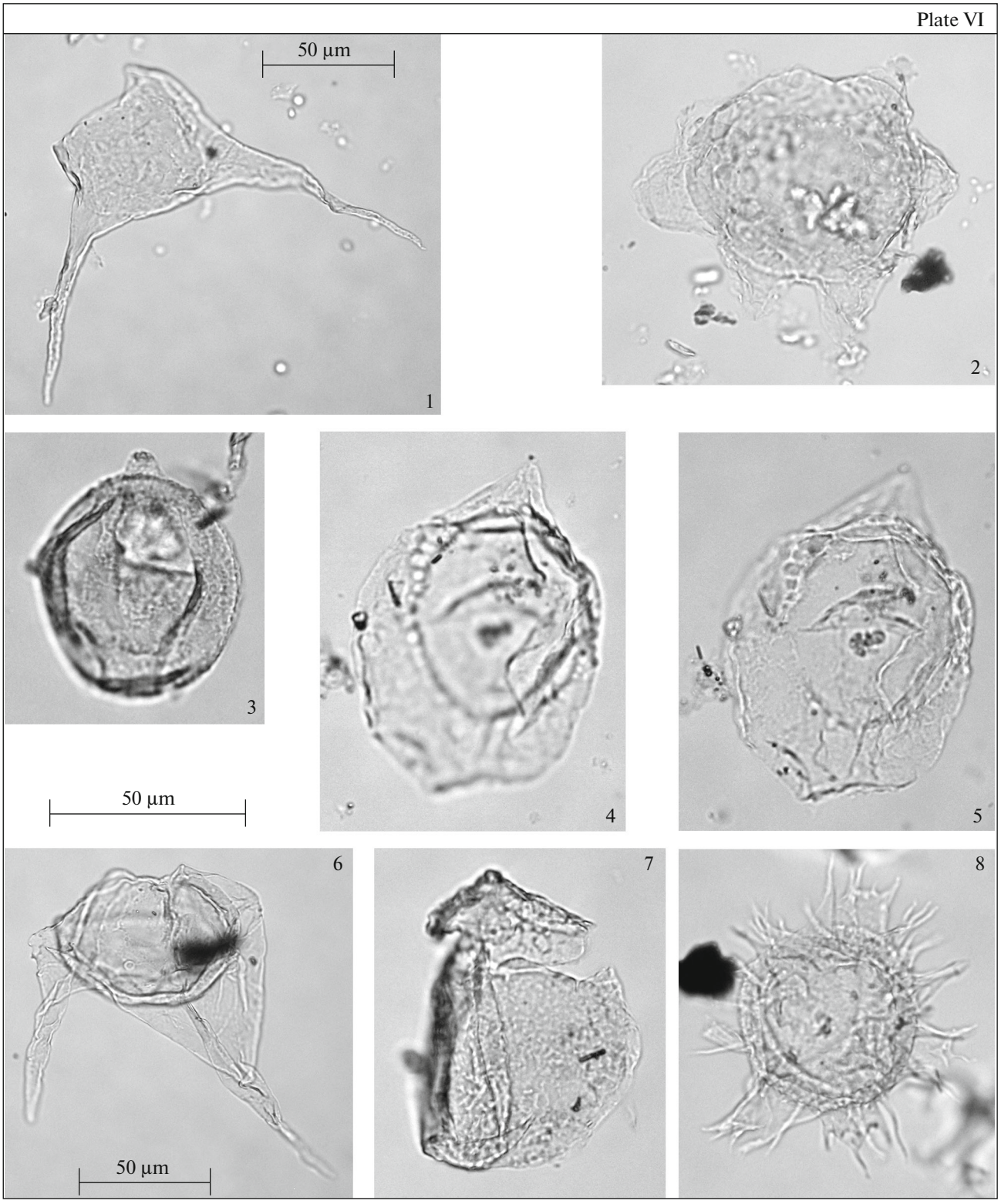

Plate VI. Palynomorphs from the Kudrino-2 and Aksu-Dere sections. (1) *Odontochitina diducta* Pearce, Kudrino-2, Sample 25; (2) *Canningia glomerata* sensu Fensome et al., 2019, Kudrino-2, Sample 25; (3) *Apteodinium* cf. *crassum* Slimani et Louwye, Aksu-Dere, Sample 64; (4, 5) *Senoniasphaera protrusa* Clarke et Verdier, Kudrino-2, Sample 30; (6) *Xenascus* sp., Aksu-Dere, Sample 44; (7) *Canningia reticulata* Cookson et Eisenack, Aksu-Dere, Sample 28; (8) *Florentinia buspina* (Davey et Verdier) Duxbury, Aksu-Dere, Sample 64.

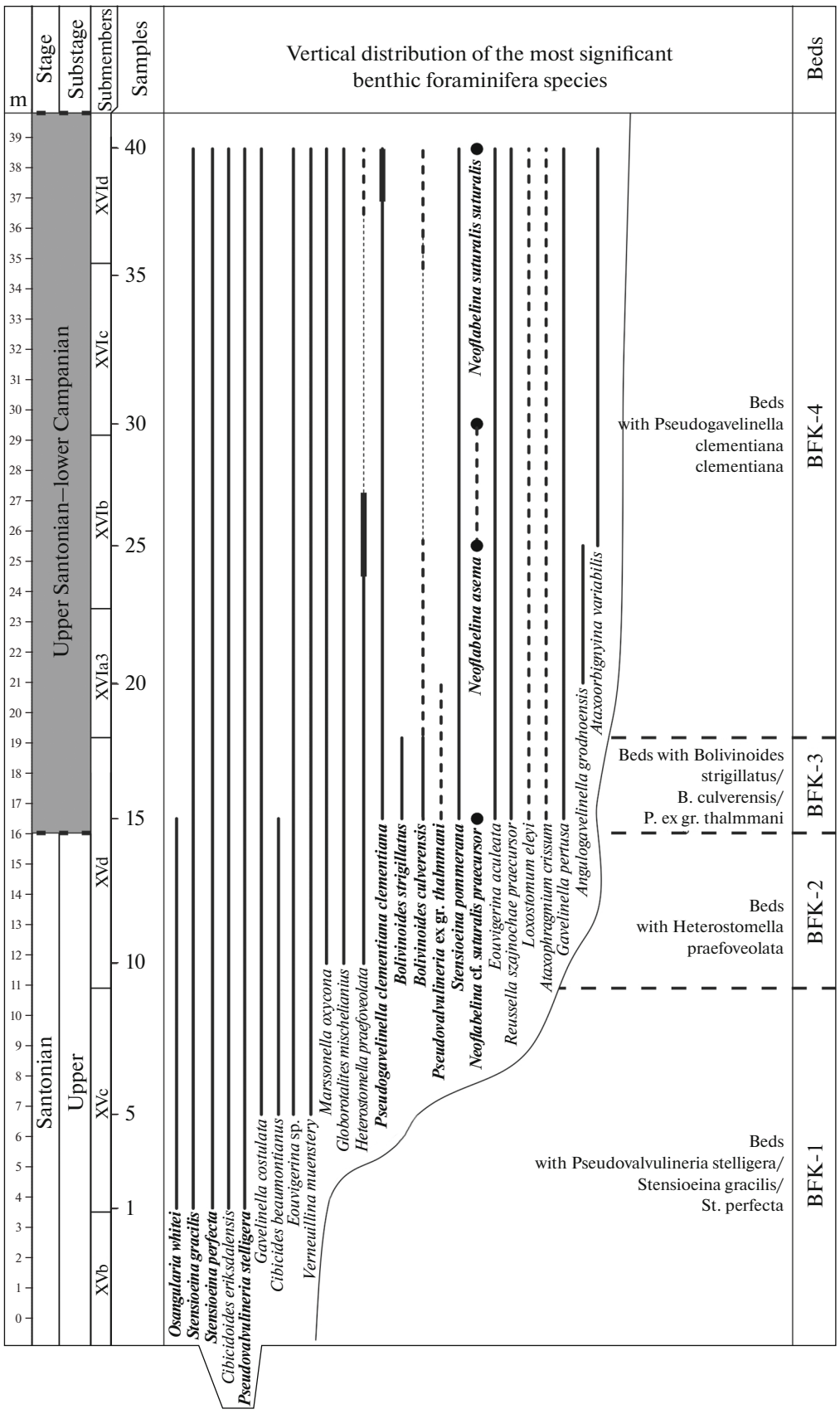

Fig. 11. Distribution of benthic foraminifers in the Kudrino-2 section. See Fig. 10 for the legend.

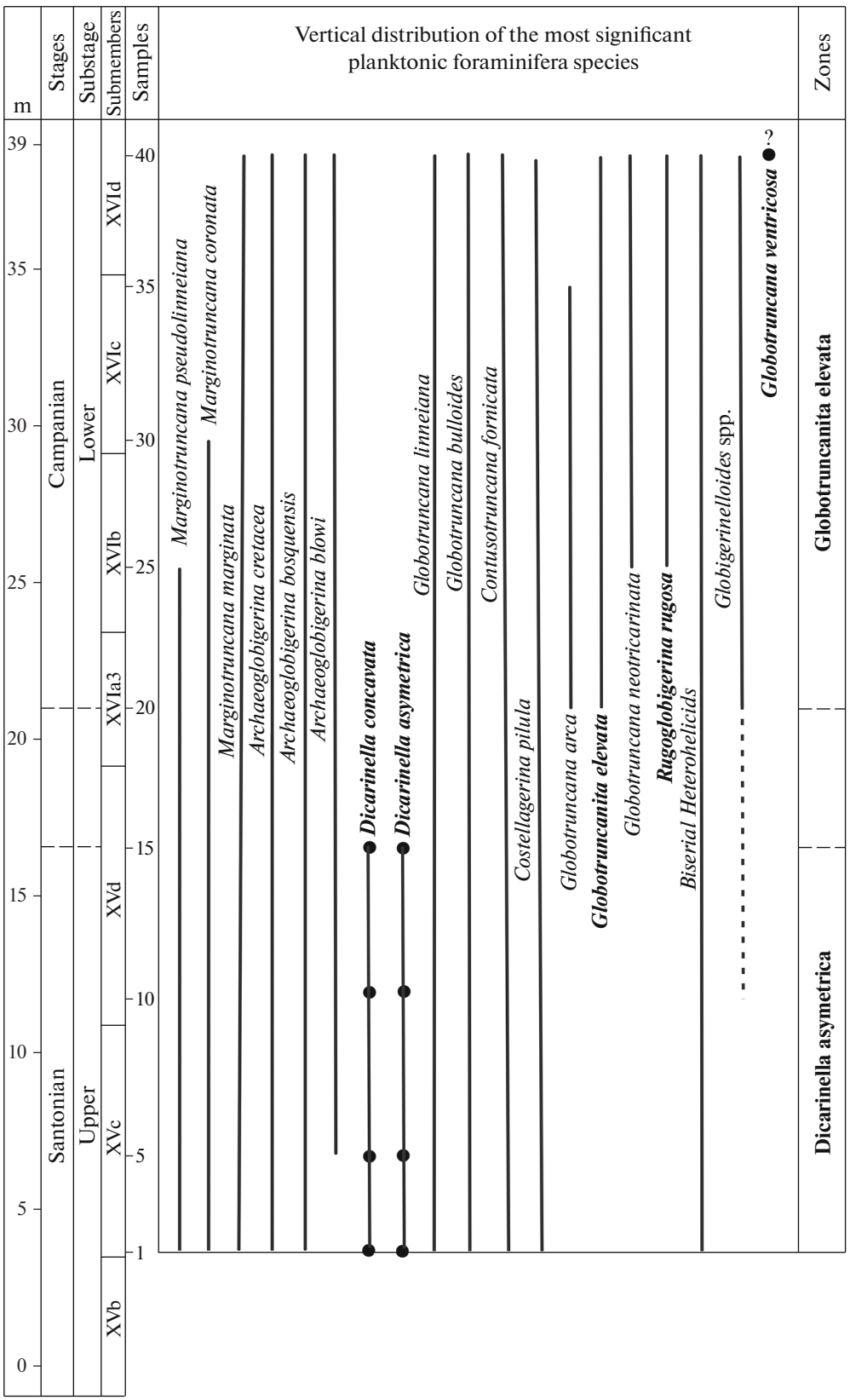

Fig. 12. Distribution of planktonic foraminifers in the Kudrino-2 section. See Fig. 10 for the legend.

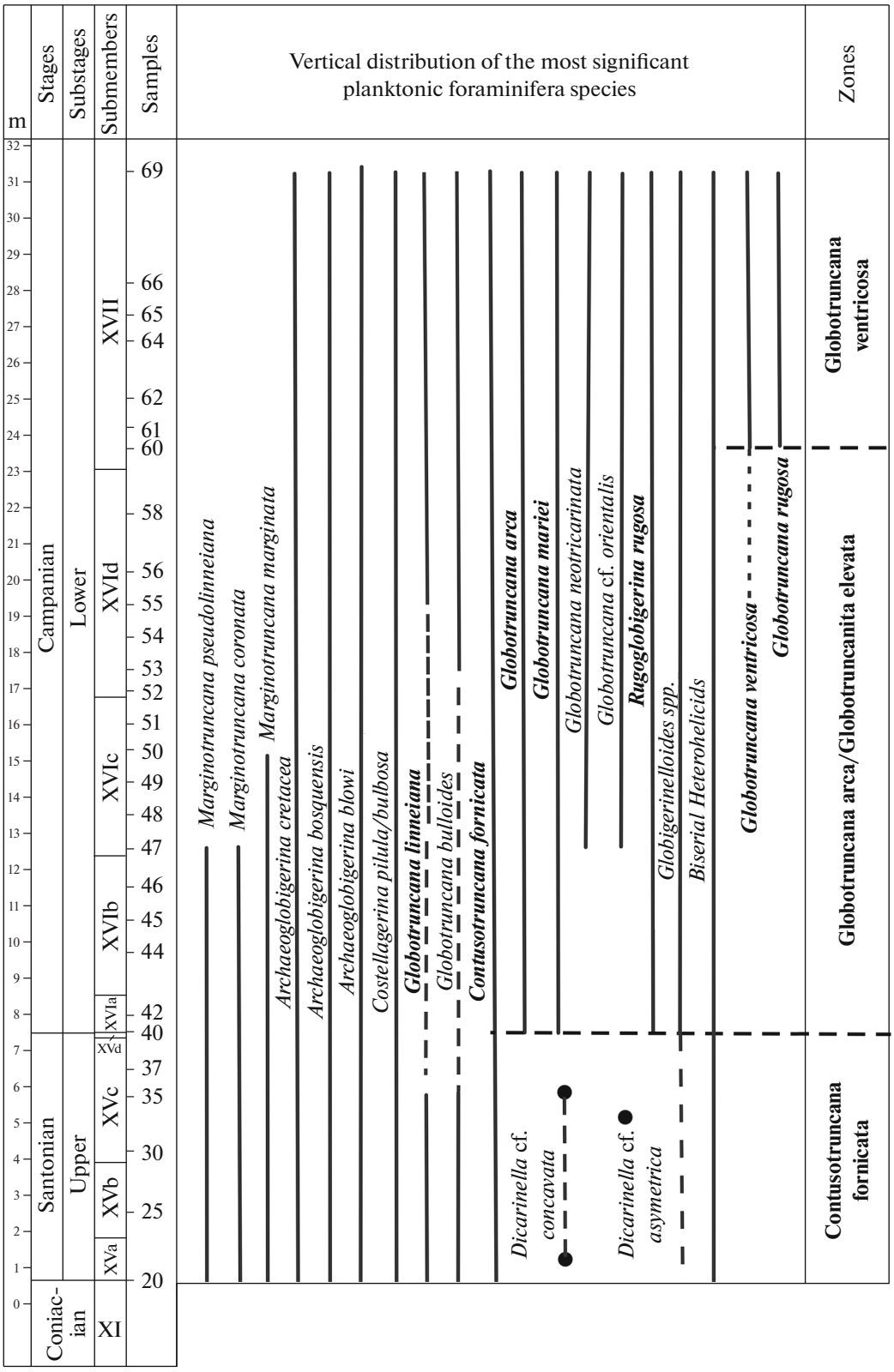

Fig. 13. Distribution of planktonic foraminifers in the Aksu-Dere section. See Fig. 10 for the legend.

tion, in the interval of samples 30 to 40. The assemblages in overlying sediments are uniform, and poor test preservation often hinders reliable identification. Unfortunately, some index species were not found in this section.

The relatively poor taxonomic diversity of the PF assemblage is explained by the gradually increasing effect of the Boreal Province on the territories of the East European Craton and its southern framework, that is, the Crimea–North Caucasus area (Kopaevich and Vishnevskaya, 2016a, 2016b; Kopaevich et al., 2020; Vishnevskaya and Kopaevich, 2020). Index species in Crimean PF assemblages often occur as single specimens or are completely absent, and it prevents the allocation of zones by PF. In such cases, one can recognize only the "analogs" of the zones by PF based on certain "bioevents" and the assemblages by the associated taxa for stratigraphic correlations.

Kudrino-2 section. It contains a PF assemblage which enables the recognition of two zones (Fig. 12).

Dicarinella asymetrica Zone has been recognized in the interval of Samples 1 to 15 inclusive (Submembers XVb and XVIc and the larger part of Submember XVd); it is characterized by a PF assemblage including the following species: keeled trochospiral *Marginotruncana pseudolinneiana* Pessagno, *M. marginata* (Reuss), *M. coronata* (Bolli); non-keeled trochospiral, morphologically more simple tests of *Archaeoglobigerina cretacea* (d'Orbigny), *A. bosquensis* Pessagno, *Costellagerina pilula* (Belford), and *C. bulbosa* (Belford); planispiral small *Globigerinelloides asper* (Ehrenberg) and *G. biforaminatus* (Hofker); and helical *Planoheterohelix/Heterohelix* spp. with biserially arranged chambers. The first occurrences of these taxa take place as early as the Turonian–Coniacian. But the presence of the bicarinate representatives of the genus *Globotruncana—G. linneiana* (d'Orbigny) and *G. bulloides* Vogler—indicates the undoubtedly Santonian age of the host rocks, because the first exemplars of this species in the Olazagutia section (Northern Spain), the GSSP for the base of the Santonian Stage, were encountered 10 cm above the first finds of *Platyceramus undulatoplicatus* (Roemer), the zonal form of the lower Santonian (Coccioni and Premoli Silva, 2015; Lamolda et al., 2014). The indicator of the late Santonian age is the constant presence of the spiral-convex, with two keels, *Contusotruncana fornicata* (Plummer) together with the two-keeled, umbilically convex *Dicarinella concavata* (Brotzen) and *D. asymetrica* (Sigal). In Crimean and North Caucasus sections, these species co-occur only in the upper Santonian sediments (Kopaevich, 2010; Kopaevich and Vishnevskaya, 2016; Maslakova, 1978), but the representatives of the genus *Dicarinella* are very rare.

Gbotruncanita elevata Zone is recognized in the interval of Samples 20 to 40 inclusive the upper part of Submember XVIa and Submembers XVIb–XVId (Fig. 13). The tests of *D. concavata/asymetrica* disappear from the sequence at the level of Sample 20, but the umbilically convex one-keeled *Globotruncanita elevata* (Brotzen) appear and occur repeatedly from this level upward. The combination of these two "bioevents" marks the boundary between two zones, Dicarinella asymetrica and Gbotruncanita elevata, which is close to the boundary between the Santonian and Campanian stages (Coccioni and Premoli Silva, 2015; Dubicka et al., 2017; Kopaevich et al., 2020; Premoli Silva and Sliter, 1999). Gbotruncanita elevata Zone continue upward to the top of the sequence (up to Sample 40). In addition to the zonal species, the PF assemblage includes the two-keeled *Globotruncana arca* (Cushman) and *G. mariei* Banner et Blow, which appeared at the level of Sample 20. In Sample 25, these forms are supplemented by *G. neotricarinata* Petrizzo, Falzoni et Premoli Silva and *Rugoglobigerina rugosa* (Plummer), the presence of which confirms the early Campanian age of this interval. The appearance of *Globotruncana ventricosa* (White) in Sample 40 suggests the possibility to recognize a zone of the same name in the overlying sediments, but this is impossible at the current stage of investigations, because the species *G. ventricosa* lacks distinct morphological signatures and has been discovered in a single sample. At present, the index species of this zone is replaced by *Contusotruncana plummerae* (Gandolfi) (Petrizzo et al., 2011), but its tests are absent in Sample 40. The last *Marginotruncana pseudolinneiana* and *M. coronata* were encountered in Sample 30; *M. marginata* continue upward to the level of Sample 40.

To summarize, the boundary between the Santonian and Campanian as determined by PF is located in the interval between Samples 15 (the top of Submember XVd) and 20 (the base of Submember XVIa). The adjustment of its position requires more detailed sampling of the Kudrino-2 section and additional studies.

Aksu-Dere section. PF are irregularly distributed in the section; analysis of the data enables the recognition of three zones (Fig. 13).

Contusotruncana fornicata Zone corresponds to Submembers XVa–XVc (Samples 20–37). PF in this part of the section are represented by various morphotypes including keeled and non-keeled trochospiral PF taxa as well as planispiral and biserial spiral-helical tests. The keeled morphotypes consist of the representatives of the genera *Marginotruncana* Hofker, *Contusotruncana* Korchagin, and *Globotruncana* Cushman. Speciments of the two-keeled umbilically convex *Dicarinella* Porthault occur sporadically. The genus *Marginotruncana* is represented by *M. pseudolinneiana*, *M. marginata*, and *M. coronata*; *Globotruncana* is represented by *G. linneiana* and *G. bulloides*; and *Contusotruncana* is represented by *C. fornicata* (Plummer). As mentioned above, the crucial aspects are the presence of the tests of *G. linneiana*, which indicates the Santonian age of host rocks, and the first occurrence and constant presence of *Contusotruncana fornicata*,

Plate VII. Nannoplankton from the Kudrino-2 and Aksu-Dere sections. The scale bar is 2 μm. All photographs are in cross-polarized light except figs. 15 and 33, which were shot under plane-polarized light. (1) *Staurolithites laffittei* Caratini, Sample 32, Aksu-Dere; (2) *Tranolithus orionatus* (Reinhardt) Reinhardt, Sample 10, Kudrino-2; (3, 4) *Reinhardtites levis* Prins et Sissingh in Sissingh: (3) Sample 10, Kudrino-2; (4) Sample 32, Aksu-Dere; (5) *Reinhardtites anthophorus* (Deflandre) Perch-Nielsen, Sample 32, Aksu-Dere; (6) *Zeugrhabdotus bicrescenticus* (Stover) Burnett in Gale et al., Sample 50, Aksu-Dere; (7) *Z. scutula* (Bergen) Rutledge et Bown, Sample 25, Kudrino-2; (8) *Z. embergeri* (Noël) Perch-Nielsen, Sample 30, Kudrino-2; (9) *Placozygus fibuliformis* (Reinhardt) Hoffmann, Sample 30, Kudrino-2; (10) *Chiastozygus bifarius* Bukry, Sample 54, Aksu-Dere; (11) *Ch. litterarius* (Górka) Manivit, Sample 48, Aksu-Dere; (12) *Eiffellithus gorkae* Reinhardt, Sample 25, Kudrino-2; (13) *E. turriseiffelii* (Deflandre in Deflandre et Fert) Reinhardt, Sample 50, Aksu-Dere; (14) *Helicolithus trabeculatus* (Górka) Verbeek, Sample 1, Aksu-Dere; (15) *Cylindralithus biarcus* Bukry, Sample 52 (Aksu-Dere); (16) *C. serratus* Bramlette et Martini, Sample 44, Aksu-Dere; (17) *Biscutum ellipticum* (Górka) Grün in Grün et Allemann, Sample 44, Aksu-Dere; (18) *Prediscosphaera grandis* Perch-Nielsen, Sample 50, Aksu-Dere; (19) *Pr. cretacea* (Arkhangelsky) Gartner, Sample 42, Aksu-Dere; (20) *Retecapsa angustiforata* Black, Sample 1, Kudrino-2; (21) *R. ficula* (Stover) Burnett, Sample 66, Aksu-Dere; (22) *R. crenulata* (Bramlette et Martini) Grün in Grün et Allemann, Sample 8, Aksu-Dere; (23) *Cyclagelosphaera margerelii* Noël, Sample 32, Aksu-Dere; (24) *Watznaueria barnesiae* (Black in Black et Barnes) Perch-Nielsen, Sample 1, Kudrino-2; (25) *W. fossacincta* (Black) Bown in Bown et Cooper, Sample 5, Kudrino-2; (26) *W. biporta* Bukry, Sample 25, Kudrino-2; (27) *Arkhangelskiella cymbiformis* Vekshina, Sample 1, Kudrino-2; (28) *Broinsonia parca expansa* Wise et Watkins in Wise, Sample 25, Kudrino-2; (29) *Br. parca parca* (Stradner) Bukry, Sample 64, Aksu-Dere; (30) *Br. parca constricta* Hattner et al., Sample 62, Aksu-Dere; (31) *Br. matalosa* (Stover) Burnett in Gale et al., Sample 50, Aksu-Dere; (32) *Microrhabdulus decorates* Deflandre, Sample 20, Kudrino-2; (33, 34) *Kamptnerius magnificus* Deflandre, Sample 66, Aksu-Dere; (35, 36) *Lucianorhabdus cayeuxii* Deflandre: (35) Sample 25, Kudrino-2; (36) Sample 54, Aksu-Dere; (37) *L. maleformis* Reinhardt, Sample 46, Aksu-Dere; (38) *Calculites obscurus* (Deflandre) Prins et Sissingh in Sissingh, Sample 30, Kudrino-2; (39) *Braarudosphaera bigelowii* (Gran et Braarud) Deflandre, Sample 66, Aksu-Dere; (40) *Eprolithus rarus* Varol, Sample 20, Kudrino-2; (41) *E. moratus* (Stover) Burnett, Sample 20, Aksu-Dere; (42) *Micula concave* (Stradner in Martini et Stradner) Verbeek, Sample 18, Aksu-Dere; (43) *M. staurophora* (Gardet) Stradner, Sample 30, Kudrino-2; (44) *M. swastika* Stradner et Steinmetz, Sample 68, Aksu-Dere.

p. 486

Plate VIII. Benthic foraminifers from the Aksu-Dere section. The scale bar is 100 μm; (a) ventral view; (b) side view; (c) dorsal view. (1) *Pseudovalvulineria stelligera* (Marie), Sample 42; (2) *Ps. stelligera* (Marie) spp., Sample 69; (3) *Stensioeina perfecta* Koch, Sample 42; (4) *Eouvigerina* sp., Sample 40; (5) *E. aculeata* (Ehrenberg), Sample 44; (6) *Pseudovalvulineria stelligera* (Marie) spp., Sample 58; (7) *Stensioeina gracilis* Brotzen, Sample 46; (8) *St. pommerana* Brotzen, 1936, Sample 44; (9) *Bolivinoides strigillatus* (Chapman), Sample 42; (10) *Pseuvalvulineria* ex gr. *thalmmani*, Sample 42; (11) *Neoflabellina* cf. *suturalis praecursor*, Sample 44; (12) *N. asema* Koch, Sample 49; (13) *Bolivinoides culverensis* Barr, Sample 48; (14) *Pseudogavelinella clementiana clementiana* (d'Orbigny), Sample 46; (15) *Pullenia dampelae* Dain, Sample 56; (16) *Bolivinoides culverensis* Barr, Sample 44; (17) *B. granulatus* Hofker, Sample 61; (18) *B.* cf. *laevigatus* Marie, Sample 66; (19) *Cibicidoides eriksdalensis* (Brotzen), Sample 46; (20) *Reussella kelleri* Vassilenko, Sample 42; (21) *R. szajnochae praecursor* De Klasz et Knipscheer, Sample 69.

p. 487

Plate IX. Benthic foraminifers from the Kudrino-2 section. The scale bar is 200 μm; (a) ventral view; (b) side view; (c) dorsal view. (1) *Spiroplectammina lingua* Akimetz, Sample 10; (2) *Bolivinoides strigillatus* (Chapman), Sample 15; (3) *Pseudogavelinella clementiana clementiana* (d'Orbigny), Sample 15; (4) *Osangularia whitei crassa* Vassilenko, Sample 10; (5) *Bolivinoides culverensis* Barr, Sample 15; (6) *Heterostomella praefoveolata* Mjatluk, Sample 25; (7) *H. praefoveolata* Mjatluk, Sample 20; (8) *Loxostomum eleyi* (Cushman), Sample 30; (9) *Angulogavelinella grodnoensis* (Akimetz), Sample 20; (10) *Neoflabellina suturalis* cf. *praecursor* (Wedekind), Sample 15; (11) *N. asema* Koch, Sample 25; (12) *N. suturalis suturalis* (Cushman), Sample 40; (13) *Ataxoorbignyina variabilis* (Orbigny), Sample 30; (14) *Pseudovalvulineria stelligera* (Marie) spp., Sample 15.

p. 488

Plate X. Planktonic foraminifers from the Santonian and Campanian sediments of the Aksu-Dere and Kudrino-2 sections. The scale bar is 200 μm. For all trochospiral tests: (a) dorsal view; (b) peripheral side view; (c) umbilical view. (1) *Archaeoglobigerina cretacea* (d'Orbigny), Aksu-Dere, Sample 20; (2) *Ar. bosquensis* Pessagno, Aksu-Dere, Sample 25; (3) *Marginotruncana pseudolinneiana* Pessagno, Kudrino-2, Sample 1; (4) *M. pseudolinneiana* Pessagno, Kudrino-2, Sample 25; (5) *M. coronata* (Bolli), Aksu-Dere, Sample 5; (6) *Globotruncana linneiana* (d'Orbigny), Aksu-Dere, Sample 1; (7) *Marginotruncana marginata* (Reuss), Kudrino-2, Sample 30; (8) *Contusotruncana fornicata* (Plummer), Aksu-Dere, Sample 20; (9) *Globotruncana linneiana* (d'Orbigny), Kudrino-2, Sample 1; (10) *Gl. arca* (Cushman), Aksu-Dere, Sample 40.

p. 489

Plate XI. Planktonic foraminifers from the Santonian and Campanian sediments of the Aksu-Dere and Kudrino-2 sections. The scale bar is 200 μm. For all trochospiral tests: (a) dorsal view; (b) peripheral side view; (c) umbilical view. (1) *Dicarinella asymetrica* (Sigal), Kudrino-2, Sample 15; (2) *Globotruncana bulloides* Vogler, Kudrino-2, Sample 5; (3) *Dicarinella concavata* (Brotzen), Kudrino-2, Sample 15; (4) *Contusotruncana fornicata* (Plummer), Kudrino-2, Sample 1; (5) *Globotruncanita elevata* (Brotzen), Kudrino-2, Sample 20; (6) *Rugoglobigerina rugosa* Plummer, Aksu-Dere, Sample 45; (7) *Globigerinelloides asper* (Ehrenberg), Aksu-Dere, Sample 40; (8) *Gl. biforaminatus* (Hofker), Aksu-Dere, Sample 44; (9) *Globotruncana mariei* Banner et Blow, Aksu-Dere, Sample 40; (10) *Gl. rugosa* (Marie), Aksu-Dere, Sample 40; (11) *Gl. ventricosa* White, Aksu-Dere, Sample 55.

Plate VII

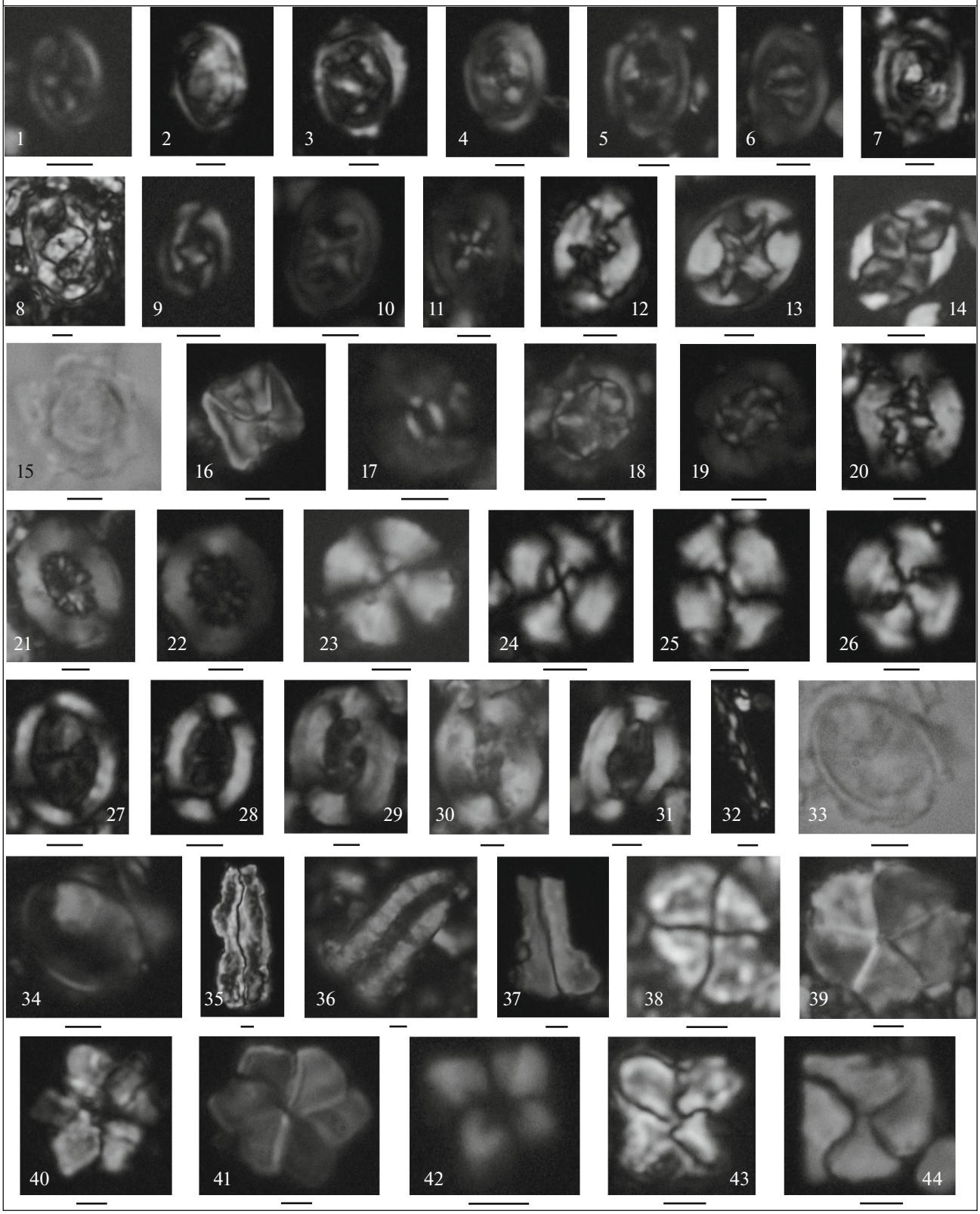
1
2
3
4
5
6
7
8
9
10
11
12
13
14
15
16
17
18
19
20
21
22
23
24
25
26
27
28
29
30
31
32
33
34
35
36
37
38
39
40
41
42
43
44

Plate VIII

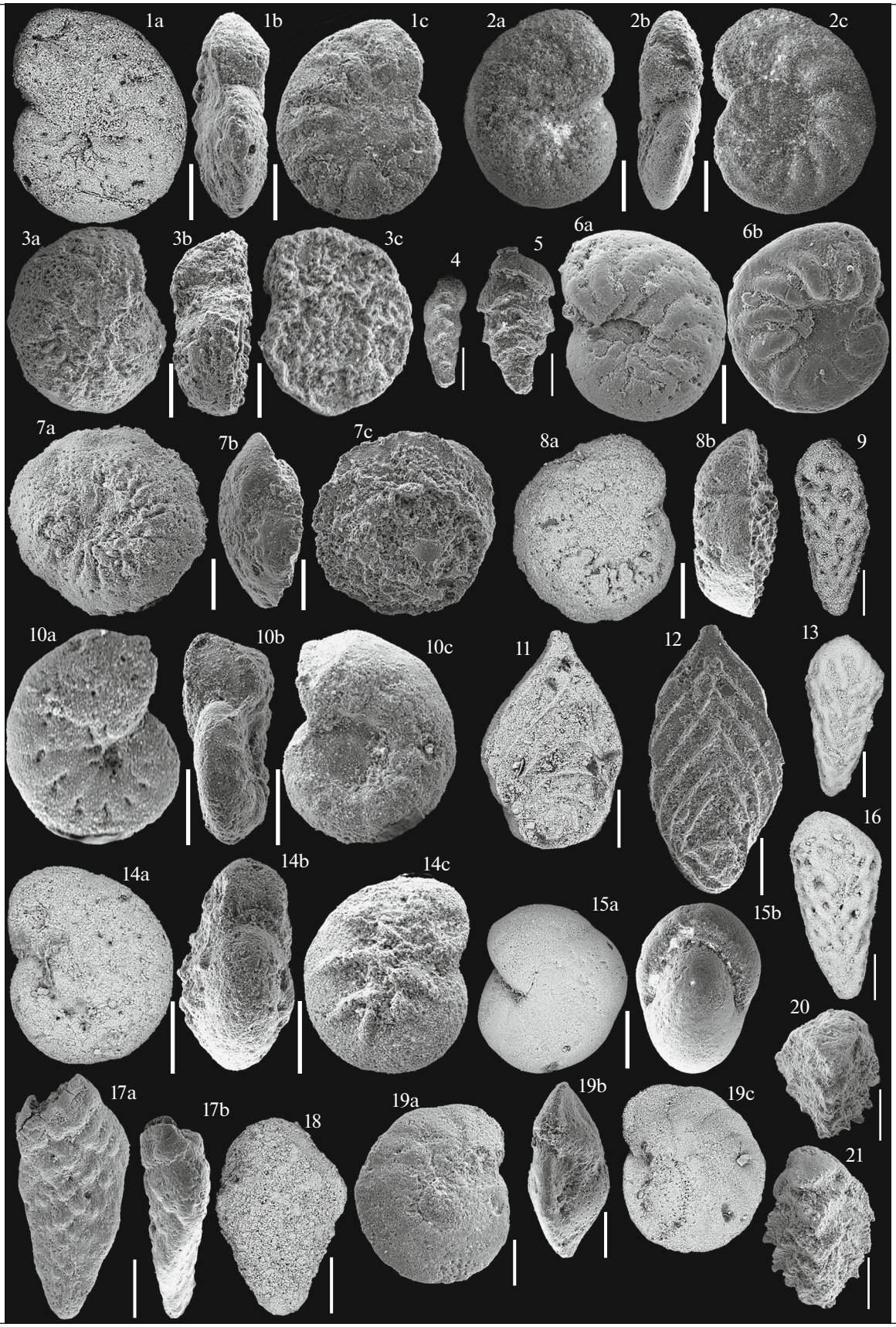
1a
1b
1c
2a
2b
2c
3a
3b
3c
4
5
6a
6b
7a
7b
7c
8a
8b
9
10a
10b
10c
11
12
13
16
14a
14b
14c
15a
15b
20
17a
17b
18
19a
19b
19c
21

Plate IX

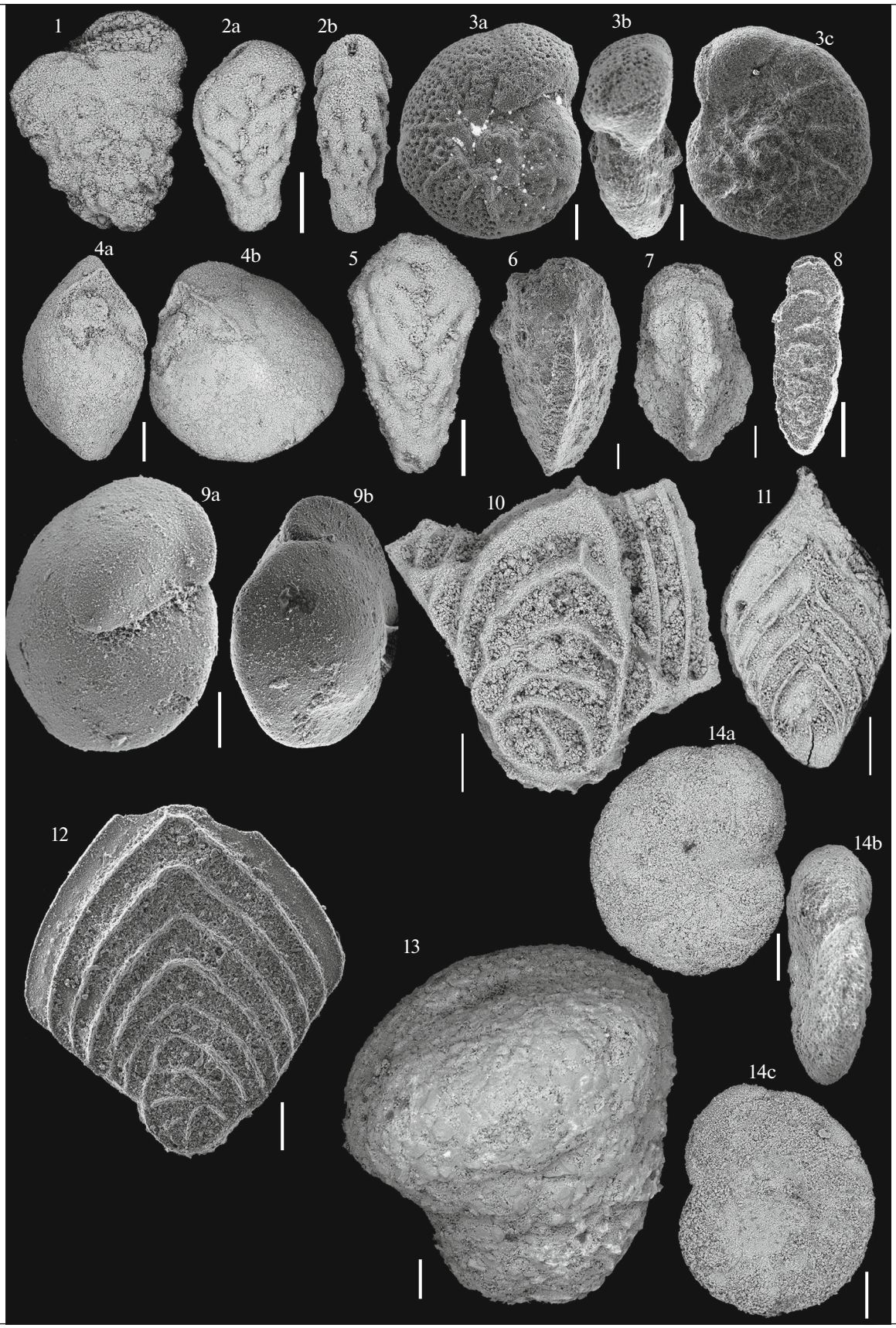

Plate X

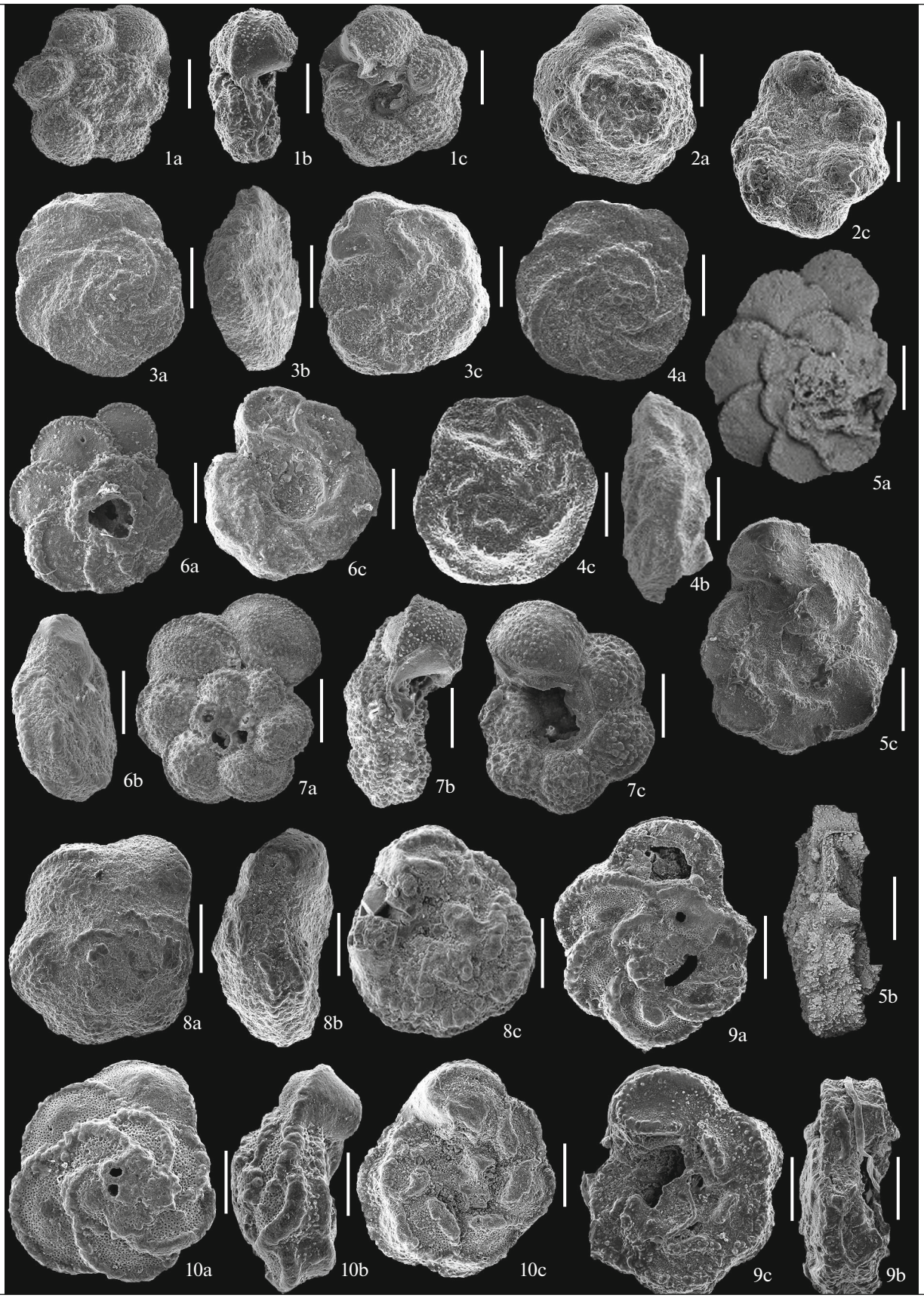
1a
1b
1c
2a
2c
3a
3b
3c
4a
5a
6a
6c
4c
4b
6b
7a
7b
7c
5c
8a
8b
8c
9a
5b
10a
10b
10c
9c
9b

Plate XI

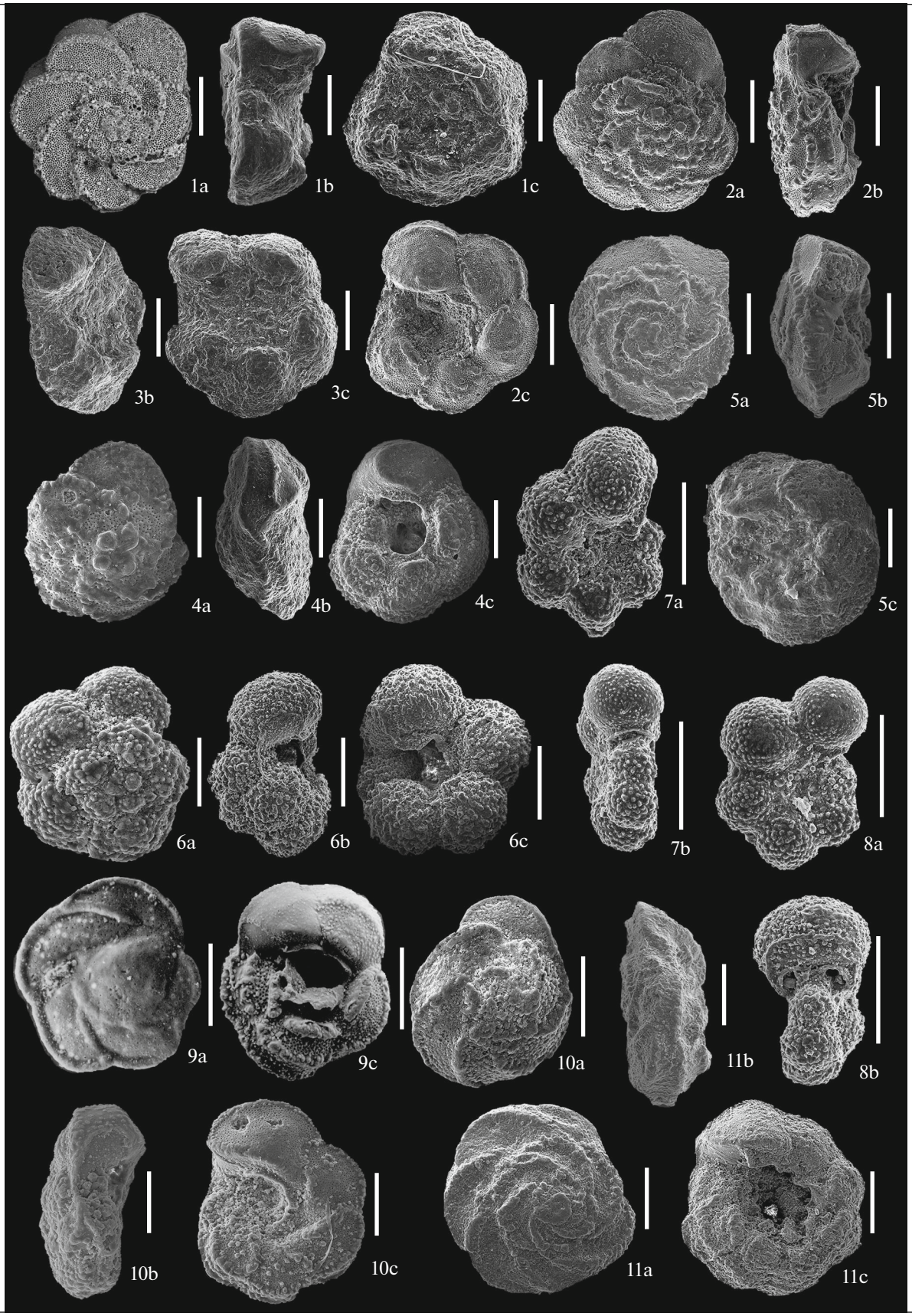
1a
1b
1c
2a
2b
3b
3c
2c
5a
5b
4a
4b
4c
7a
5c
6a
6b
6c
7b
8a
9a
9c
10a
11b
8b
10b
10c
11a
11c

typical of the upper Santonian sediments of the Crimean Mountains and Central Poland (Maslakova, 1978; Walaszczyk and Peryt, 1998). The sporadic specimens of the genus *Dicarinella* present in this interval were successfully identified only in terms of the open nomenclature, because they lack clearly expressed morphological signatures. They can be considered as morphotypes transitional from the moderately convex (umbilically) *Marginotruncana marginata* to more contrastingly convex (umbilically) *Dicarinella* cf. *concavata* or *D.* cf. *asymetrica*. The rest of the assemblage consists of the tests of non-keeled taxa with high trochospiral tests and globular chambers. They are represented by *Archaeoglobigerina cretacea*, *A. bosquensis*, *Costellagerina pilula*, and *C. bulbosa*. The planispiral tests of the genus *Globigerinelloides* in this interval occur repeatedly but still sporadically. The biserial taxa of the Heterohelicidae are, on the contrary, ubiquitous and highly abundant. Starting from Sample 35, tests of non-keeled taxa, which occur virtually throughout the Aksu-Dere section, are obviously predominant in Member XV.

Globotruncana arca/Globotruncanita elevata Zone (Member XVI, Samples 40–58). The tests of the species *Globotruncana arca* (Cushman), which is considered as the marker of the Santonian–Campanian boundary in Crimea and Northern Poland (although its first occurrence was also mentioned in the upper Santonian in Poland), appear at the level of Sample 40. *G. mariei* Banner et Blow appears at the level of Sample 46, and *G. neotricarinata* and *G.* cf. *orientalis* El Naggar appear in Sample 47. *Rugoglobigerina rugosa* appears in the same sample and is present in each sample afterwards. The occurrence of these species indicates the Campanian age of sediments. Along with the increase in numbers of *Globotruncana*, the number of *Marginotruncana* decreases rapidly. The last representatives of the latter genus were encountered in Submember XVIc as single specimens. Together with the holdover *Costellagerina* and *Archaeoglobigerina*, the small planispiral tests of the genus *Globigerinelloides*, belonging to *G. asper* and *G. biforaminatus*, increase in abundance substantially.

The top of the section (Member XVII, Samples 60–66) is characterized by the first occurrence of *Globotruncana ventricosa* and *G. rugosa* (Marie). These species were encountered in a small amount, but their occurrence enables the recognition of the **middle zone of the Campanian—Globotruncana ventricosa Zone** (Caron, 1985; Petrizzo et al., 2011; Premoli Silva and Sliter, 1995). Considering the two-member subdivision of the Campanian adopted in Russia, this zone corresponds largely to the lower Campanian in this case.

To summarize, the boundary by PF between the Santonian and Campanian stages in the Aksu-Dere section is drawn at the base of the Globotruncana arca Zone, which corresponds to the Globotruncanita elevata Zone in the Kudrino-2 section, and can be combined with the base of Submember XVIa.

The magneto- and chemostratigraphic data as well as the discussion of the results of the integrated studies will be presented in Article 2.

ACKNOWLEDGMENTS

We are grateful to A.G. Manikin, V.A. Grishchenko, and E.V. Naumov (Saratov State University) and D.S. Bolotova (Moscow State University) for the participation in the field studies of the section; A.M. Zakharevich (Saratov State University) for assistance in SEM imaging; P.A. Proshina (Geological Institute, Russian Academy of Sciences) for the processing of the microfaunistic samples from Aksu-Dere in the laboratory; and V.A. Musatov (Lower Volga Scientific Research Institute for Geology and Geophysics) for creating conditions necessary for processing of microfaunistic samples.

FUNDING

This work was supported by the Russian Foundation for Basic Research (project no. 18-05-00784-a); planktonic foraminifer studies were supported by the Russian Foundation for Basic Research (project no. 18-05-00-503-a); identification of the benthic foraminifers and nannoplankton from the Aksu-Dere section was supported by the Russian Science Foundation (project no. 20-77-00028) and the State Assignment to GIN RAS (project no. 0114-2021-0003), respectively; ichnofossil studies and cephalopod identification were supported by the State Assignment to Moscow State University (project no. AAAA-A16-116033010096-8).

Reviewers V.V. Arkadiev, V.A. Zakharov, and B.N. Shurygin

REFERENCES

Aleksandrova, G.N., Beniamovsky, V.N., Vishnevskaya, V.S., and Zastrozhnov, A.S., New data on Upper Cretaceous biostratigraphy of the Lower Volga region, *Stratigr. Geol. Correl.,* 2012, vol. 20, no. 5, pp. 426–465.

Alekseev, A.S., Upper Cretaceous, in *Geologicheskoe stroenie Kachinskogo podnyatiya Gornogo Kryma. Stratigrafiya mezozoya* (Geological structure of the Kacha Uplift in the Crimean Mountains. Mesozoic Stratigraphy), Mazarovich, O.A. and Mileev, V.S., Eds., Moscow: Mosk. Gos. Univ., 1989, pp. 123–157.

Alekseev, A.S., Kopaevich, L.F., Baraboshkin, E.Yu., Gabdullin, R.R., Olferiev, A.G., and Yakovishina, E.V., Palaeogeography of the south of the East European Platform and its folded frame in the Late Cretaceous. Article 1. Introduction and stratigraphic framework, *Byull. Mosk. O–va Ispyt. Prir., Otd. Geol.*, 2005, vol. 80, no. 2, pp. 80–92.

Bailey, H.W., Hart, M.B., and Swiecicki, A., Evolutionary lineages of benthic foraminifera in the chalk seas of N.W. Europe and their application to problem solving, in *Geologic Problem Solving with Microfossils: A Volume in Honor of Garry D. Jones*, Demchuk, T.D. and Gary, A.C., Eds., *SEPM Spec. Publ.*, 2009, vol. 93, pp. 233–249.

Baraboshkin, E.Yu., Ichnoassemblages from the Santonian–Campanian deposits (Upper Cretaceous) of the southwestern Crimea, in *Mater. Desyatogo Vseross. soveshch. "Melovaya sistema Rossii i blizhnego zarubezh'ya: problemy stratigrafii i paleogeografii," Magadan, 20-25 sentyabrya 2020 g.* (Proc. X All-Russ. Conf. "Cretaceous System of Russia and CIS Countries: Problems of Stratigraphy and Palaeogeography," Magadan, September 20–25, 2020), Baraboshkin, E.Yu. and Guzhikov, A.Yu., Eds., Magadan: OAO "MAOBTI", 2020, pp. 24–27.

Baraboshkin, E.Yu. and Fokin, P.A., Cephalopods from Santonian/Campanian (Upper Cretaceous) boundary interval of the Aksu-Dere section (Crimean Mountains), *Byull. Mosk. O–va Ispyt. Prir., Otd. Geol.*, 2019, vol. 94, no. 4, pp. 77–84.

Baraboshkin, E.Yu., Veimarn, A.B., Kopaevich, L.F., and Naidin, D.P., *Izuchenie stratigraficheskikh pereryvov pri proizvodstve geologicheskoi s"emki. Metodicheskie rekomendatsii* (Studies of Stratigraphic Hiatuses during the Geological Mapping. Methodical Recommendations), Moscow: Mosk. Gos. Univ., 2002 [in Russian].

Beniamovsky, V.N., Infrazonal biostratigraphy of the Upper Cretaceous in the East European Province based on benthic foraminifers, Part 1: Cenomanian and Coniacian, *Stratigr. Geol. Correl.*, 2008a, vol. 16, no. 3, pp. 257–266.

Beniamovsky, V.N., Infrazonal biostratigraphy of the Upper Cretaceous in the East European province based on benthic foraminifers, Pt. 2: Santonian–Maastrichtian, *Stratigr. Geol. Correl.*, 2008b, vol. 16, no. 5, pp. 515–527.

Beniamovsky, V.N. and Kopaevich, L.F., The Alan-Kyr Coniacian–Campanian section (Crimean Mountains): Biostratigraphy and paleobiogeography aspects, *Moscow Univ. Geol. Bull.*, 2016, vol. 71, no. 2, pp. 217–233.

Bown, P.R. and Young, J.R., Techniques, in *Calcareous Nannofossil Biostratigraphy (British Micropalaeontol. Soc. Ser.)*, Bown, P.R., Ed., London: Chapman and Hall, 1998, pp. 16–28.

Bragina, L.G., Beniamovsky, V.N., and Kopaevich, L.F., Radiolarians, foraminifers, and biostratigraphy of the Coniacian–Campanian deposits of the Alan-Kyr Section, Crimean Mountains, *Stratigr. Geol. Correl.*, 2016, vol. 24, no. 1, pp. 39–57.

Burnett, J.A., Upper Cretaceous, in *Calcareous Nannofossil Biostratigraphy (British Micropalaeontol. Soc. Ser.)*, Bown, P.R., Ed., London: Chapman and Hall, 1998, pp. 132–199.

Caron, M., Cretaceous planktic foraminifera, in *Plankton Stratigraphy*, Bolli, H.M., Saunders, J., and Perch-Nielsen, K., Eds., Cambridge Univ. Press, 1985, pp. 17–86.

Coccioni, R. and Premoli Silva, I., Revised Upper Albian–Maastrichtian planktonic foraminiferal biostratigraphy and magnetostratigraphy of the classical Tethyan Gubbio section (Italy), *Newsl. Stratigr.*, 2015, vol. 48, pp. 47–90.

Droser, M.L. and Bottjer, D.J., A semiquantitative field classification of ichnofabric, *J. Sediment. Petrol.*, 1986, vol. 56, no. 4, pp. 558–559.

Dubicka, Z. and Peryt, D., Bolivinoides (benthic foraminifera) from the Upper Cretaceous of Poland and western Ukraine: Taxonomy, evolutionary changes and stratigraphic significance, *J. Foraminiferal Res.*, 2016, vol. 46, pp. 75–94.

Dubicka, Z., Jurkowska, A., Thibault, N., Razmjooei, M.J., Wójcik, K., Gorzelak, K., and Felisiak, I., An integrated stratigraphic study across the Santonian/Campanian boundary at Bocieniec, southern Poland: A new boundary stratotype candidate, *Cretaceous Res.*, 2017, vol. 20, pp. 61–85.

Flügel, E., *Microfacies Analysis of Limestones. Analysis, Interpretation and Application*, Berlin: Springer, 2010.

Fokin, P.A., Kopaevich, L.F., Ustinova, M.A., and Kosorukov, V.L., The Santonian–Campanian boundary deposits in the Aksu-Dere section (Crimea, Bakhchisaray district), in *Mater. IX Vseross. soveshch. "Melovaya sistema Rossii i blizhnego zarubezh'ya: Problemy stratigrafii i paleogeografii." 17–21 sentyabrya 2018, Belgorod* (Proc. IX All-Russ. Conf. "Cretaceous System of Russia and CIS Countries: Problems of Stratigraphy and Palaeogeography." Belgorod, September 17–21, 2018), Baraboshkin, E.Yu. et al., Eds., Belgorod: POLITERRA, 2018, pp. 278–282.

Gale, A.S., Hancock, J.M., Kennedy, J.W., Petrizzo, M.R., Lees, J., Walaszczyk, I., and Wray, D., An integrated study (geochemistry, stable oxygen and carbon isotopes, nannofossils, planktonic foraminifera, inoceramid bivalves, ammonites and crinoids) of the Waxahachie Dam Spillway section, north Texas: A possible boundary stratotype for the base of the Campanian Stage, *Cretaceous Res.*, 2008, vol. 29, pp. 131–167.

Gawor-Biedowa, E., Campanian and Maastrichtian foraminifera from the Lublin Upland, eastern Poland, *Palaeontol. Pol.*, 1992, vol. 52.

Gozhik, P.F., Semenenko, V.M., Maslun, N.V., Poletaev, V.I., Ivanik, M.M., Mikhnits'ka, T.M., Velikanov, V.Ya., Melnichuk, V.G., Konstantinenko, L.I., Kir'yanov, V.V., Tsegelnyuk, P.D., Kotlyar, O.Yu., Berchenko, O.I., Vdovenko, M.V., Shul'ga, V.F., Nemirovs'ka, T.I., Shchegolev, O.K., Boyarina, N.I., Pyatkova, D.M., Plotnikova, L.F., Leshchukh, R.I., Zhabina, N.M., Shevchuk, O.A., Yakushin, L.M., Anikeeva, O.V., Veklich, O.D., Prikhod'ko, M.G., Tuzyak, Ya.M., Matlai, L.M., Dorotyak, Yu.B., Shainoga, I.V., Klimenko, Yu.V., and Gotsanyuk, G.I., *Stratigrafiya verkhn'ogo proterozoyu ta fanerozoyu Ukraïni. Tom 1. Stratigrafiya verkhn'ogo proterozoyu, paleozoyu ta mezozoyu Ukraïni* (The Upper Proterozoic and Phanerozoic Stratigraphy of Ukraine (in 2 Vols.). Vol. 1: Upper Proterozoic, Paleozoic, and Mesozoic Stratigraphy of Ukraine), Kiev: Inst. Geol. Nauk Nats. Akad. Nauk Ukraïni, Logos, 2013 [in Ukrainian].

Guzhikov, A.Yu., Aleksandrova, G.N., and Baraboshkin, E.Yu., New sedimentological, magnetostratigraphic, and palynological data on the Upper Cretaceous Alan-Kyr Section (Central Crimea), *Moscow Univ. Geol. Bull.*, 2020, vol. 75, no. 1, pp. 20–30.

Guzhikov, A.Yu., Aleksandrova, G.N., Baraboshkin, E.Yu., Ryabov, I.P., and Ustinova, M.A., New data on bio- and magnetostratigraphy of the Santonian–Campanian boundary interval, southwestern Crimea, in *Mater. Desyatogo Vseross. soveshch. "Melovaya sistema Rossii i blizhnego zarubezh'ya: problemy stratigrafii i paleogeografii," Magadan, 20–25 sentyabrya 2020 g.* (Proc. X All-Russ. Conf. "Cretaceous System of Russia and CIS Countries: Problems of Stratigraphy and Palaeogeography," Magadan, September 20–25, 2020), Baraboshkin, E.Yu. and Guzhikov, A.Yu., Eds., Magadan: OAO "MAOBTI", 2020, pp. 76–80.

Hampton, M.J., Bailey, H.W., Gallagher, L.T., Mortimore, R.N., and Wood, C.J., The biostratigraphy of Seaford Head, Sussex, southern England: An international reference section for the basal boundaries for the Santonian

and Campanian Stages in chalk facies, *Cretaceous Res.*, 2007, vol. 28, pp. 46–60.

Hancock, J.M., Gale, A.S., Gardin, S., Kennedy, W.J., Lamolda, M.A., Matsumoto, T.M., and Naidin, D.P., The Campanian Stage, in *Proc. Second Int. Symp. on Cretaceous Stage Boundaries*, Rawson, P.F., Dhondt, J.M., Hancock, J.M., and Kennedy, W.J., Eds., *Bull. Inst. R. Sci. Nat. Belg., Sci. Terre*, 1996, vol. 66 (Suppl.), pp. 103–109.

Haq, B.U., Hardenbol, J., and Vail, P.R., Chronology of fluctuating sea levels since the Triassic, *Science*, 1987, vol. 235, pp. 1156–1167.

Hart, M.B., Bailey, H.W., Crittenden, S., Fletcher, B.N., Price, R.J., and Swiecicki, A., Cretaceous, in *Stratigraphical Atlas of Fossil Foraminifera*, 2nd ed., Jenkins, D.G. and Murray, J.W., Eds., Chichester, U.K.: Ellis Horwood Ltd., 1989, pp. 273–371.

Jarvis, I., Mabrouk, A., Moody, R.T.J., and de Cabrera, S., Late Cretaceous (Campanian) carbon isotope events, sea level change and correlation of the Tethys and Boreal realms, *Palaeogeogr., Palaeoclimatol., Palaeoecol.*, 2002, vol. 188, pp. 215–248.

Jarvis, I., Gale, A.S., Jenkyns, H.C., and Pearce, M., Secular variations in Late Cretaceous carbon isotopes: A new $\delta^{13}C$ carbonate reference curve for the Cenomanian–Campanian (99.6–70.6 Ma), *Geol. Mag.*, 2006, vol. 143, pp. 561–608.

Jenkyns, H.C., Gale, A.S., and Corfield, R.M., Carbon and oxygen isotope stratigraphy of the English chalk and Italian Scaglia and its paleoclimatic significance, *Geol. Mag.*, 1994, vol. 131, pp. 1–34.

Jolkichev, N.A. and Naidin, D.P., Upper Cretaceous of North Bulgaria, Crimea, and Mangyshlak. 2. Upper Cretaceous stratigraphy of southwestern Mountain Crimea, *Byull. Mosk. O–va Ispyt. Prir., Otd. Geol.*, 1999, vol. 75, no. 5, pp. 48–59.

Kirsch, K.-H., Dinoflagellatenzysten aus der Oberkreide des Helvetikums und Nordultrahelvetikums von Oberbayern, *Munchener Geowiss. Abh., Reihe A*, 1991, vol. 22, pp. 1–306.

Klikushin, V.G., Crinoids from the Upper Cretaceous deposits of the USSR, *Byull. Mosk. O–va Ispyt. Prir., Otd. Geol.*, 1980, vol. 55, no. 5, pp. 80–84.

Klikushin, V.G., Paleofaunistic characteristic of the Upper Cretaceous deposits of the southwestern Crimea, *Zap. Leningrad. Gorn. Inst.*, 1981, vol. LXXV, pp. 107–124.

Klikushin, V.G., Turonian, Coniacian, and Santonian deposits of the Belbek River valley (Crimea), *Byull. Mosk. O-va Ispyt. Prir., Otd. Geol.*, 1985, vol. 60, no. 2, pp. 69–82.

Knaust, D., *Atlas of Trace Fossils in Well Core: Appearance, Taxonomy and Interpretation*, Springer, 2017.

Koch, W., Stratigraphie der Oberkreide in Nordwestdeutchland (Pompeckjsche Scholle). Teil 2. Biostratigraphie in der Oberkreide und Taxonomie von Foraminiferen, *Geol. Jahrb.*, 1977, A. 38, pp. 11–123.

Kopaevich, L.F., Upper Cretaceous zonal scheme for the Crimea–Caucasus area on the base of globotruncanids (planktonic foraminifers), *Byull. Mosk. O-va Ispyt. Prir., Otd. Geol.*, 2010, vol. 85, no. 5, pp. 40–52.

Kopaevich, L.F. and Khotylev, A.O., The stratigraphic setting of Cretaceous volcanic rocks in Crimea and in the North Caucasus, *Moscow Univ. Geol. Bull.*, 2014, vol. 69, no. 6, pp. 433–444.

Kopaevich, L.F. and Vishnevskaya, V.S., Distribution of water masses and paleogeographic dynamics in the Crimea–North Caucasus region in the Late Cretaceous, in *Paleontologiya. Stratigrafiya. Astrobiologiya. K 80-letiyu A.Yu. Rozanova* (Paleontology. Stratigraphy. Astrobiology. Coll. Sci. Works to the 80th Anniversary of A.Yu. Rozanov), Moscow: Paleontol. Inst. Ross. Akad. Nauk, 2016a, pp. 243–256.

Kopaevich, L.F. and Vishnevskaya, V.S., Cenomanian–Campanian (Late Cretaceous) planktonic assemblages of the Crimea-Caucasus area: Palaeoceanography, palaeoclimate and sea level changes, *Palaeogeogr., Palaeoclimatol., Palaeoecol.*, 2016b, vol. 441, Spec. Iss., pp. 493–515.

Kopaevich, L.F. and Walaszczyk, I.P., An integrated inoceramid-foraminiferal biostratigraphy of the Turonian and Coniacian strata in southwestern Crimea, Soviet Union, *Acta Geol. Polon.*, 1990, vol. 40, nos. 1–2, pp. 83–96.

Kopaevich, L.F., Proshina, P.A., Ryabov, I.P., Ovechkina, M.N., and Grechikhina, N.O., Santonian–Campanian boundary position in the Alan-Kyr section (Central Crimea): New micropaleontological data, *Moscow Univ. Geol. Bull.*, 2020, vol. 75, no. 3, pp. 246–253.

Lamolda, M.A., Paul, C.R.C., Peryt, D., and Pons, J.M., The Global Boundary Stratotype and Section Point (GSSP) for the base of the Santonian Stage, "Cantera de Margas," Olazagutia, northern Spain, *Episodes*, 2014, vol. 37, pp. 2–13.

Lebedeva, N.K., Dinocyst biostratigraphy of Upper Cretaceous deposits in the Usa River basin (Polar Cis-Urals), *Stratigr. Geol. Correl.*, 2005, vol. 13, no. 3, pp. 310–326.

Lebedeva, N.K., Dinocyst biostratigraphy of the Upper Cretaceous of Northern Siberia, *Doctoral (Geol.-Mineral.) Dissertation*, Novosibirsk: Inst. Neftegaz. Geol. Geofiz. Sib. Otd. Ross. Akad. Nauk, 2006a.

Lebedeva, N.K., Dinocyst biostratigraphy of the Upper Cretaceous of Northern Siberia, *Paleontol. J.*, 2006b, vol. 40, no. 5, pp. 604–S621.

Linnert, C., Robinson, S.A., Lees, J.A., Bown, P.R., Pérez-Rodríguez, I., Petrizzo, M.R., Falzoni, F., Littler, K., Arz, J.A., and Russel, E.E., Evidence for global cooling in the Late Cretaceous, *Nat. Commun.*, 2014, vol. 5, no. 4194. www.nature.com/articles/ncomms5194.

Linnert, C., Robinson, S.A., Lees, J.A., Perez-Rodriguez, I., Jenkyns, H.C., Bown, P.R., and Falzoni, F., Did Late Cretaceous cooling trigger the Campanian–Maastrichtian Boundary Event? *Newsl. Stratigr.*, 2018, vol. 51, no. 2, pp. 145–166.

Maslakova, N.I., The Crimea, in *Atlas verkhnemelovoi fauny Severnogo Kavkaza i Kryma* (Atlas of Upper Cretaceous Fauna of the Northern Caucasus and Crimea), Moskvin, M.M., Ed., Moscow; Gostoptekhizdat, 1959, pp. 60–84.

Maslakova, N.I., Globotrunkanids and their stratigraphic significance for the Upper Cretaceous stratigraphy of the Crimea, Caucasus, and Soviet Carpathians, *Doctoral (Geol.-Mineral.) Dissertation*, Moscow: Mosk. Gos. Univ., 1967.

Maslakova, N.I., *Globotrunkanidy yuga evropeiskoi chasti SSSR* (Globotrunkanids of the South of the European Part of the USSR), Moscow: Nauka, 1978 [in Russian].

Maslakova, N.I. and Naidin, D.P., The Santonian deposits of the southwestern Crimea, *Izv. Akad. Nauk SSSR. Ser. Geol.*, 1958, no. 1, pp. 75–77.

McArthur, J.M., Kennedy, W.J., Gale, A.S., Thirlwall, M.F., Chen, M., Burnett, J., and Hancock, J.M., Strontium isotope stratigraphy in the Late Cretaceous: Intercontinental correlation of the Campanian/Maastrichtian boundary, *Terra Nova*, 1992, vol. 4, pp. 385–393.

McArthur, J.M., Thirlwall, M.F., Chen, M., Gale, A.S., and Kennedy, W.J., Strontium isotope stratigraphy in the Late Cretaceous: numerical calibration of the Sr isotope curve and intercontinental correlation of the Campanian, *Paleoceanography*, 1993, vol. 8, no. 6, pp. 859–873.

Melinte-Dobrinescu, M.C., Uppermost Cretaceous calcareous nannofossils in red pelagic sediments (Romanian Carpathians), *Acta Palaeontol. Roman.*, 2018, vol. 14, no. 2, pp. 35–44.

Mitchell, S.F., New data on the biostratigraphy of the Flamborough Chalk Formation (Santonian, Upper Cretaceous) between South Landing and Danes Dyke, North Yorkshire, *Proc. Yorkshire Geol. Soc.*, 1994, vol. 50, no. 2, pp. 113–118.

Mitchell, S.F., The Cretaceous crinoid *Uintacrinus socialis* from Jamaica and its significance for global correlation, *Geol. Mag.*, 2009, vol. 146, no. 6, pp. 937–940.

Montgomery, P., Hailwood, E.A., Gale, A.S., and Burnett, J.A., The magnetostratigraphy of Coniacian–Late Campanian chalk sequences in southern England, *Earth Planet. Sci. Lett.*, 1998, vol. 156, pp. 209–224.

Naidin, D.P., A new belemnite from the Upper Cretaceous deposits of Crimea, *Byull. Mosk. O–va Ispyt. Prir., Otd. Geol.*, 1953, vol. 28, no. 2, pp. 64-65.

Naidin, D.P., Subclass Endocochlia. Endocochleate Cehalopods, in *Atlas verkhnemelovoi fauny Severnogo Kavkaza i Kryma* (Atlas of Late Cretaceous Fauna of the Northern Caucasus and Crimea), Moskvin, M.M., Ed., Moscow: Gostoptekhizdat, 1959, pp. 198–209.

Naidin, D.P., *Verkhnemelovye belemnity Russkoi platformy i sopredel'nykh oblastei. Aktinokamaksy, gonioteitisy i belemnellokamaksy* (Upper Cretaceous Belemnites from the Russian Platform and Adjacent Areas. Actinocamax, Gonioteuthis, and Belemnellocamax), Moscow: Mosk. Gos. Univ., 1964 [in Russian].

Naidin, D.P., Alekseev, A.S., and Kopaevich, L.F., Fauna from Turonian deposits of the Kacha–Bodrak interfluve (Crimea) and the Senomanian–Turonian boundary, in *Evolyutsiya organizmov i biostratigrafiya serediny melovogo perioda* (Organic Evolution and Biostratigraphy in the mid-Cretaceous Time), Naidin, D.P. and Krassilov, V.A., Eds., Vladivostok: Dalnevost. Nauchn. Tsentr Akad. Nauk SSSR, 1981, pp. 22–40.

Nøhr-Hansen, H., Upper Cretaceous dinoflagellate cyst stratigraphy, onshore West Greenland, *Grønlands Geol. Undersøgelse Bull.*, 1996, vol. 170.

Nøhr-Hansen, H., Piasecki, S., and Alsen, P., A Cretaceous dinoflagellate cyst zonation for NE Greenland, *Geol. Mag.*, 2019.
https://doi.org/10.1017/S0016756819001043

Ogg, J.G. and Hinnov, L.A., Cretaceous, in *The Geologic Time Scale*, Gradstein, F.M., Ogg, J.G., Schmitz, M.D., and Ogg, G.M., Eds., Amsterdam: Elsevier, 2012, pp. 793–855.

Okay, A.I. and Nikishin, A.M., Tectonic evolution of the southern margin of Laurasia in the Black Sea region, *Int. Geol. Rev.*, 2015, vol. 57, nos. 5–8, pp. 1051–1076.

Olferiev, A.G. and Alekseev, A.S., *Stratigraficheskaya skhema verkhnemelovykh otlozhenii Vostochno-Evropeiskoi platformy. Ob"yasnitel'naya zapiska* (Stratigraphic Scheme of the Upper Cretaceous Sediments of the East European Platform. Explanatory Note), Moscow: Paleontol. Inst. Ross. Akad. Nauk, 2005 [in Russian].

Ovechkina, M.N., Kopaevich, L.F., Aleksandrova, G.N., Proshina, P.A., Ryabov, I.A., Baraboshkin, E.Yu., Guzhikov, A.Yu., and Mostovski, M.B., Calcareous nannofossils and other proxies define the Santonian–Campanian boundary in the Central Crimean Mountains (Alan-Kyr section), *Cretaceous Res.*, 2021, vol. 119, no. 104706.
https://doi.org/10.1016/j.cretres.2020.104706

Pearce, M.A., New genera and species of organic-walled dinoflagellate cysts from the Cenomanian to lower Campanian of the Trunch Borehole, southeast England, *J. Micropalaeontol.*, 2010, vol. 29, pp. 51–72.

Pearce, M.A., Jarvis, I., Ball, P.J., and Laurin, J., Palynology of the Cenomanian to lowermost Campanian (Upper Cretaceous) Chalk of the Trunch Borehole (Norfolk, UK) and a new dinoflagellate cyst bioevent stratigraphy for NW Europe, *Rev. Palaeobot. Palynol.*, 2020.
https://doi.org/10.1016/j.revpalbo.2020.104188

Petrizzo, M.R., Falzoni, F., and Premoli Silva, I., Identification of the base of the lower-to-middle Campanian Globotruncana ventricosa Zone: comments on reliability and global correlations, *Cretaceous Res.*, 2011, vol. 32, pp. 387–405.

Prauss, M., Sea-level changes and organic-walled phytoplankton response in a Late Albian epicontinental setting, Lower Saxony basin, NW Germany, *Palaeogeogr., Palaeoclimatol., Palaeoecol.*, 2001, vol. 174, pp. 221–249.

Premoli Silva, I. and Sliter, W.V., Cretaceous planktonic foraminiferal biostratigraphy and evolutionary trends from the Botaccione section, Gubbio, Italy, *Palaeontigr. Ital.*, 1995, vol. 82, pp. 1–89.

Premoli Silva, I. and Sliter, W.V., Cretaceous paleoceanography: evidence from planktonic foraminiferal evolution, in *The Evolution of Cretaceous Ocean-Climatic System*, Barrera, E. and Jonson, C.C., Eds., *Spec. Pap.—Geol. Soc. Am.*, 1999, vol. 332, pp. 301–328.

Prince, I.M., Jarvis, I., and Tocher, B.A., High-resolution dinoflagellate cyst biostratigraphy of the Santonian–Basal Campanian (Upper Cretaceous): New data from Whitecliff, Isle of Wight, England, *Rev. Palaeobot. Palynol.*, 1999, vol. 105, pp. 143–169.

Prince, I.M., Jarvis, I., Pearce, M.A., and Tocher, B.A., Dinoflagellate cyst biostratigraphy of the Coniacian–Santonian (Upper Cretaceous): new data from the English Chalk, *Rev. Palaeobot. Palynol.*, 2008, vol. 150, pp. 59–96.

Radmacher, W., Tyszka, J., Mangerud, G., and Pearce, M.A., Dinoflagellate cyst biostratigraphy of the Upper Albian to Lower Maastrichtian in the southwestern Barents Sea, *Mar. Petrol. Geol.*, 2014, vol. 57, pp. 109–121.

Radmacher, W., Mangerud, G., and Tyszka, J., Dinoflagellate cyst biostratigraphy of Upper Cretaceous strata from two wells in the Norwegian Sea, *Rev. Palaeobot. Palynol.*, 2015, vol. 216, pp. 18–32.

Razmjooei, M.J., Thibault, N., Kani, A., Mahanipour, A., Boussaha, M., and Korte, C., Coniacian–Maastrichtian calcareous nannofossil biostratigraphy and carbon-isotope stratigraphy in the Zagros Basin (Iran): Consequences for

the correlation of Late Cretaceous Stage Boundaries between the Tethyan and Boreal realms, *Newsl. Stratigr.*, 2014, vol. 47/2, pp. 183–209.

Razmjooei, M.J., Thibault, N., Kani, A., Dinarès-Turell J., Pucéat E., Shahriari, S., Radmacher, W., Jamali, A.M., Ullmann, C.V., Voigt, S., and Cocquerez, T., Integrated bio- and carbon-isotope stratigraphy of the Upper Cretaceous Gurpi Formation (Iran): A new reference for the eastern Tethys and its implications for large-scale correlation of stage boundaries, *Cretaceous Res.*, 2018, vol. 91, pp. 312–340.

Remane, J., Basset, M.G., Cowie, J.W., Gohrbandt, K.H., Lane, H.R., Michelsen, O., and Wang, N., Revised guidelines for the establishment of global chronostratigraphic standards by the International Commission on Stratigraphy (ICS), *Episodes*, 1996, vol. 19, no. 3, pp. 77–81.

Russo, F., Calcareous nannofossil revised biostratigraphy of the latest Albian–earliest Campanian time interval (Late Cretaceous), *Ph. D. Thesis. Matricola R08989*, Universitá degli Studi di Milano, Dottorato di Ricerca in Scienze de la Terra Ciclo XXVI, Anno Academico, 2012–2013.

Sanjary, S., Hadavi, F., Notghi-Moghaddam, M., and Allameh, M., Calcareous nannofossils from chalky limestone interval of the Abderas Formation in the Kopet Dagh range, NE Iran, *Iran. J. Earth Sci.*, 2019, vol. 11, pp. 47–55.

Schulz, M-G., Erns, G., Ernst, H., and Schmid, F., Coniacian to Maastrichtian stage boundaries in the standard section for the Upper Cretaceous white chalk of NW Germany (Lägerdorf-Kronsmoor-Hemmoor): Definitions and proposals, *Bull. Geol. Soc. Denmark*, 1984, vol. 33, pp. 203–215.

Shcherbinina, E.A. and Gavrilov, Yu.O., The nannoplankton zoning of Senomanian–Santonian deposits of southwestern Crimea, in *Melovaya sistema Rossii i blizhnego zarubezh'ya: problemy stratigrafii i paleogeografii. Sb. nauch. trudov* (Coll. Sci. Works "Cretaceous System of Russia and CIS Countries: Problems of Stratigraphy and Paleogeography"), Baraboshkin, E.Yu., Ed., Simferopol: Izd. Dom Chernomorpress, 2016, pp. 292–294.

Shumenko, S.I. and Stetsenko V.P., Calcareous nannofossils from Upper Cretaceous deposits of Crimea, *Byull. Mosk. O-va Ispyt. Prir., Otd. Geol.*, 1978, vol. 53, no. 1, pp. 130–137.

Siegl-Farkas, Á., Dinoflagellate stratigraphy of the Senonian formations of the Transdanubian Range, *Acta Geol. Hungarica*, 1997, vol. 40/1, pp. 73–100.

Siegl-Farkas, Á. and Wagreich, M., Correlation of palyno- (spores, pollen, dinoflagellates) and calcareous nannofossil zones in the Late Cretaceous of the Northern Calcareous Alps (Austria) and the Transdanubian Central Range (Hungary), in *Advances in Austrian-Hungarian Joint Geological Research. 1000 Years Austria & 1100 years Hungary*, Budapest: MÁFI (Geol. Inst. Hungary), 1996, pp. 127–135.

Sissingh, W., Biostratigraphy of Cretaceous calcareous nannoplankton, *Geol. Mijnbouw*, 1977, vol. 56, pp. 37–65.

Slimani, H., Les kystes de dinoflagellés du Campanien au Danien dans la région de Maastricht (Belgique, Pays-Bas) et de Turnhout (Belgique): Biozonation et correlation avec d'autres régions en Europe occidentale, *Geol. Palaeontol.*, 2001, no. 35, pp. 161–201.

Stratigraphy.org – International Commission on Stratigraphy. https://stratigraphy.org/gssps/#cretaceous.

Thibault, N., Jarvis, I., Voigt, S., Gale, A.S., Attree, K., and Jenkyns, H.C., Astronomical calibration and global correlation of the Santonian (Cretaceous) based on the marine carbon isotope record, *Paleoceanography*, 2016, vol. 31, pp. 847–865.

Vishnevskaya, V.S., Kopaevich, L.F., and Benyamovsky, V.N., and Ovechkina, M.N., Correlation of the Upper Cretaceous zonal schemes of the Eastern European Platform based on foraminifera, radiolarians, and nanoplankton, *Moscow Univ. Geol. Bull.*, 2018, vol. 73, no. 1, pp. 131–140.

Vishnevskaya, V.S. and Kopaevich, L.F., Microfossil assemblages as key to reconstruct sea-level fluctuations, cooling episodes and palaeogeography: The Albian to Maastrichtian of Boreal and Peri-Tethyan Russia, *Spec. Publ.—Geol. Soc. London.*, 2020, no. 498, pp. 165–187. https://doi.org/10.6084/m9.figshare.c.4737236

Walaszczyk, I. and Peryt, D., Inoceramid-foraminiferal biostratigraphy of the Turonian through Santonian deposits of the Middle Vistula Section, Central Poland, *Zentralbl. Geol. Palaontol.*, 1998, vol. I, nos.11/12, pp. 1501–1513.

Walaszczyk, I., Dubicka, Z., Olszewska-Nejbert, D., and Remin, Z., Integrated biostratigraphy of the Santonian through Maastrichtian (Upper Cretaceous) of extra-Carpathian Poland, *Acta Geol. Polon.*, 2016, vol. 66, no. 3, pp. 313–350.

Weber, G. and Malychef, V., Sur la stratigraphie du Mesocretace et du Neocretace de la Crimee, *Bull. Soc. Geol. France. Ser. 4*, 1923, vol. XXIII, nos. 5–6, pp. 193–204.

Wolfgring, E., Wagreich, M., Dinarés-Turell, J., Gier, S., Böhm, K., Sames, B., and Spötl, K., The Santonian–Campanian boundary and the end of the Long Cretaceous Normal Polarity-Chron: isotope and plankton stratigraphy of a pelagic reference section in NW Tethys (Austria), *Newsl. Stratigr.*, vol. 51, no. 4. https://doi.org/10.1127/nos/2018/0392

Mikrotax.org – A System for Web-Delivery of Taxonomy. www.mikrotax.org

Translated by E. Murashova